

Simulation of Groundwater Flow in the Shallow Aquifer System of the Delmarva Peninsula, Maryland and Delaware



Open-File Report 2012–1140

Cover. Flows in the Choptank River (shown) and other streams are used to calibrate the groundwater model. Photograph by Sharon Shahan, used with permission.

Simulation of Groundwater Flow in the Shallow Aquifer System of the Delmarva Peninsula, Maryland and Delaware

By Ward E. Sanford, Jason P. Pope, David L. Selnick, and Ryan F. Stumvoll

Open-File Report 2012–1140

U.S. Department of the Interior
U.S. Geological Survey

U.S. Department of the Interior
KEN SALAZAR, Secretary

U.S. Geological Survey
Marcia K. McNutt, Director

U.S. Geological Survey, Reston, Virginia: 2012

For more information on the USGS—the Federal source for science about the Earth, its natural and living resources, natural hazards, and the environment, visit <http://www.usgs.gov> or call 1–888–ASK–USGS.

For an overview of USGS information products, including maps, imagery, and publications, visit <http://www.usgs.gov/pubprod>

To order this and other USGS information products, visit <http://store.usgs.gov>

Any use of trade, firm, or product names is for descriptive purposes only and does not imply endorsement by the U.S. Government.

Although this information product, for the most part, is in the public domain, it also may contain copyrighted materials as noted in the text. Permission to reproduce copyrighted items must be secured from the copyright owner.

Suggested citation:

Sanford, W.E., Pope, J.P., Selnick, D.L., and Stumvoll, R.F., 2012, Simulation of groundwater flow in the shallow aquifer system of the Delmarva Peninsula, Maryland and Delaware: U.S. Geological Survey Open-File Report 2012–1140, 58 p.

Contents

Abstract.....	1
Introduction.....	1
Purpose and Scope	1
Previous Investigations	2
Location and Setting of Study Area	2
Simulation of Groundwater Flow in the Shallow Aquifer System.....	2
Assembly of the Groundwater Model	2
Model Grid Characteristics	3
Boundary Conditions	7
Land-Surface Characteristics	10
Climate Characteristics	10
Hydrologic Characteristics	10
Geologic Characteristics	19
Model Calibration	26
Simulation Results	44
Summary and Conclusions.....	52
References Cited.....	57

Figures

1. Map showing location of the study area	3
2. Map showing locations of counties, and state boundaries on the Delmarva Peninsula.....	4
3. Map showing region covered by the groundwater flow model including the active model area	5
4. Map showing location of watersheds by U.S. Geological Survey 8-digit hydrologic unit code.....	6
5. Map showing elevation of land surface on the Delmarva Peninsula derived from light detection and ranging and bathymetry from National Oceanic and Atmospheric Administration National Geophysical Data Center, U.S. Coastal Relief Model.....	8
6. Map showing general land-cover types based on the U.S. Geological Survey 2001 National Land-Cover Dataset	9
7. Map showing percentage of impervious surface based on the U.S. Geological Survey 2001 National Land-Cover Database.....	11
8. Map showing texture of soils on the Delmarva Peninsula shown as percent sand	12
9. Map showing texture of soils on the Delmarva Peninsula shown as percent clay	13
10. Map showing mean annual precipitation on the Delmarva Peninsula from 1971 to 2000 based on the PRISM climate dataset.....	14
11. Map showing mean maximum daily temperature on the Delmarva Peninsula from 1971 to 2000 based on the PRISM climate dataset	15
12. Map showing mean minimum daily temperature on the Delmarva Peninsula from 1971 to 2000 based on the PRISM climate dataset	16

13.	Map showing mean annual temperature on the Delmarva Peninsula from 1971 to 2000 based on the PRISM climate dataset.....	17
14.	Map showing mean annual difference between the maximum and minimum daily temperature on the Delmarva Peninsula from 1971 to 2000 based on the PRISM climate dataset.....	18
15.	Map showing mean annual estimated evapotranspiration on the Delmarva Peninsula from 1971 to 2000 based on the climate regression equation of Sanford and others (2012).....	20
16.	Map showing mean-annual estimated surface runoff on the Delmarva Peninsula from 1971 to 2000 based on the regression equations of Sanford and others (2012) for the Coastal Plain physiographic province and the clay content of the soils.....	21
17.	Map showing mean annual estimated total runoff on the Delmarva Peninsula from 1971 to 2000 calculated by subtracting evapotranspiration from precipitation.....	22
18.	Map showing mean annual estimated recharge on the Delmarva Peninsula from 1971 to 2000 based on the precipitation from the PRISM climate database and the climate and runoff regression equations of Sanford and others (2012).....	23
19.	Map showing bottom surface of the Cretaceous deposits on the Delmarva Peninsula relative to sea-level datum NGVD 29.....	24
20.	Map showing locations where various Cretaceous and Tertiary deposits outcrop at the land surface or subcrop beneath Quaternary deposits on the Delmarva Peninsula.....	25
21.	Cross-sectional view showing dipping of confined hydrogeologic units beneath the surficial aquifer along the line <i>B–B'</i>	26
22.	Map showing bottom surface of the Quaternary deposits on the Delmarva Peninsula relative to sea-level datum NGVD 29.....	27
23.	Map showing distribution of geologic units within layer 1 of the model grid.....	28
24.	Map showing distribution of geologic units within layer 2 of the model grid.....	29
25.	Map showing distribution of geologic units within layer 3 of the model grid.....	30
26.	Map showing distribution of geologic units within layer 4 of the model grid.....	31
27.	Map showing distribution of geologic units within layer 5 of the model grid.....	32
28.	Map showing distribution of geologic units within layer 6 of the model grid.....	33
29.	Map showing distribution of geologic units within layer 7 of the model grid.....	34
30.	Map showing locations of the 48 wells used for water-level observations.....	37
31.	Map showing locations of U.S. Geological Survey stream gages and watersheds on the Delmarva Peninsula with real-time water data.....	39
32.	Map showing locations of the 23 well sites where samples were collected for groundwater-age observations.....	41
33.	Graphs showing observed versus simulated water levels, and simulated water levels versus the difference between the observed and simulated water levels.....	45
34.	Map showing spatial distribution of errors in the simulated water-level observations.....	46
35.	Graphs showing observed versus simulated groundwater ages, and simulated ages versus the difference between the observed and simulated ages.....	47
36.	Map showing spatial distribution of errors in the simulated age observations.....	48
37.	Map showing the simulated water table on the Delmarva Peninsula represented by water levels in layer 1 of the model.....	49
38.	Map showing the simulated water levels in layer 7 of the model.....	50
39.	Map showing the simulated depth of the water table beneath the land surface.....	51
40.	Map showing simulated net recharge across the Delmarva Peninsula calculated by subtracting the seepage discharge from the recharge.....	54

41. Map showing simulated groundwater age 80 feet below land surface in layer 4 of the model grid.....	55
42. Map showing simulated return time of groundwater travelling from the water table to its discharge location	56

Tables

1. Observation wells and associated groundwater levels used to calibrate the groundwater model in this study.....	35
2. Watersheds used to compare observed and simulated total runoff from the land surface.....	38
3. Observation wells and associated groundwater ages used for comparison with simulated groundwater ages in this study	40
4. Hydraulic conductivity values reported and specified or calibrated in the groundwater model in this study.....	42
5. Composite scaled sensitivities for hydraulic conductivity parameters in the groundwater model	43
6. Water budget terms in the groundwater model by model layer	52
7. Water budget terms in the groundwater model by geologic unit.....	53

Conversion Factors and Abbreviations

Inch/Pound to SI

Multiply	By	To obtain
Length		
inch (in.)	2.54	centimeter (cm)
inch (in.)	25.4	millimeter (mm)
foot (ft)	0.3048	meter (m)
mile (mi)	1.609	kilometer (km)
Flow rate		
million gallons per day (Mgal/d)	0.04381	cubic meter per second (m ³ /s)
inch per year (in/yr)	25.4	millimeter per year (mm/yr)
Hydraulic conductivity		
foot per day (ft/d)	0.3048	meter per day (m/d)

Temperature in degrees Fahrenheit (°F) may be converted to degrees Celsius (°C) as follows:

$$^{\circ}\text{C}=(^{\circ}\text{F}-32)/1.8$$

Vertical coordinate information is referenced to the National Geodetic Vertical Datum of 1929 (NGVD 29).

Horizontal coordinate information is referenced to the North American Datum of 1983 (NAD 83).

Elevation, as used in this report, refers to distance above the vertical datum.

Abbreviations

CSS	composite scaled sensitivity
ET	evapotranspiration
RAM	random access memory
USGS	U.S. Geological Survey

Simulation of Groundwater Flow in the Shallow Aquifer System of the Delmarva Peninsula, Maryland and Delaware

By Ward E. Sanford, Jason P. Pope, David L. Selnick, and Ryan F. Stumvoll

Abstract

Estimating future loadings of nitrogen to the Chesapeake Bay requires knowledge about the groundwater flow system and the traveltime of water and chemicals between recharge at the water table and the discharge to streams and directly to the bay. The Delmarva Peninsula has a relatively large proportion of its land devoted to agriculture and a large associated nitrogen load in groundwater that has the potential to enter the bay in discharging groundwater. To better understand the shallow aquifer system with respect to this loading and the traveltime to the bay, the U.S. Geological Survey constructed a steady-state groundwater flow model for the region. The model is based on estimates of recharge calculated using recently developed regression equations for evapotranspiration and surface runoff. The hydrogeologic framework incorporated into the model includes unconfined surficial aquifer sediments, as well as subcropping confined aquifers and confining beds down to 300 feet below land surface. The model was calibrated using 48 water-level measurements and 24 tracer-based ages from wells located across the peninsula. The resulting steady-state flow solution was used to estimate ages of water in the shallow aquifer system through the peninsula and the distribution and magnitude of groundwater traveltime from recharge at the water table to discharge in surface-water bodies (referred to as return time). Return times vary but are typically less than 10 years near local streams and greater than 100 years near the stream divides. The model can be used to calculate nitrate transport parameters in various local watersheds and predict future trends in nitrate loadings to Chesapeake Bay for different future nitrogen application scenarios.

Introduction

Groundwater plays a prominent role in the transport of nutrients to Chesapeake Bay. Over half of the freshwater entering the bay has travelled through the subsurface and discharged into streams beforehand (Phillips and Lindsey, 2003). The traveltime for groundwater is much longer than

that of surface runoff, with the typical time of travel (return time or lag time) from recharge at the water table to stream discharge ranging from years to centuries. The variability in the return times creates difficulties in predicting the magnitude and timing of the effect of reducing nitrogen loading (in fertilizer, for example) at land surface on the resulting timing of nitrogen loading to the streams and the bay. To better predict the effects of nitrogen loading practices on the health of the bay, better estimates are needed for the distribution of groundwater return times to local streams across the Chesapeake Bay watershed. The purpose of this study is to obtain a map of groundwater return times that can be used in estimating and forecasting nitrogen loading to the Chesapeake Bay. The best type of tool currently available to estimate groundwater return times is a groundwater simulation model calibrated using environmental tracers. A series of such models is currently being developed by the U.S. Geological Survey (USGS), as part of its Priority Ecosystems Science Initiative, for major sections of the Chesapeake Bay watershed. The Delmarva Peninsula is the first section for which this type of groundwater model is being constructed. The peninsula was chosen as the first study site because a large percentage of its area is devoted to agriculture and is near the bay; it was also chosen because the surficial aquifer is composed of porous sediments of the Atlantic Coastal Plain, the effect of which is to increase the length and effect impact of the groundwater lag time relative to that in fractured rock terrains west and north of the plain. The return times obtained from the current modeling effort can be used to estimate the timing of nitrogen delivery to Chesapeake Bay for different regions, and help environmental managers assess current and future nitrogen application practices.

Purpose and Scope

The purpose of this report is to describe the construction a groundwater model of the shallow aquifer system of the Delmarva Peninsula that can be used to calculate ranges of groundwater return times from recharge areas to streams. The aquifer system simulated by the model is the surficial aquifer

and subcropping confined aquifers and confining units down to 300 feet (ft) below land surface. The model grid, boundary conditions, and the hydrologic and geologic factors used to construct this model are all described herein. The grid was constructed with a horizontal discretization of 500 ft over the entire peninsula (the Virginia section of the southernmost peninsula was mostly excluded) in order to incorporate details of the local flow system. Because the model was designed to study the transport of nitrogen (mostly as nitrate) from the land surface to streams, only the shallow flow system (approximately the top 300 ft) was included in the model. Much of the groundwater used for public supply on the peninsula is extracted from deeper confined aquifers, but the impact of those withdrawals on the deeper groundwater system is beyond the purpose of this study, and therefore, the extent of this model. Also described herein are the development and initial results of the model in terms of the simulated steady-state water table, groundwater ages, and return-time distributions.

Previous Investigations

To date, no comprehensive groundwater model has been constructed that covers the majority of the Delmarva Peninsula. During the 1980s and 1990s, the USGS constructed a regional model of the Atlantic Coastal Plain (Leahy and Martin, 1993; Fleck and Vroblesky, 1996), but the Delmarva Peninsula was only represented in a very rudimentary manner because of the relatively large discretization used. In addition, the shallow unconfined aquifer that contributes most of the flow to the local streams was represented only as a constant-head boundary in that model. Groundwater models of the Coastal Plain aquifers in other states (North Carolina and Virginia) have been constructed recently (Heywood and Pope, 2009), but no equivalent model has been constructed in Maryland or Delaware, and as with previous work on the Delmarva Peninsula, the focus of the other models was the deeper aquifers that are used for most of the water-supply withdrawals. The flow system of the surficial aquifer on the peninsula and its role in nutrient transport have been studied by use of environmental tracers (Dunkle and others, 1993; Bohlke and Denver, 1995) and local representative cross-sectional flow modeling (Reilly and others, 1994). The hydrogeologic characterization of the peninsula has also been described recently (Ator and others, 2005), and this characterization was used to estimate variations in recharge in the Coastal Plain sediments of Virginia (Sanford and others, 2012). The southern portion of the Delmarva Peninsula that lies in Virginia was included in a groundwater model that also addressed the potential for saltwater intrusion (Sanford and others, 2009), and because this section has already been simulated, it was mostly excluded from the current study; this excluded portion of the peninsula is referred to hereafter as the “Virginia section.” The Virginia Delmarva model was also used for a preliminary estimate of nitrate delivery to Chesapeake Bay (Sanford and Pope, 2007).

Location and Setting of Study Area

The Delmarva Peninsula is that portion of land bordered by Chesapeake Bay, Delaware Bay, and the Atlantic Ocean (fig. 1). The groundwater model was constructed to include the entire peninsula except the Virginia section. Excluding the Virginia section also allowed for a more efficient use of computer storage in that large portions of areas outside the peninsula did not have to be included in the model. Counties in the study area include Kent, Queen Anne’s, Talbot, Caroline, Dorchester, Wicomico, Somerset, Worcester, and part of Cecil in Maryland; Sussex, Kent and part of New Castle in Delaware; and a small part of northern Accomack County in Virginia (fig. 2). Although some areas of Maryland west of the bay and areas of New Jersey are included in the model grid, they are not included in the active area of the model where groundwater flow is simulated (fig. 3).

Simulation of Groundwater Flow in the Shallow Aquifer System

As noted earlier, the focus of the model in this study is to calculate the distribution of groundwater return times present in the shallow aquifer system across the majority of the Delmarva Peninsula.

Assembly of the Groundwater Model

The major watersheds within the peninsula can be divided into two groups—those that drain westward into Chesapeake Bay and those that drain eastward into Delaware Bay or the Atlantic Ocean (fig. 4). The watershed divide between the two is oriented north-south through Delaware and is relatively close to the coastal bays of Maryland, resulting in about two-thirds of the peninsula draining into Chesapeake Bay (fig. 4). Although future use of the model is to focus on using the groundwater return times to estimate the timing of nutrient transport to Chesapeake Bay, the entire peninsula was included in the model in case future studies of nitrogen transport in the eastern watersheds are initiated. The objective of creating the model was to provide the ability to calculate distributions of groundwater return times within individual watersheds of interest, and because seasonal variations in flow and stresses do not typically cause any substantial variations in the overall distribution of these times (Reilly and Pollock, 1996), a steady-state flow simulation was deemed sufficient for the return-time calculations. In addition, although the volumes of groundwater extracted for human and agricultural use from the shallow system are substantial, they are relatively small compared to the overall recharge and discharge fluxes in the aquifer; therefore, withdrawals of water by pumping were excluded from the simulation. For example, the total pumping of groundwater from the model area in 2005 was less than 60 million gallons per day (Mgal/d) (Kenny and

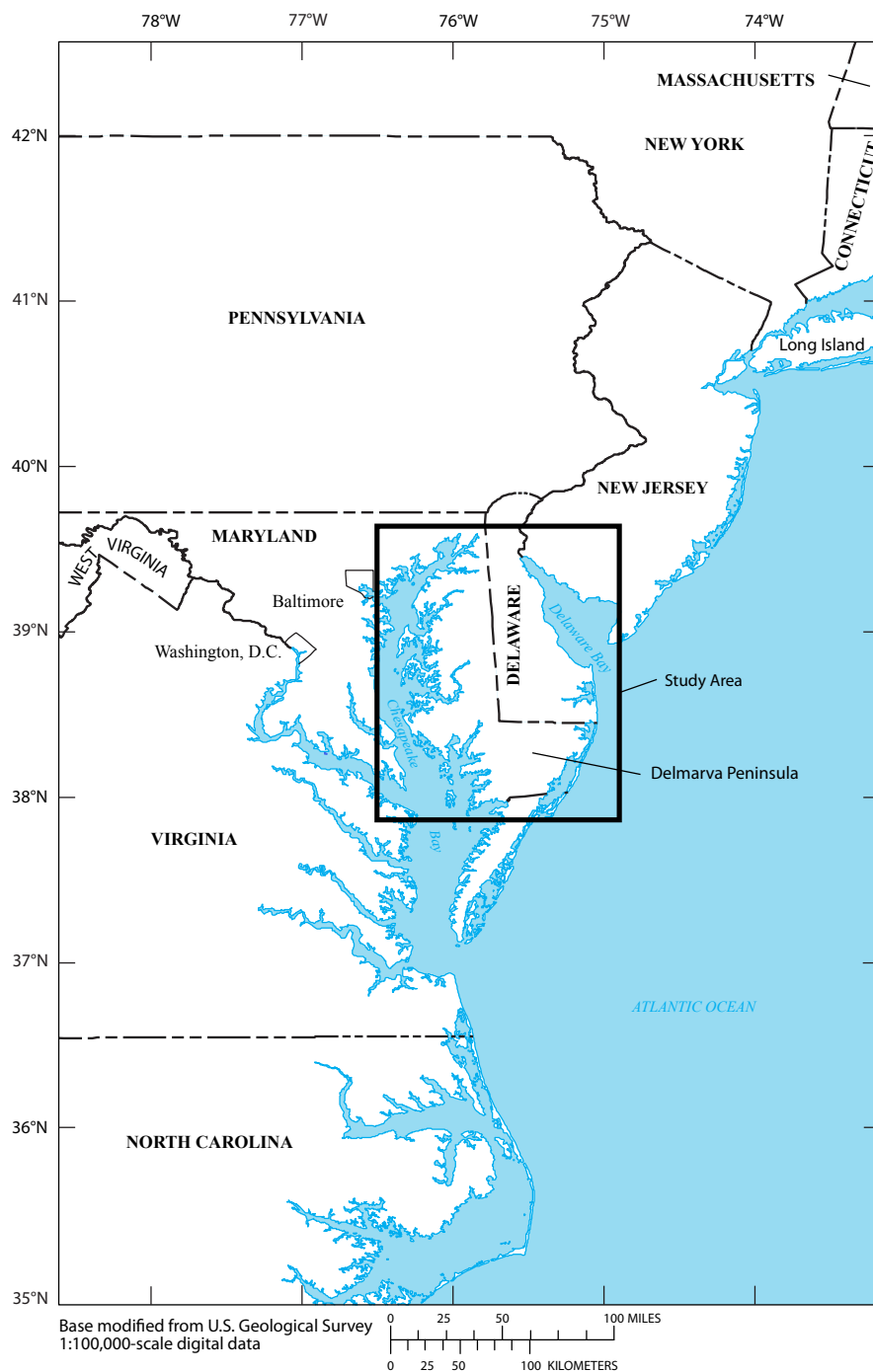


Figure 1. Location of the study area.

others, 2009), but the total mean annual recharge to the area is in excess of 3,300 Mgal/d (see section Simulation Results). Likewise, water withdrawals from the deeper confined aquifers are substantial quantities themselves, as they are derived partly from storage losses as the aquifers and confining units compress. Consequently, the remaining flux downward from the shallow aquifers is small relative to the natural recharge and discharge to the streams. The simulation of only steady-state, natural flow in the shallow system substantially reduced the amount of work

required to construct and calibrate the model, yet was more than adequate to meet the objective of the study.

Model Grid Characteristics

A major requirement of the model development was to obtain the distributions of groundwater traveltimes for various subwatersheds within the peninsula, and thus, a discretization

4 Simulation of Groundwater Flow in the Shallow Aquifer System of the Delmarva Peninsula, Maryland and Delaware



Figure 2. Locations of counties, and state boundaries on the Delmarva Peninsula.

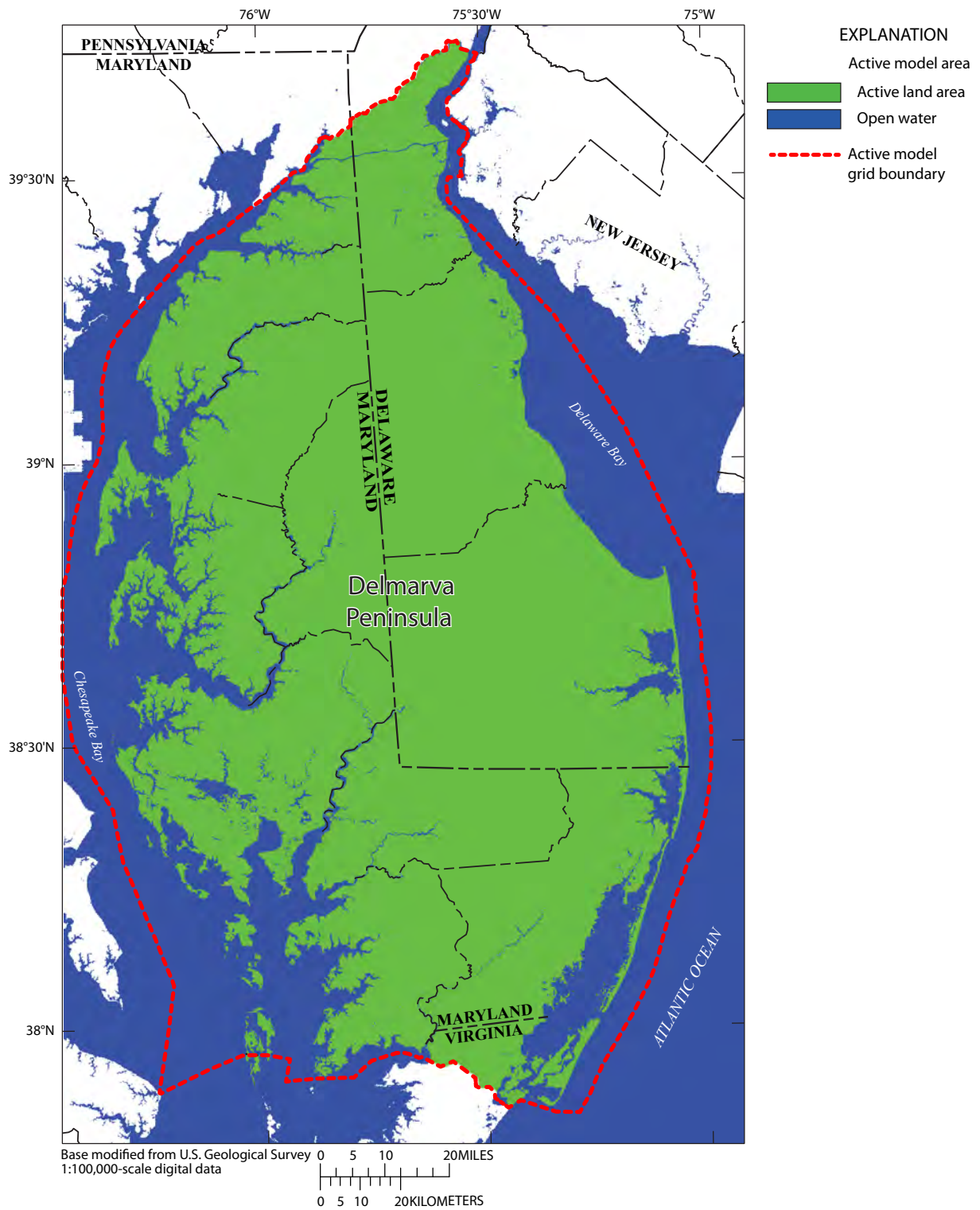


Figure 3. Region covered by the groundwater flow model (875 columns by 1,435 rows) including the active model area.

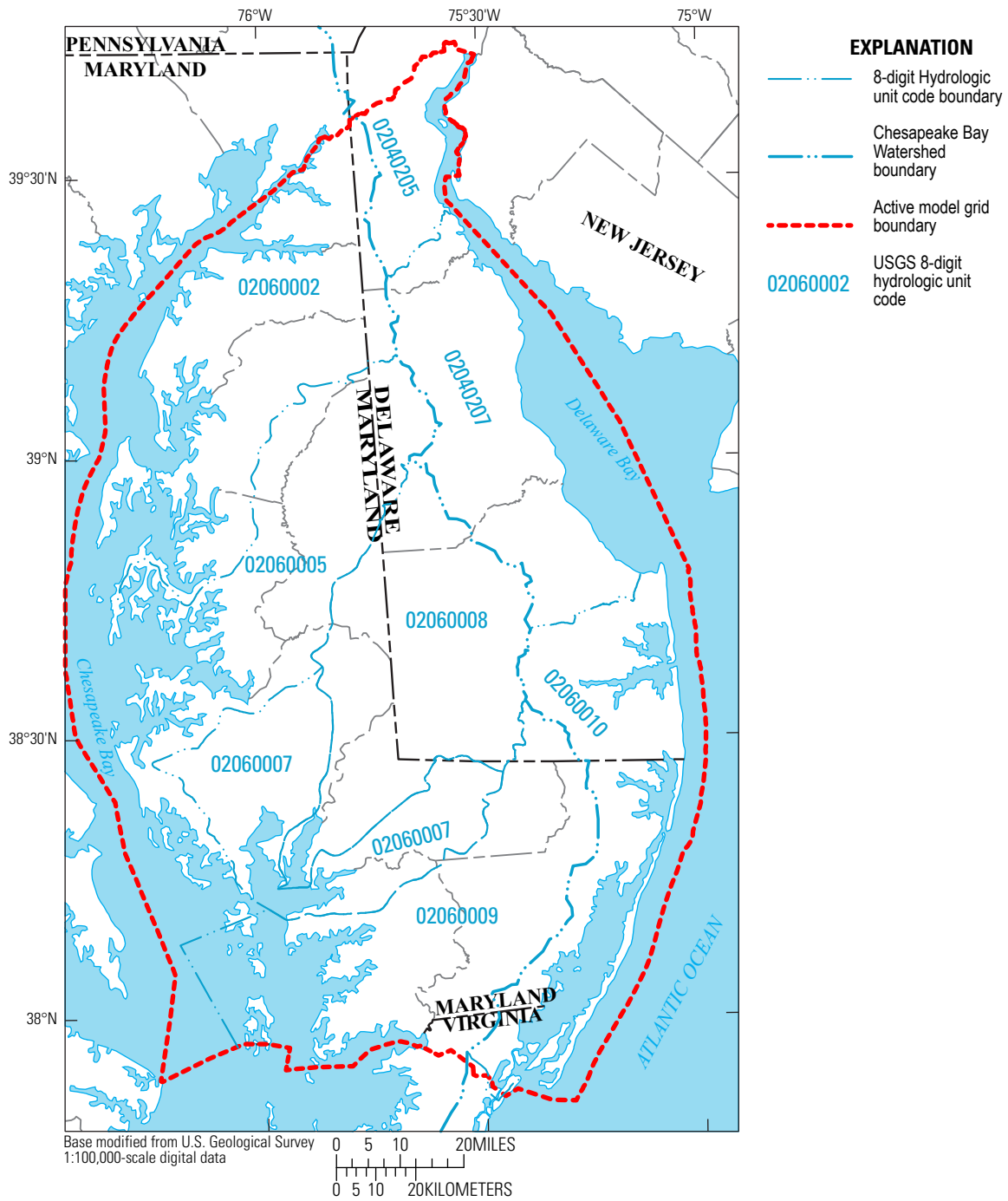


Figure 4. Location of watersheds by U.S. Geological Survey 8-digit hydrologic unit code (HUC-8).

was required that was fine enough to give a good resolution of flow paths, even for watersheds as small as several square miles. In accordance with this criterion, a uniform horizontal discretization of 500 ft was used across the entire model area. Coverage of the entire model area at this spatial discretization yielded 1,435 rows and 875 columns in the model grid. The USGS MODFLOW–2005 simulation code (Harbaugh, 2005), a three-dimensional finite-difference groundwater flow model, was used to simulate the flow system.

Although much of the groundwater flow in the shallow system is local flow to streams, a vertical discretization was required that would still allow characterization of the vertical aspect of the flow. This aspect included vertical flow near streams and the variable nature of the Coastal Plain strata (including permeable aquifers sediments and fine-grained confining units) that dip toward the southeast and subcrop beneath a layer of overlying Quaternary sediments that are commonly breached in the stream valleys. To achieve this, seven layers were used in the model that progressively increase in thickness with depth. The uppermost layer, layer 1, is 10 ft thick and has a top elevation equal to the land surface elevation throughout the model area. The remaining six layers, progressing downward, are 20, 30, 40, 50, 60, and 90 ft thick, for a total model thickness of 300 ft. Although the model grid extends to 300 ft below land surface, the fine-grained confining beds form a relative barrier to any substantial vertical flow penetrating this deep in many areas of the peninsula. The model grid consists of nearly 8.8 million cells, of which about 5.5 million (62 percent) are active. The model requires close to 4 gigabytes of random access memory (RAM) to run on a personal computer, as well as a 64-bit operating system that can appropriate 4 or more gigabytes of RAM.

In general, the water table is relatively close to the land surface across the peninsula, although it is more than 60 ft below land surface in a few places. Consequently, the top few model layers are dry in a number of locations, creating a nonlinear flow condition in which the aquifer transmissivity is dependent upon the elevation of the water table, and vice versa. This strong nonlinearity, along with a variability of up to five orders of magnitude in hydraulic conductivity between certain units, created severe difficulties in achieving numerical convergence using the standard numerical solvers found in MODFLOW. The Newton version of MODFLOW (Niswonger and others, 2011) was used to overcome this difficulty during the calibration and achieve the final steady-state flow solution. The processing time required to solve the steady-state solution with MODFLOW–NWT is about 10 minutes on a T7500 Dell Precision with 3.33 gigahertz (GHz) Intel Xeon processors.

Boundary Conditions

Simulation of any groundwater flow system requires appropriate boundary conditions. The active model area (fig. 3) in this study includes both land and areas of open water in the Chesapeake and Delaware Bays and the Atlantic Ocean. The model cells that are below sea level in these water bodies

are treated with a general-head boundary condition. The conductance term was set to a sufficiently high value ($50,000 \text{ ft}^{-1}$) so that the water-sediment interface would behave similarly to a constant-head boundary. This is equivalent to a hydraulic conductivity in the each cell of 10 feet per day (ft/d) connecting the center of the 10-ft thick cell with the top boundary of the cell at which the external head is located. This external head is equivalent to sea level (defined as zero), but is also adjusted to account for the additional pressure head created by the excess density of the salt in the column of water above the cell. For this calculation, a salinity value equivalent to that of standard ocean water was used in the Delaware Bay and Atlantic Ocean, and values that were representative of the mean Chesapeake Bay salinity distribution were used beneath Chesapeake Bay. The effect of the excess salt head in these regions was minimal because of the relatively shallow surface-water depths close to shore (fig. 5) and the shallow extent of the groundwater flow system relative to the horizontal distances involved. The majority of the flow along the Chesapeake Bay shoreline was usually restricted to the top few model layers and was relatively small in magnitude because much of the nearshore sediment is relatively fine-grained. The minor perceived effect of density variation justified the constant-density assumption, as well as the use of MODFLOW rather than a more computationally intensive variable-density code, such as SEAWAT (Langevin and others, 2003). The latter code was used, for example, in the Virginia Eastern Shore model (Sanford and others, 2009), where the objective was to track saltwater intrusion in deeper confined aquifers.

The land surface is treated in the model as a combination of a recharge and seepage-face boundary as described in Sanford (2002). This combination of boundary conditions is very effective where relief is relatively low and the water table is relatively shallow, and it allows the model to calculate the magnitude and distribution of discharge within the stream valleys. With this approach, recharge is applied to all cells above sea level. The recharge values applied were estimated using the same water-balance method applied recently to the Coastal Plain of Virginia (Sanford and others, 2012); more detail about these values is provided later in this report. A “drain” boundary condition, as defined in drain package of MODFLOW, is also assigned to every cell above sea level to represent a seepage face. In this approach, the elevation of the land surface (fig. 5) is commonly used as the elevation of the drain. On the Delmarva Peninsula, however, drains have been installed in much of the agricultural land where the water table is near the land surface. In riparian areas, evapotranspiration from the water table keeps the water table near the bottom of the root zone. Although including drain locations in the model was beyond the scope of this study, the model-drain elevations at each cell were adjusted downward to represent these conditions. Land-cover types on the peninsula were also included in the model grid (fig. 6). For each cell that represented agricultural land cover, the drain elevation for the cell was set to 6 ft below the land surface. Where forest was present, the

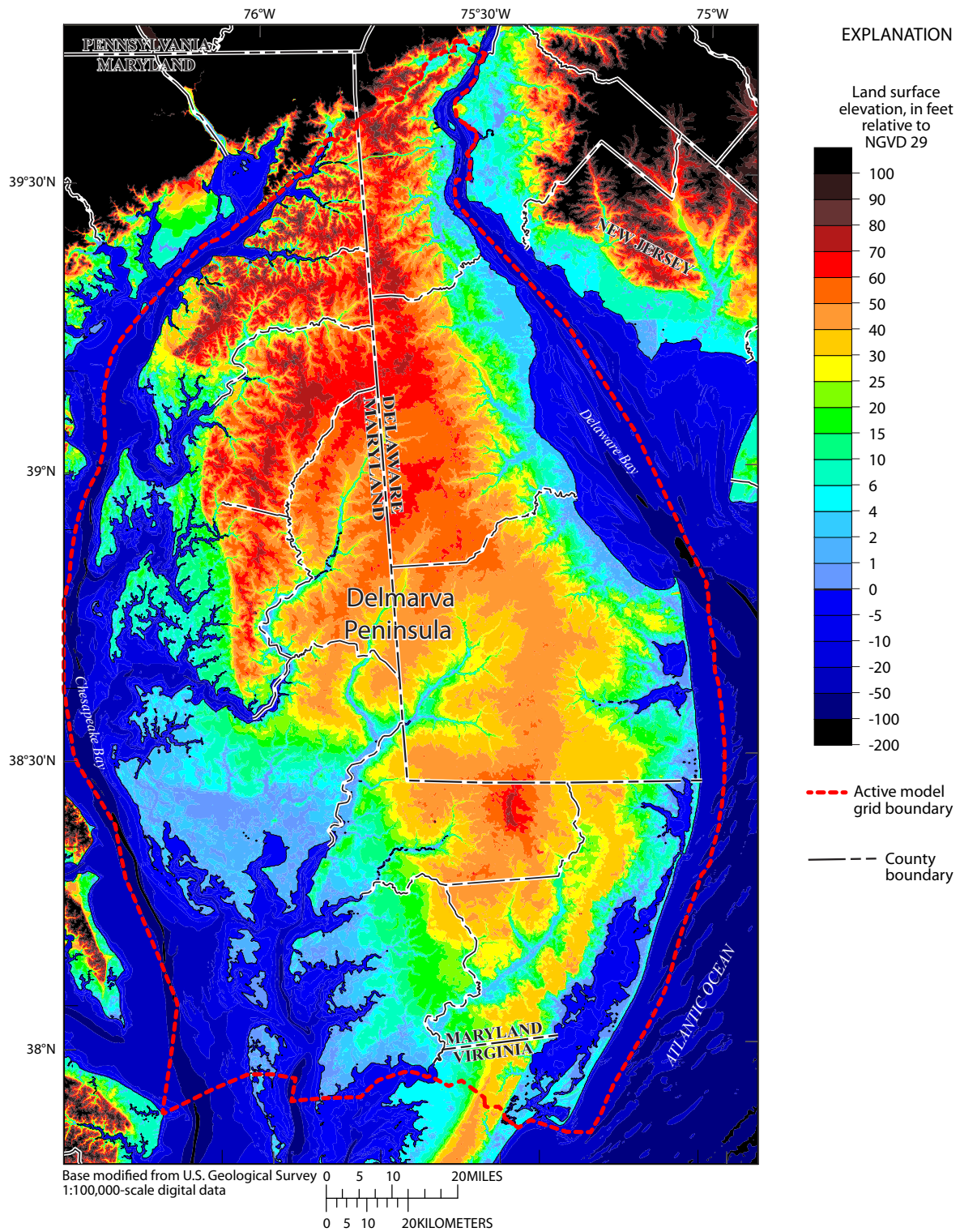


Figure 5. Elevation of land surface on the Delmarva Peninsula derived from light detection and ranging (LIDAR) (Roger Barlow, U.S. Geological Survey, unpub. data, 2010), and bathymetry from National Oceanic and Atmospheric Administration National Geophysical Data Center, U.S. Coastal Relief Model. Retrieved July 2007 from <http://www.ngdc.noaa.gov/mgg/coastal/crm.html>.

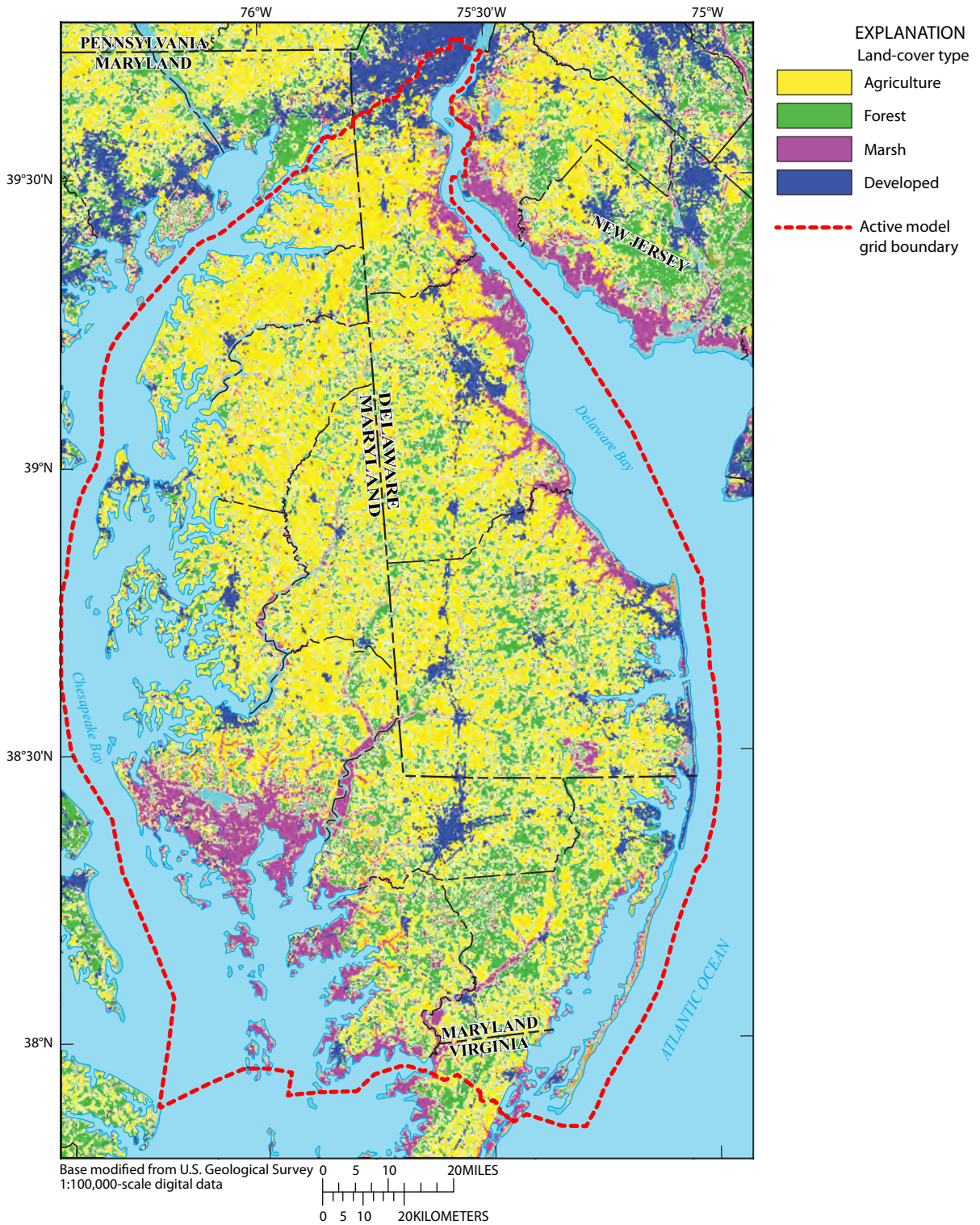


Figure 6. General land-cover types based on the U.S. Geological Survey 2001 National Land-Cover Dataset. Data retrieved August 2007 from <http://landcover.usgs.gov/natl/landcover.php>.

elevation was set at 3.5 ft below the surface, and where urban development or marsh was present, the elevation was set to 2 ft below the surface. These values were chosen to represent the typical depths of agricultural drains, forest root systems, and urban grass or marsh root systems, respectively. The values only made a difference in areas where the water table was close to the land surface, typically near streams. If the water level in a given cell is calculated to be above the drain elevation, then discharge is calculated by the model automatically; if the water level is below drain elevation, then discharge is zero. The conductance of the drain is specified as a value equal to the area of the cell multiplied by the hydraulic conductivity of the local cell material and divided by the distance between the land surface and the center of the cell in layer 1 (5 ft). Although cells having discharge were mostly in the stream valleys, the hydraulic conductivity of the streambeds was not assumed to differ from that of the local aquifer material. Riparian evapotranspiration is not calculated explicitly in the model, but its flux, which is much smaller than the direct seepage discharge to the streams, is an implicit part of the drain discharge.

The bottom of the model grid is treated as a no-flow boundary. The cells representing the confining units in the system, however, are assigned a hydraulic conductivity value of 0.001 ft/d, which is at least three orders of magnitude lower than that of the aquifer cells. Thus, in many parts of the peninsula, the effective bottom of the flow system is the top of the local confining layer and much shallower than the 300-ft depth of the bottom of the model.

Land-Surface Characteristics

Because the top of the water table is relatively close to the land surface across the Delmarva Peninsula, land-surface characteristics strongly affect the shallow groundwater flow system. The topography of the peninsula is relatively low in relief (fig. 5), with the highest elevation being 93 ft above NGVD 29 in the northeastern region. Coastal areas, however, are mostly within a few feet of NGVD 29. The land cover (fig. 6) is mostly agricultural, but there are also substantial areas of forest, swamp, and urban or suburban development. The developed areas create impervious surfaces that alter the runoff and recharge potentials that affect the shallow groundwater flow system. A map showing percentages of impervious surface (fig. 7) compiled from 2001 data (Homer and others, 2004) illustrates that areas with highly impervious surfaces are concentrated around the towns and small cities. Soil texture was an important factor in recent estimates of recharge on the Coastal Plain of Virginia and Maryland (Sanford and others, 2012), and it was used to estimate recharge for this model. Surficial sediments range in composition from clays to sands. Maps of the percentages of sand (fig. 8) and clay (fig. 9) in the soil indicated sand content was greatest in the eastern and central portions of the peninsula and clay content was greatest along the margins, especially in the low-lying tidal regions along Chesapeake Bay.

Climate Characteristics

Climatic conditions on the peninsula influence the shallow groundwater flow system through precipitation, which affects the recharge rate, and the air temperature, which affects the evapotranspiration rate. A recent study by Sanford and others (2012) used climatic factors to help estimate evapotranspiration and subsequent recharge in Virginia. The factors of importance for calculating long-term mean annual evapotranspiration (ET) and recharge were mean annual precipitation and mean-annual daily maximum and minimum temperatures. Because the groundwater model in the current study is a steady-state model that does not incorporate temporal variations in precipitation and recharge, the long-term average ET and recharge regression equations developed for the Virginia study were also applied to this study. All climate data were obtained from the PRISM climate dataset (Daly and others, 2008) and represented average values from 1971 to 2000. Mean annual precipitation during the period (fig. 10) did not vary greatly across the peninsula, and ranged from 41 inches in northernmost Virginia at the southern end of the Delmarva Peninsula to over 45 inches in portions of Delaware and southeastern Maryland. The mean maximum daily temperature ranged from less than 65°F in the northernmost peninsula to more than 67°F in south-central portions of Maryland (fig. 11). The mean minimum daily temperature ranged from less than 44°F in the northernmost peninsula to 49°F in the southernmost coastal regions of the study area (fig. 12). The mean daily temperature ranged from 54°F in the northernmost peninsula to over 57°F in the southernmost section (fig. 13). The ET rate, as estimated by Sanford and others (2012), was a function not only of the mean annual daily temperature, but also of the difference between the mean annual daily maximum and minimum temperatures. Daily differences in temperature are smallest near the coast where humidity is greater, and as a result, solar radiation and ET are less (fig. 14). The greatest range in daily temperature on the peninsula was about 21°F in the central region, and the lowest was less than 17°F along the coastlines of Maryland and Virginia.

Hydrologic Characteristics

The climatic factors and their spatial distributions described in the preceding section were used to estimate ET in the following regression equation from Sanford and others (2012):

$$ET = 0.370 P + 0.957 T_{max} - 0.383 T_{min} - 34.277 \quad (1)$$

where

- ET is the evapotranspiration rate, in inches per year;
- P is the precipitation rate, in inches per year;
- T_{max} is the mean maximum daily temperature, in degrees Fahrenheit; and
- T_{min} is the mean minimum daily temperature, in degrees Fahrenheit.

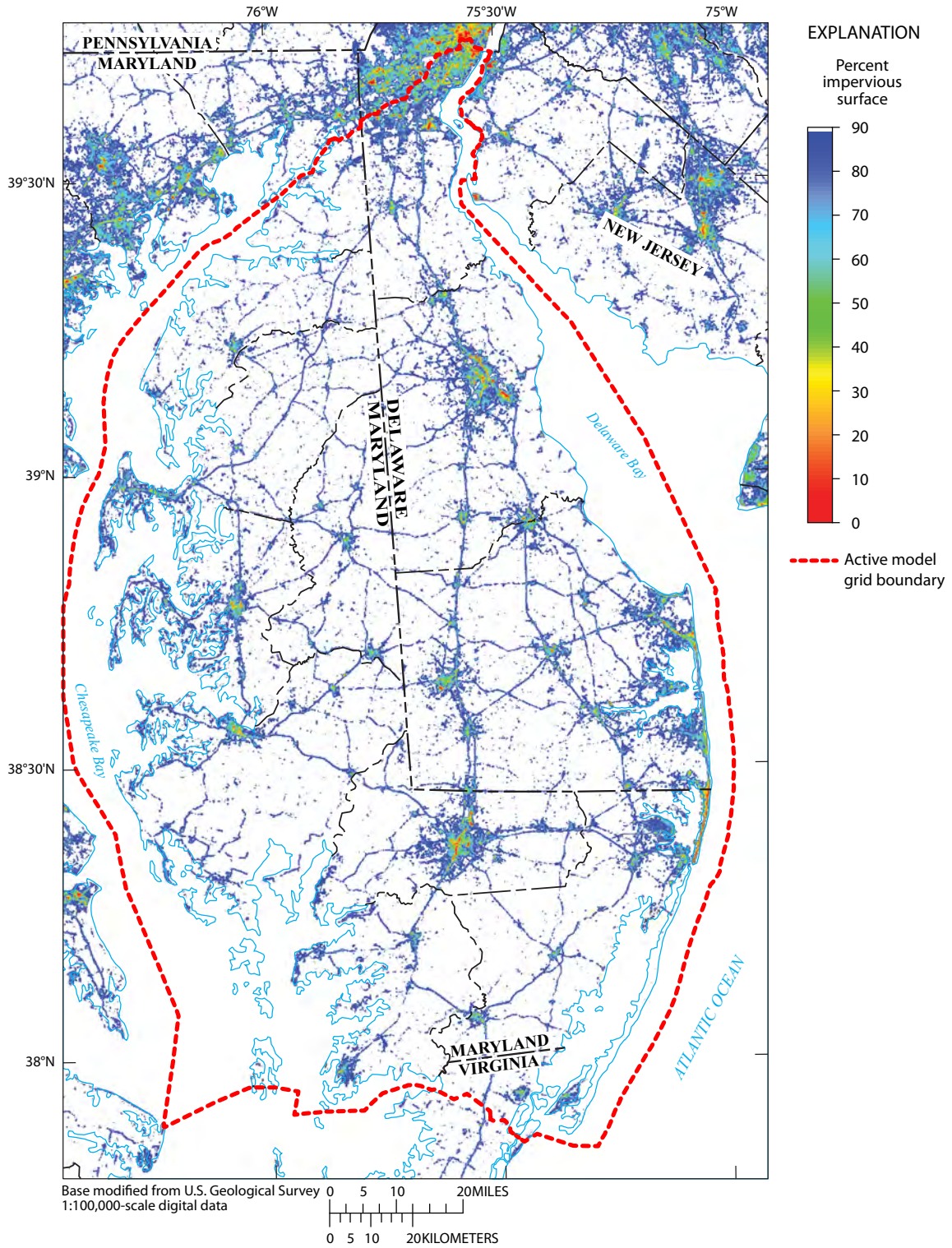


Figure 7. Percentage of impervious surface based on the U.S. Geological Survey 2001 National Land-Cover Database (Homer and others, 2004).

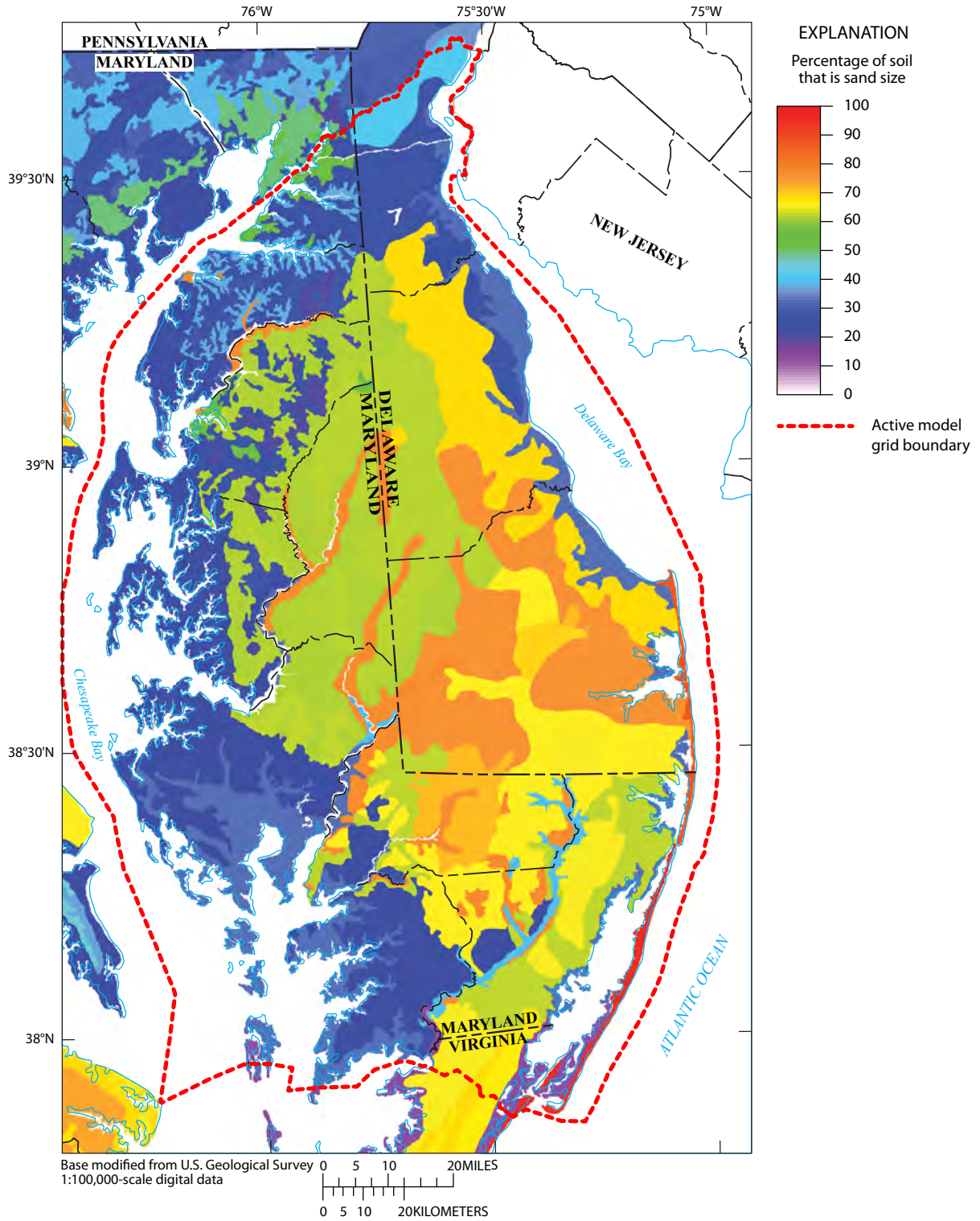


Figure 8. Texture of soils on the Delmarva Peninsula shown as percent sand. Data retrieved September 2007 from <http://soildatamart.nrcs.usda.gov>.

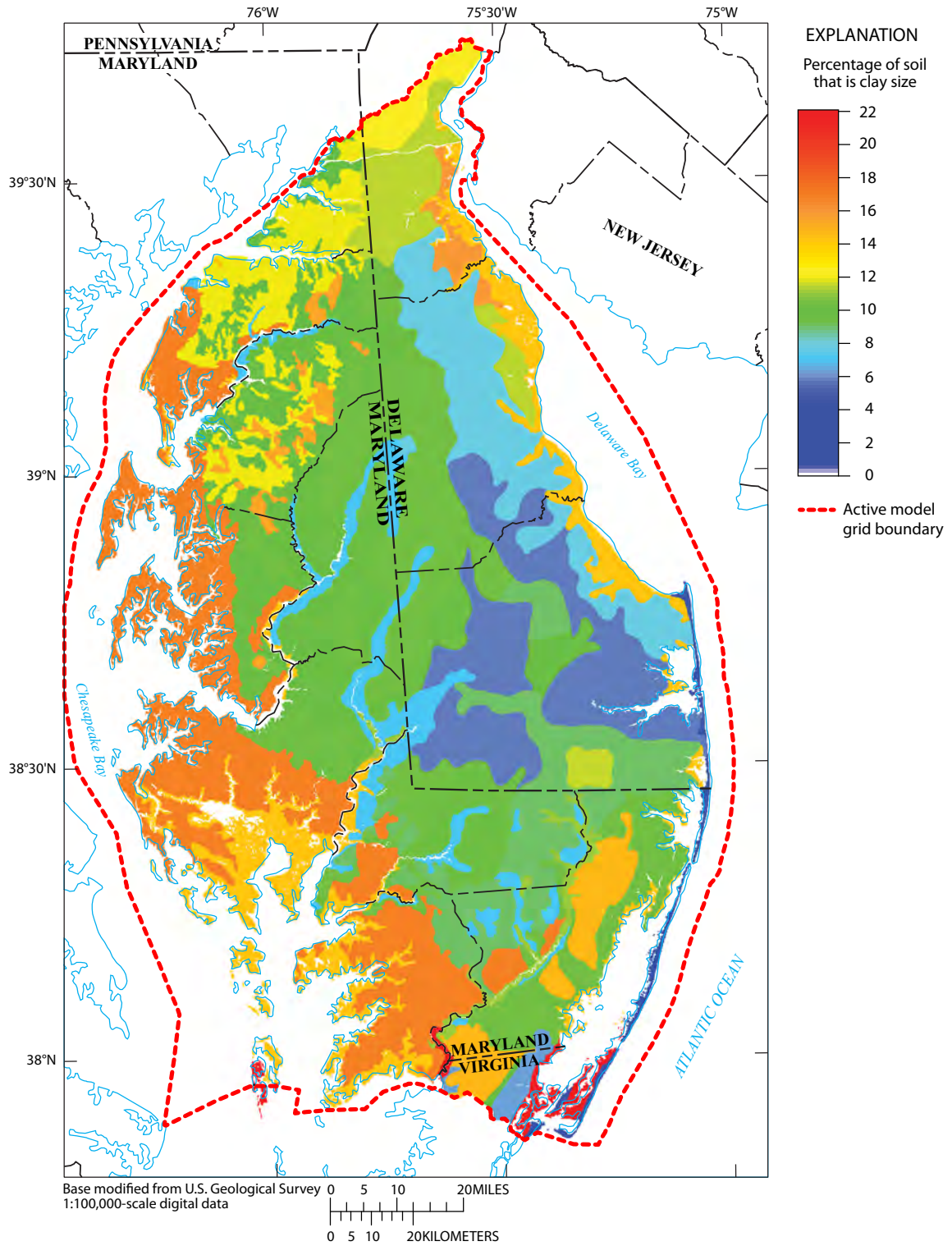


Figure 9. Texture of soils on the Delmarva Peninsula shown as percent clay. Data retrieved September 2007 from <http://soildatamart.nrcs.usda.gov>.

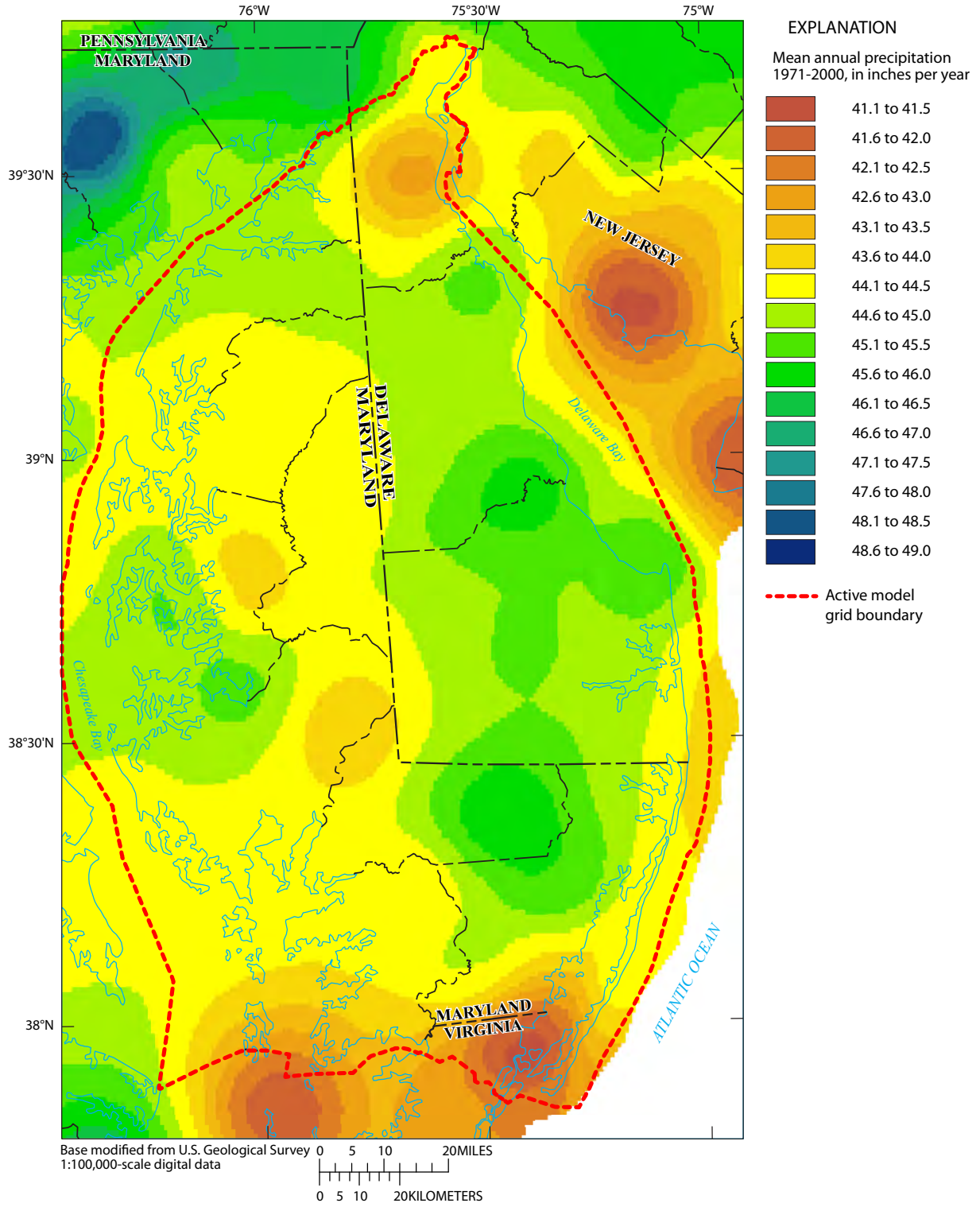


Figure 10. Mean annual precipitation on the Delmarva Peninsula from 1971 to 2000 based on the PRISM climate dataset (Daly and others, 2008). Data retrieved July 2009 from <http://www.prism.oregonstate.edu>.

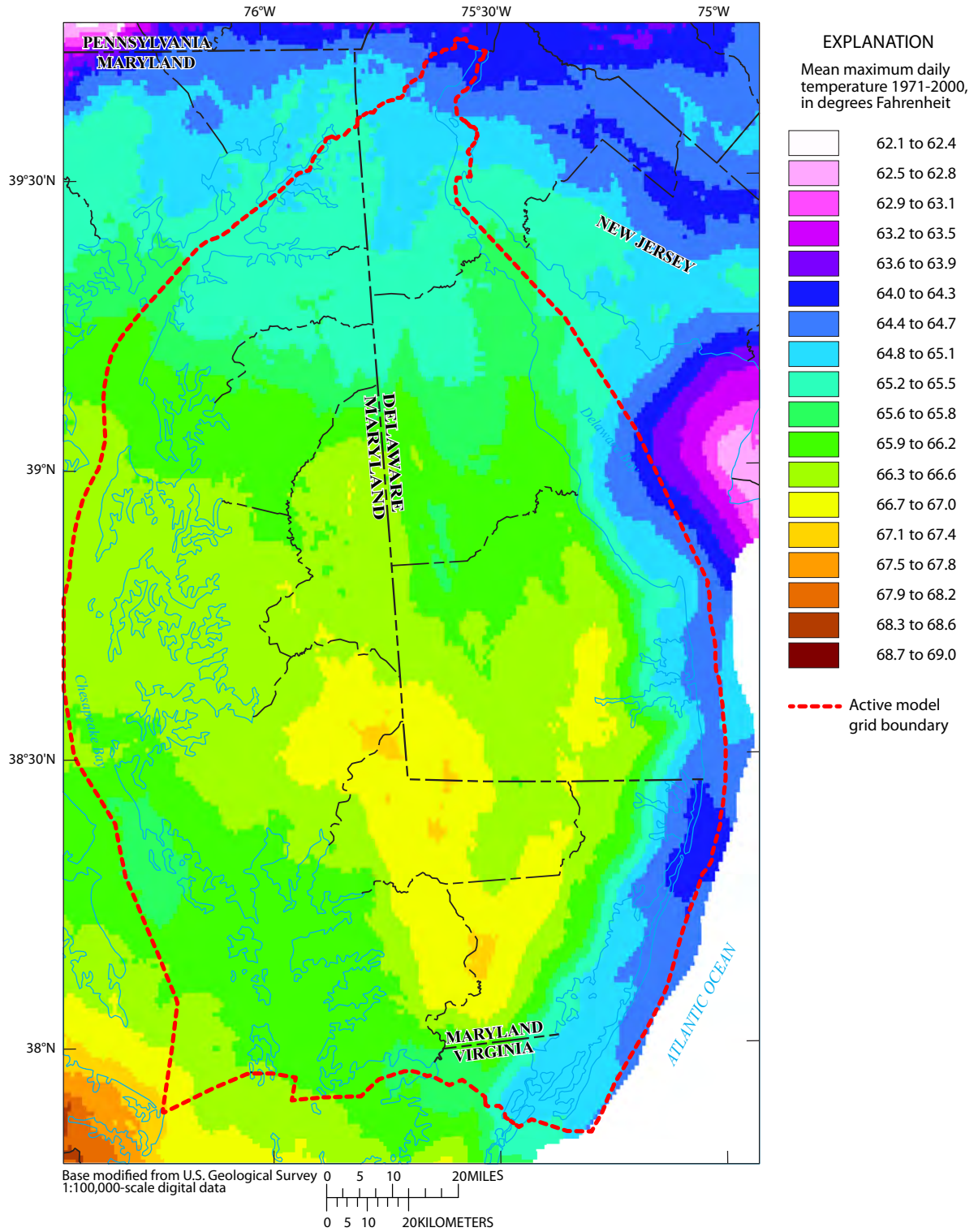


Figure 11. Mean maximum daily temperature on the Delmarva Peninsula from 1971 to 2000 based on the PRISM climate dataset (Daly and others, 2008). Data retrieved July 2009 from <http://www.prism.oregonstate.edu>.

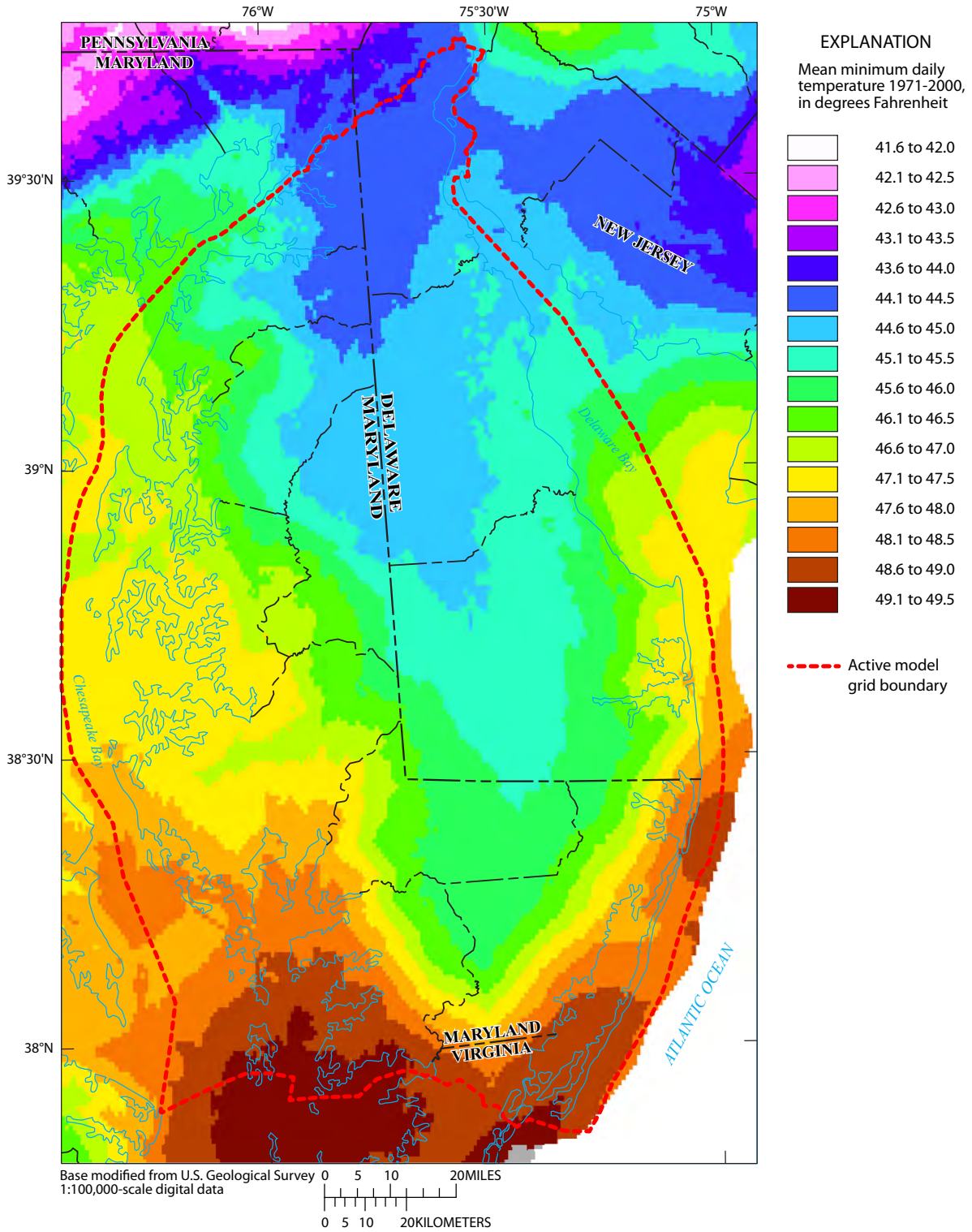


Figure 12. Mean minimum daily temperature on the Delmarva Peninsula from 1971 to 2000 based on the PRISM climate dataset (Daly and others, 2008). Data retrieved July 2009 from <http://www.prism.oregonstate.edu>.

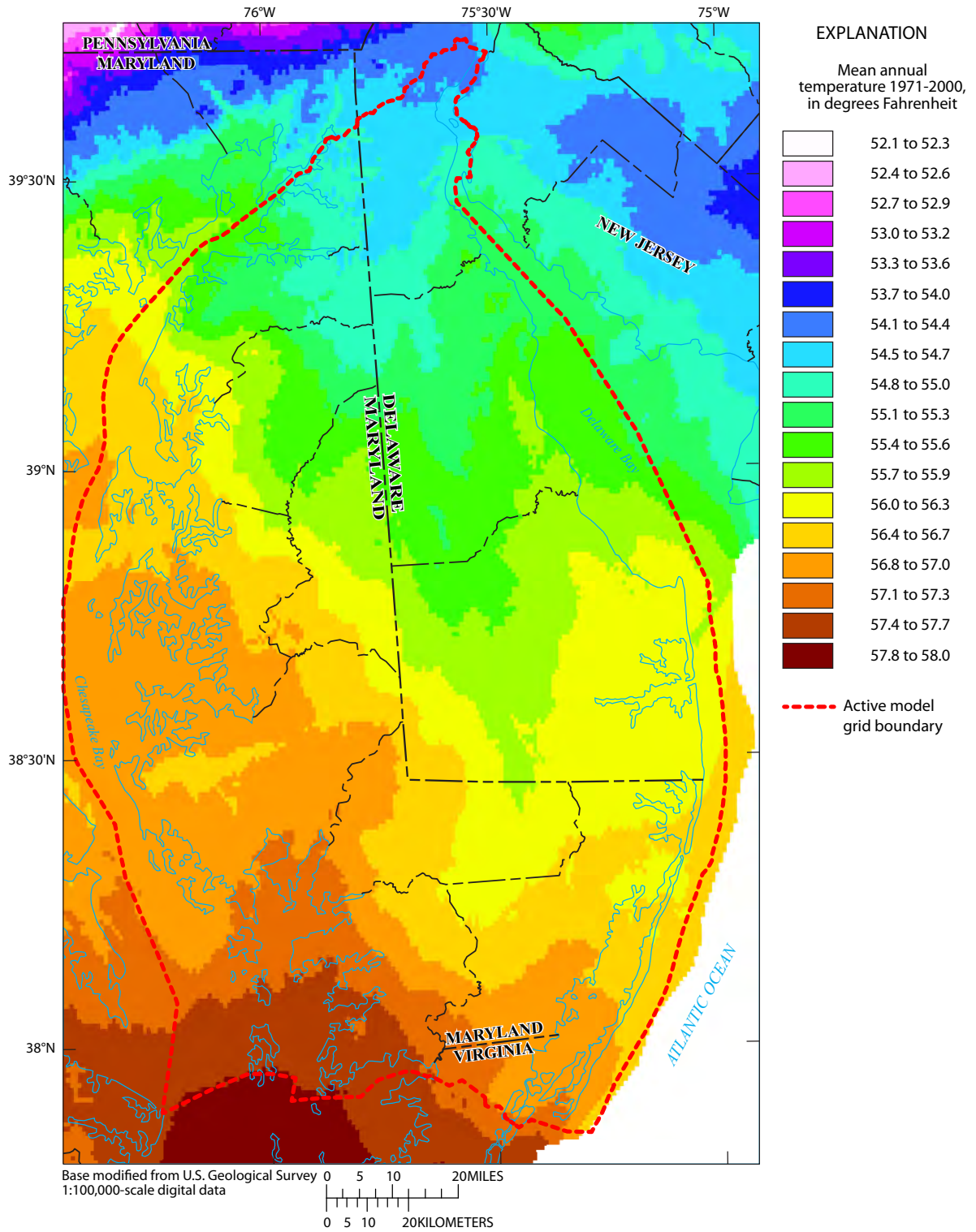


Figure 13. Mean annual temperature on the Delmarva Peninsula from 1971 to 2000 based on the PRISM climate dataset (Daly and others, 2008). Data retrieved July 2009 from <http://www.prism.oregonstate.edu>.

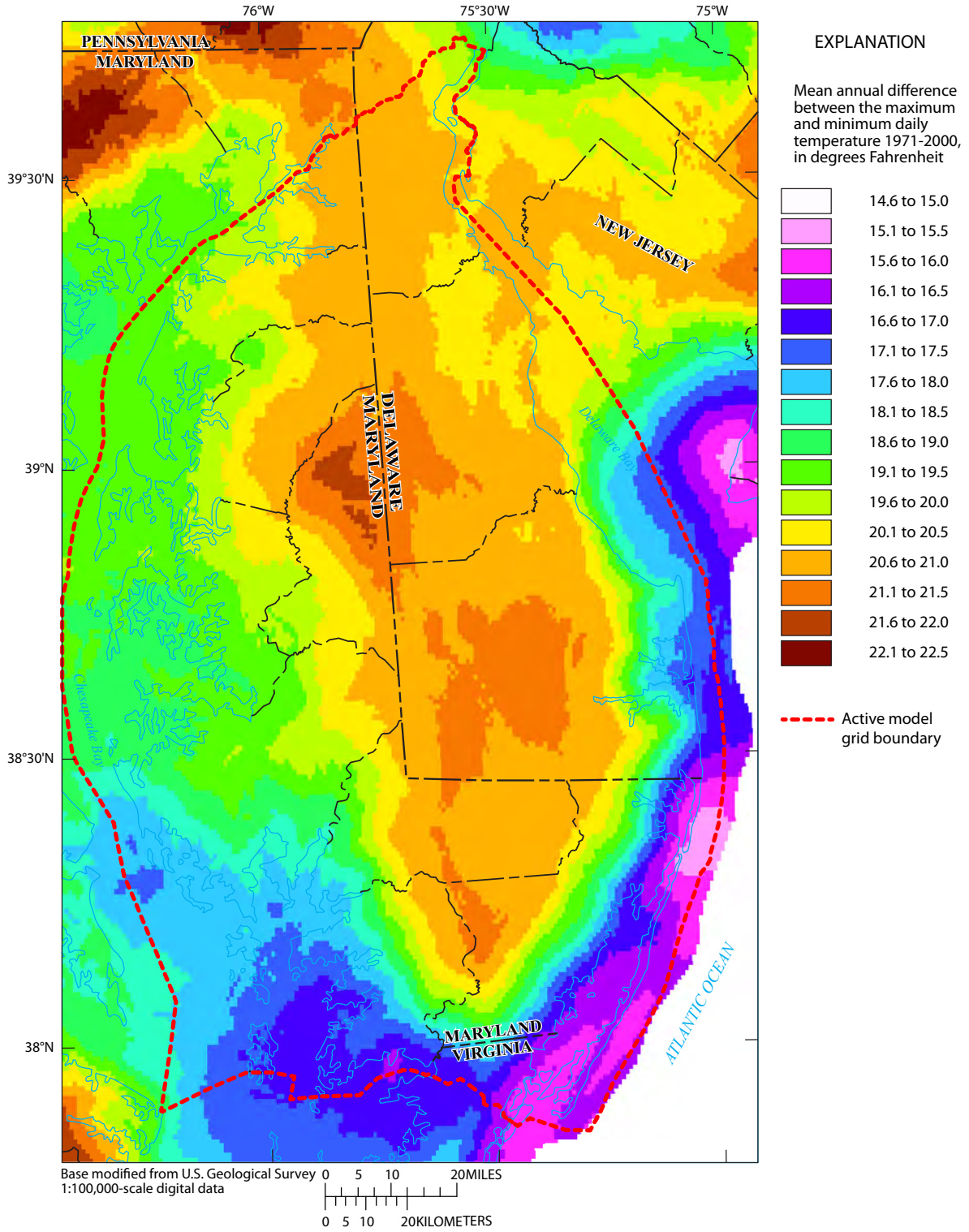


Figure 14. Mean annual difference between the maximum and minimum daily temperature on the Delmarva Peninsula from 1971 to 2000 based on the PRISM climate dataset (Daly and others, 2008). Data retrieved July 2009 from <http://www.prism.oregonstate.edu>.

This regression was based on estimates of ET using a water-balance approach for several dozen watersheds across the entire State of Virginia. The ET rate was also reduced by 1.3 percent for each one percent of the land surface that was impervious, as in the study of Sanford and others (2012). The resulting distribution of ET is relatively uniform across the study area, having a value of about 28 inches per year (in/yr), except within a few miles of the Atlantic coastline where higher humidity results in ET values that are slightly lower, typically 25 to 26 in/yr (fig. 15). Areas with impervious surface were estimated to have values of 24 in/yr or less.

Surface runoff is the portion of precipitation that travels over the soil or impervious surface to the nearest stream channel. Surface runoff was estimated for the Coastal Plain environments in the recent study by Sanford and others (2012), which used a regression equation that related surface runoff on the Coastal Plain to soil and sediment character. The regression equation that was used in that study and for comparison in this study is

$$R_o = 11.0 FG + 7.5 MG + 4.1 CG, \quad (2)$$

where

R_o	is surface runoff, in inches per year;
FG	is the fraction of the watershed that is underlain by fine-grained sediment;
MG	is the fraction underlain by medium-grained sediment; and
CG	is the fraction underlain by coarse-grained sediment.

The Nanticoke River watershed in southern Maryland has surface runoff estimated to be about 4 percent of precipitation, or 1.8 in/yr (Sanford and others, 2012). This rate was compared to the percentage of clay in the Nanticoke watershed soil (fig. 9). A similar comparison was made to watersheds having greater clay contents, and it was determined that the percentage of clay content in the soil divided by a factor of 2 yielded a reasonable estimate of surface runoff in inches per year. Similar to the calculations by Sanford and others (2012), the surface runoff values were adjusted to account for the percentage of impervious surface. This was accomplished by increasing the runoff by 0.58 percent of the precipitation rate for each one percent of impervious surface. The resulting surface runoff across the peninsula (fig. 16) was estimated to be between 1 and 2 in/yr for sandy soils in the east-central region, and up to 3 to 4 in/yr in the western tidal region of Chesapeake Bay. Many locations having a high percentage of impervious surface have estimated surface-runoff values that exceed 5 in/yr.

The total runoff for the peninsula was calculated by subtracting the evapotranspiration from the precipitation (fig. 17). The mean-annual total runoff for the peninsula varied from less than 16 in/yr in the central region in Maryland to over 18 in/yr near the Atlantic coast. The recharge to the water table was calculated by subtracting the surface runoff from the total runoff. The mean annual recharge across the peninsula

(fig. 18) was estimated to be from 12 to 13 in/yr in some areas with a high clay content in the western and southwestern regions, to 14 in/yr in much of the central region, to 15 to 17 in/yr in eastern areas with sandy soils and along the Atlantic coastline; all of these recharge values (fig. 18) were entered into the MODFLOW model in this study. The values were specified and did not require adjustment during the calibration procedure, as discussed further in the model calibration section herein.

Geologic Characteristics

The Delmarva Peninsula is underlain by Coastal Plain sediments that are Cretaceous through Quaternary in age and alternate between fluvial and marine sands, silts, and clays (Andreasen and others, 2007). The sediments overlie Paleozoic and Precambrian crystalline bedrock, and dip and thicken to the southeast (fig. 19). Within the study area, the Cretaceous-age sediments crop out above sea level along the western side of northernmost Chesapeake Bay toward the northeast into northernmost Delaware. The bottom surface of the Cretaceous-age sediments dips to the southeast and is more than 6,000 ft below sea level along the Atlantic coast of Maryland and Delaware. Cretaceous- and Tertiary-age sedimentary layers thicken toward the southeast accordingly, pinching out at various locations beneath the peninsula (figs. 20 and 21). These sediments are overlain by Quaternary deposits that are fluvial, marine, and eolian in origin (Owens and Denny, 1979). The bottom surface of the Quaternary deposits varies in elevation from over 60 ft above NGVD 29 in the northern peninsula to more than 100 ft below NGVD 29 near the east-west border between Maryland and southern Delaware (fig. 22).

Because the model layers are constant in thickness areally, each represents the geologic framework by uniquely representing the corresponding stratigraphic unit in space based on how the grid layer intersects the strata at each cell location. This hydrogeologic representation in the model was constructed by intersecting the model layers with the digital stratigraphic-unit surfaces created in a hydrogeologic framework by Andreasen and others (2007). Layer 1, being the shallowest layer and 10 ft thick, mostly represents the Quaternary deposits, except where they have been breached in the northern region by stream erosion that has exposed the underlying Tertiary and Cretaceous units (fig. 23). Layer 2 is 20 ft thick and also dominated by Quaternary deposits, but it has a larger region of Tertiary and Cretaceous units represented in the western and northern peninsula compared to layer 1 (fig. 24). Layer 3 is 30 ft thick and composed of the Quaternary units, mostly in the central and southeastern peninsula, with only a few scattered areas of Quaternary deposits present in the northern and northwestern peninsula (fig. 25). The remainder of layer 3 is composed of the Tertiary and Cretaceous units that underlie the Quaternary units. Layer 4 is 40 ft thick and composed of Tertiary and Cretaceous units, except for the southeastern quadrant of the peninsula and few isolated cells in the northwestern part (fig. 26). Layer 5 is 50 ft thick and

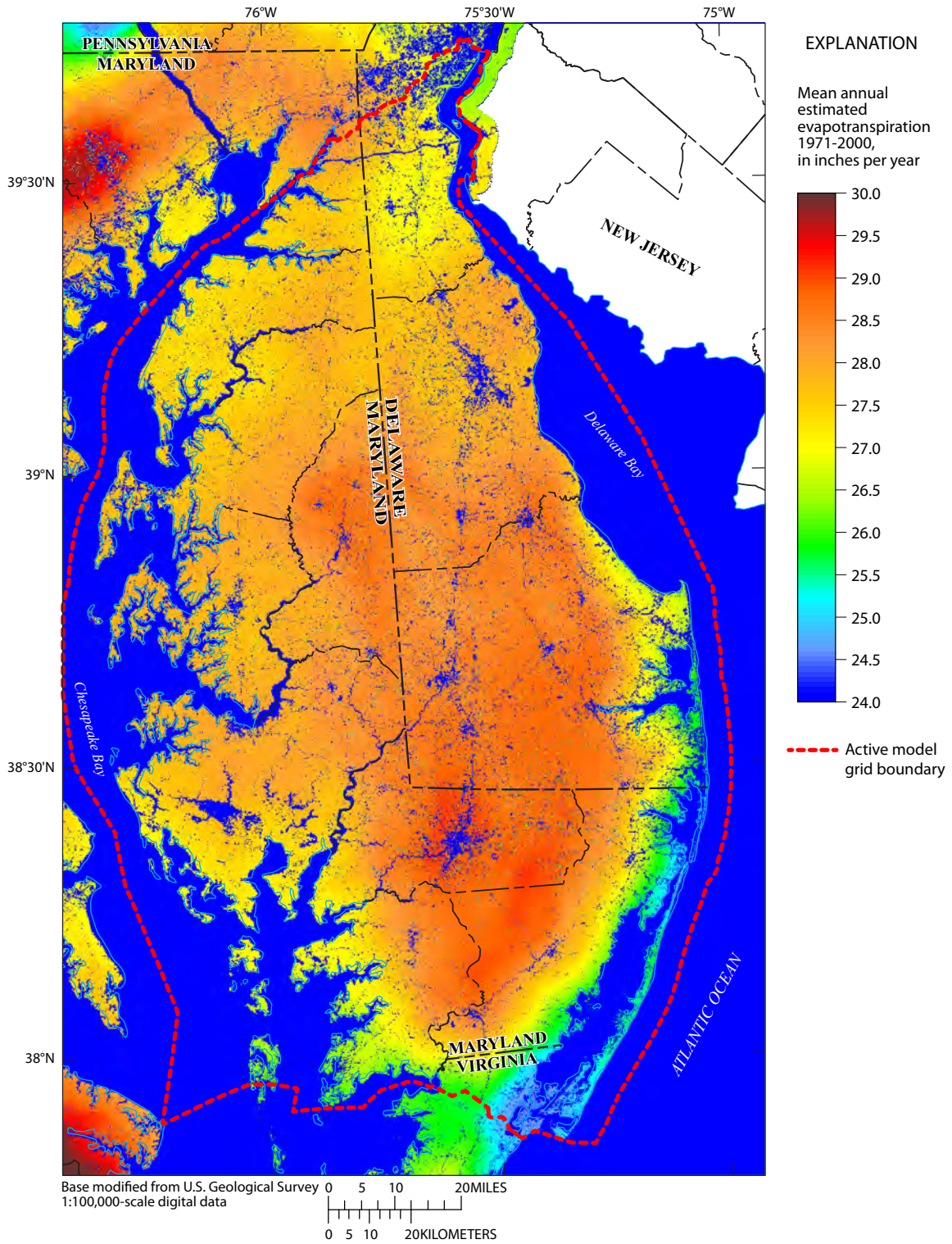


Figure 15. Mean annual estimated evapotranspiration on the Delmarva Peninsula from 1971 to 2000 based on the climate regression equation of Sanford and others (2012).

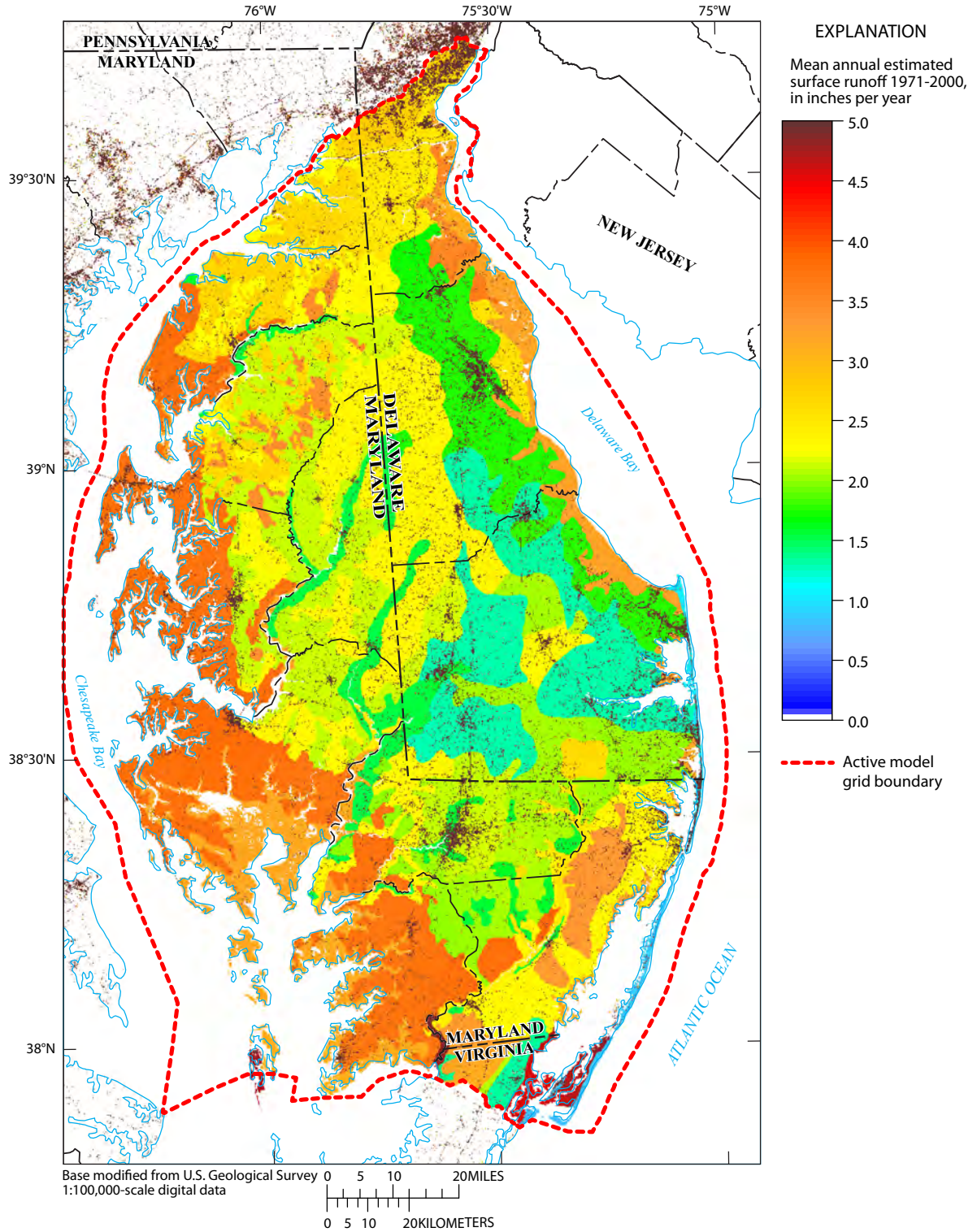


Figure 16. Mean-annual estimated surface runoff on the Delmarva Peninsula from 1971 to 2000 based on the regression equations of Sanford and others (2012) for the Coastal Plain physiographic province and the clay content of the soils. Regions outside the active model area only show runoff for impervious surfaces.

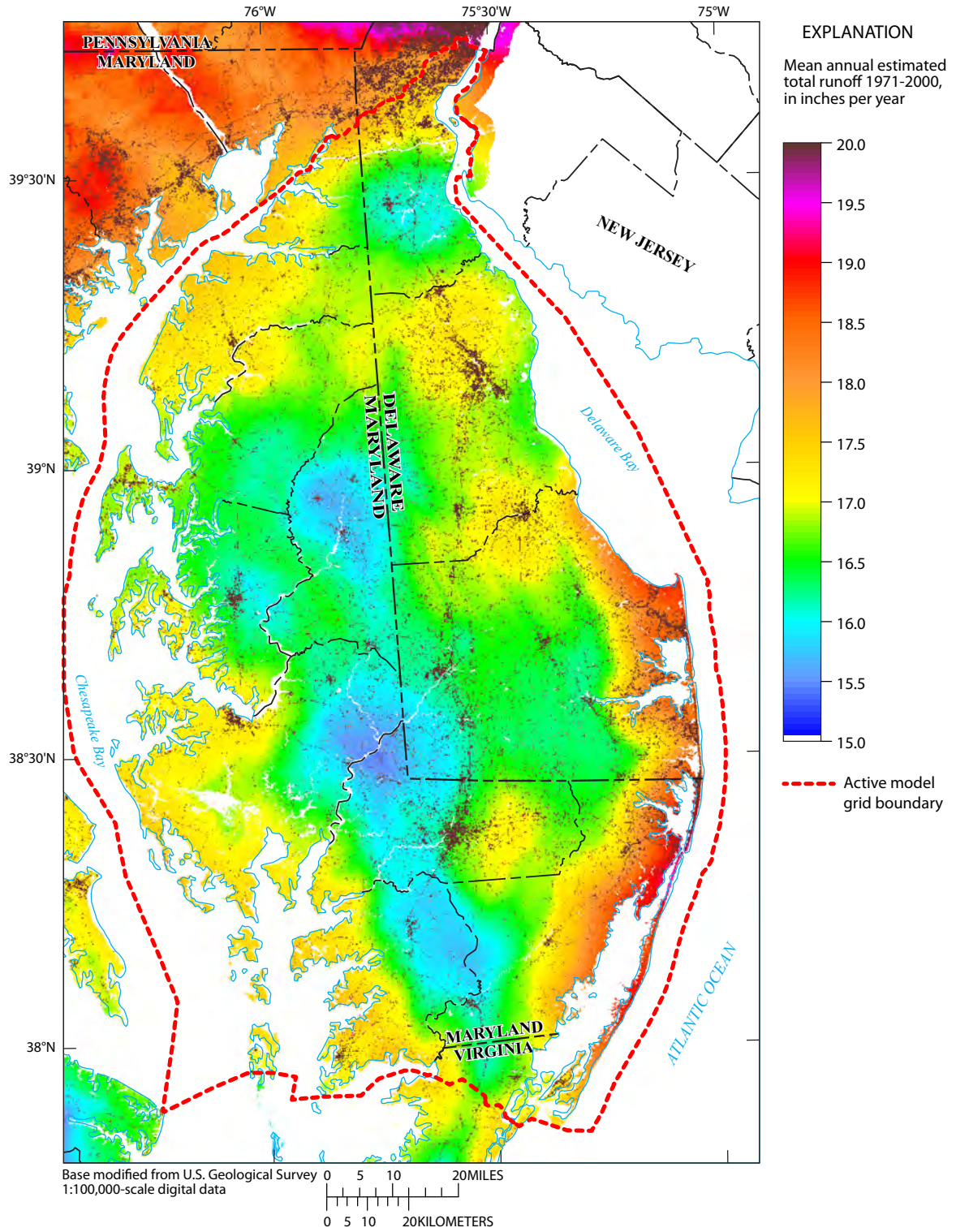


Figure 17. Mean annual estimated total runoff on the Delmarva Peninsula from 1971 to 2000 calculated by subtracting evapotranspiration (fig. 14) from precipitation (fig. 9).

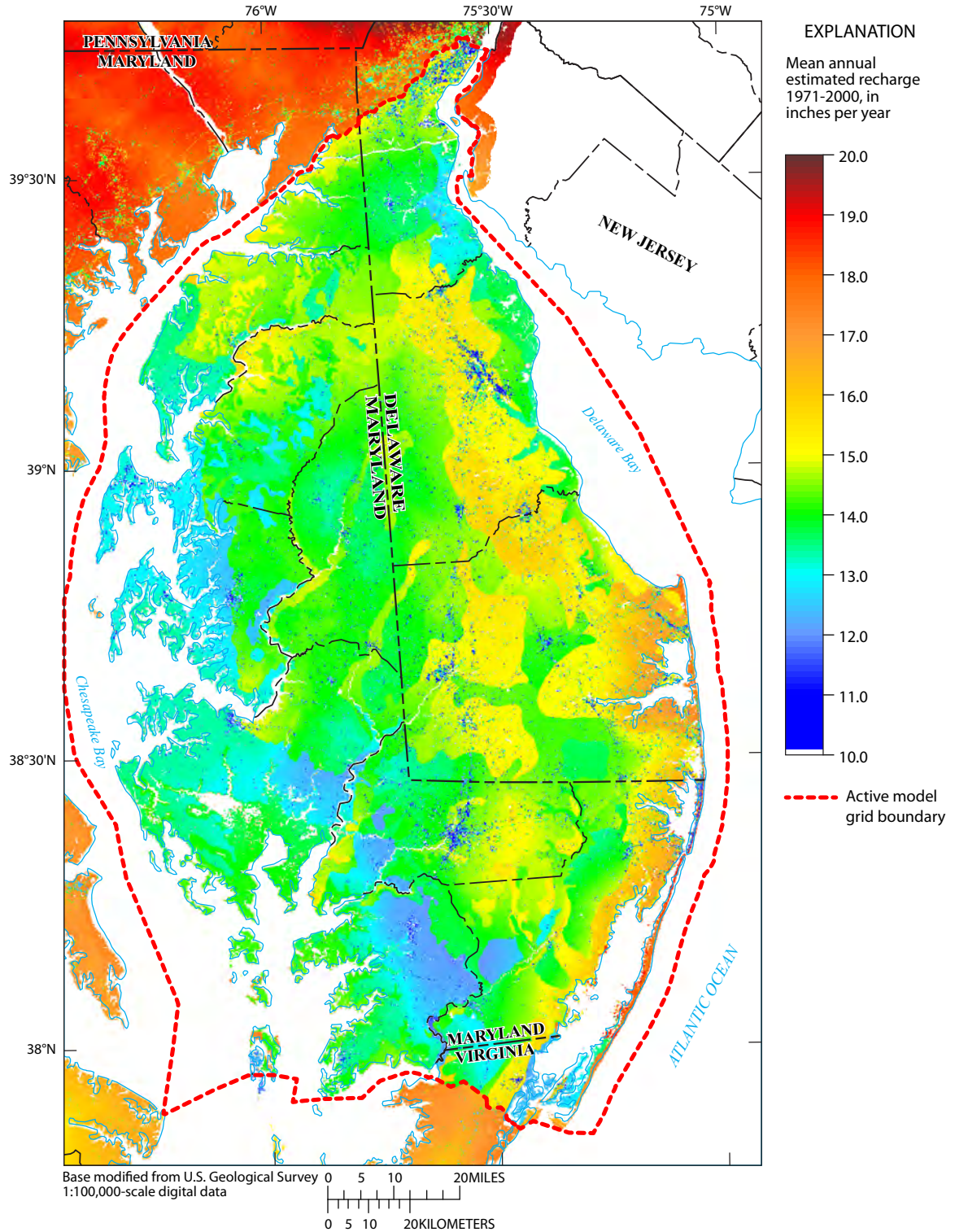


Figure 18. Mean annual estimated recharge on the Delmarva Peninsula from 1971 to 2000 based on the precipitation from the PRISM climate database and the climate and runoff regression equations of Sanford and others (2012). Values outside the active model area (fig. 3) represent total runoff rather than recharge.

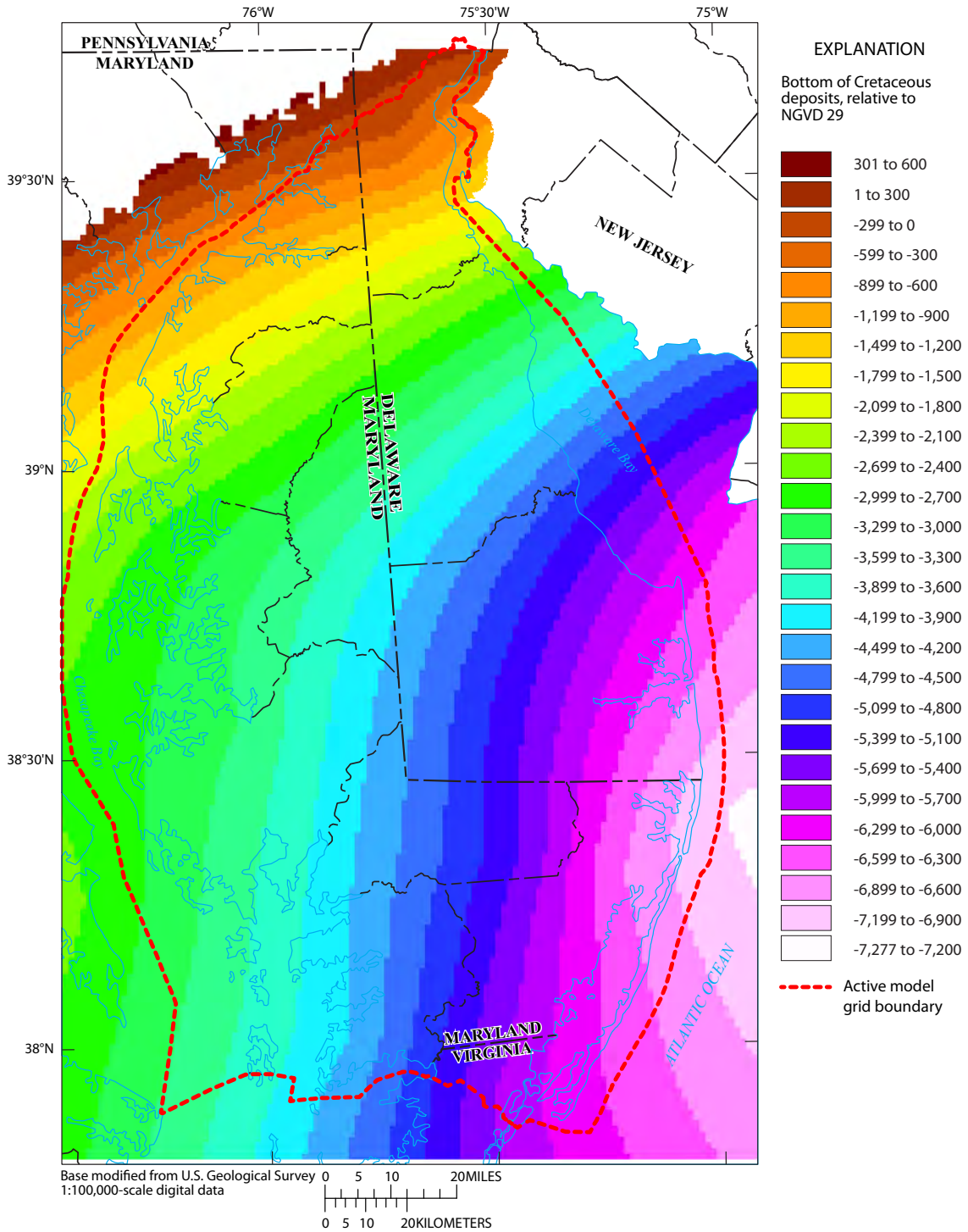


Figure 19. Bottom surface of the Cretaceous deposits on the Delmarva Peninsula relative to sea-level datum NGVD 29. Data surface from Andreasen and others (2007).

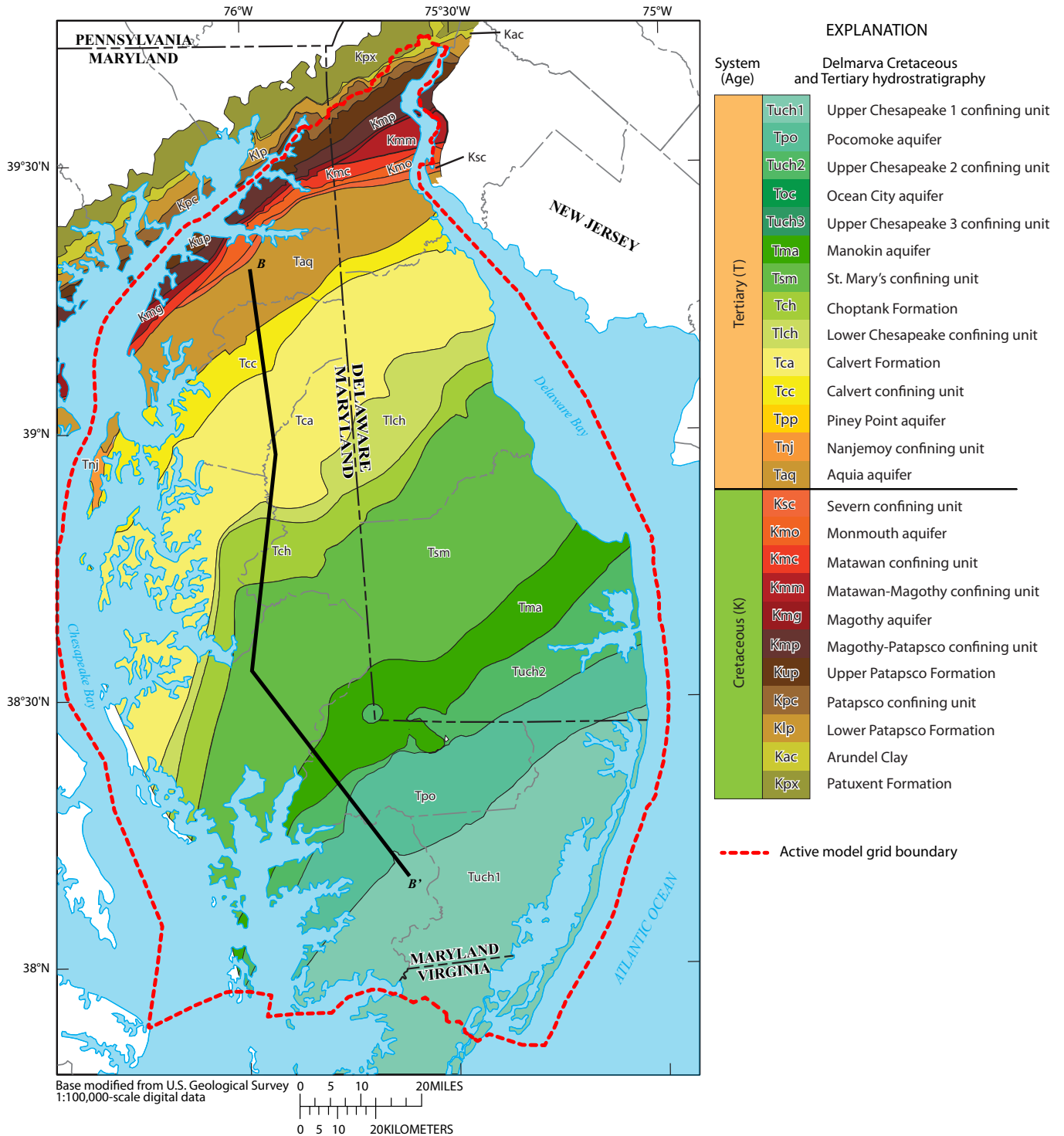


Figure 20. Locations where various Cretaceous (K) and Tertiary (T) deposits outcrop at the land surface or subcrop beneath Quaternary deposits on the Delmarva Peninsula. Section along line B-B' is shown in figure 21. Data files from Andreasen and others (2007).

composed almost entirely of Tertiary and Cretaceous units except for a few isolated patches of Quaternary units (fig. 27). Layers 6 and 7 are 60 and 90 ft thick, respectively, and composed entirely of Tertiary and Cretaceous units (figs. 28 and 29), except for one isolated cell in layer 6. In all of the layers, the Cretaceous units are represented only in the far northern and northeastern peninsula, because the remainder of the Cretaceous units dipping to the southeast exceed the 300-ft depth represented in the model. Various units also extend beneath the Chesapeake and Delaware Bays and the Atlantic Ocean within the active model area (not shown in figs. 23 to 29). Hydraulic conductivity values were assigned to each of the units, as described in the next section.

Model Calibration

The groundwater model was calibrated using water levels and tracer-based ages determined from a number of observation wells across the peninsula. The water-level observations

used to calibrate the model were selected from existing USGS wells and had to represent good spatial coverage and consist of at least 12 measurements made over several seasons (to eliminate seasonal variation) per well. The observations also had to represent natural conditions and not have been under the influence of pumping. The number of candidate wells was reduced to 48 using these criteria (table 1) and ranged in depth from 10 to 85 ft below land surface. The wells were chosen to be distributed as evenly as possible across the peninsula in order to represent different regions and formations during the calibration procedure (fig. 30). In Queen Anne’s County (fig. 2), the two northernmost wells (fig. 30) are located very close to the same site.

Base flows to streams are frequently used to calibrate models that represent humid regions, such as the Delmarva Peninsula, in order to constrain water fluxes to a degree that cannot be accomplished using water levels alone (Hill and Tiedeman, 2007). Base flow is considered here to be that portion of the total streamflow that originates as groundwater

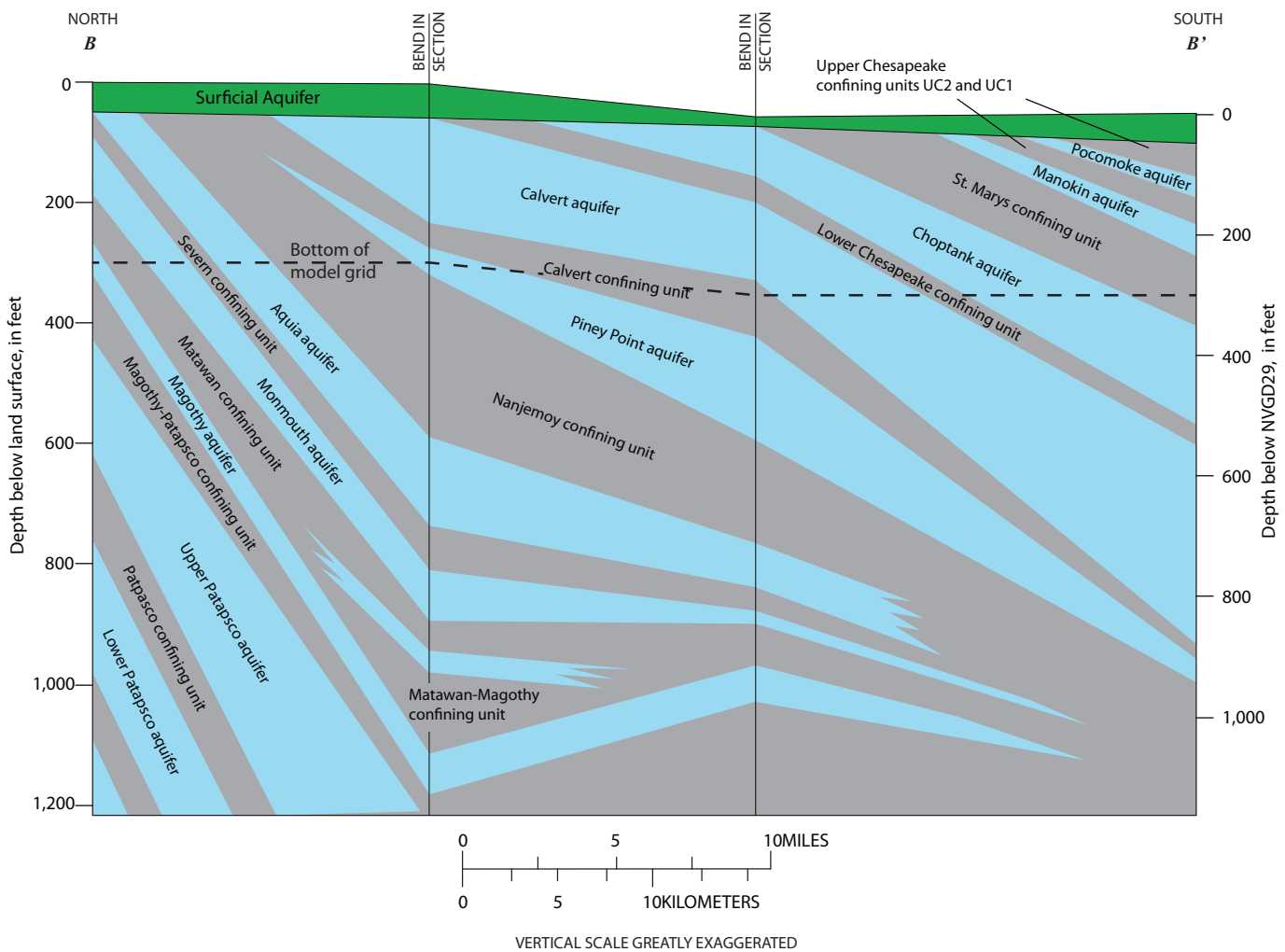


Figure 21. Cross-sectional view showing dipping of confined hydrogeologic units beneath the surficial aquifer along the line B–B’. See figure 20 for location of section line. Modified from Andreasen and others (2007).

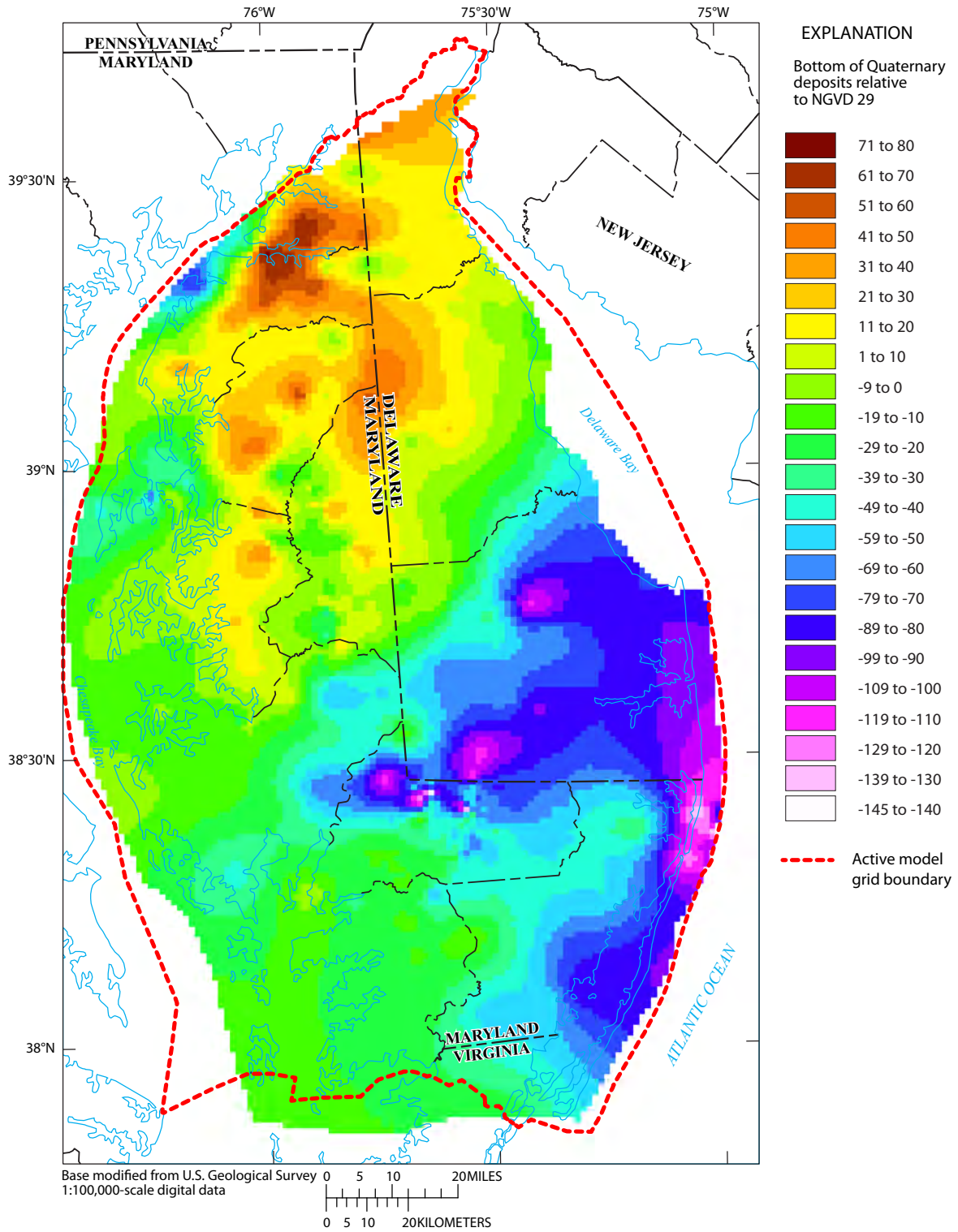


Figure 22. Bottom surface of the Quaternary deposits on the Delmarva Peninsula relative to sea-level datum NGVD 29. Data surface from Andreasen and others (2007).

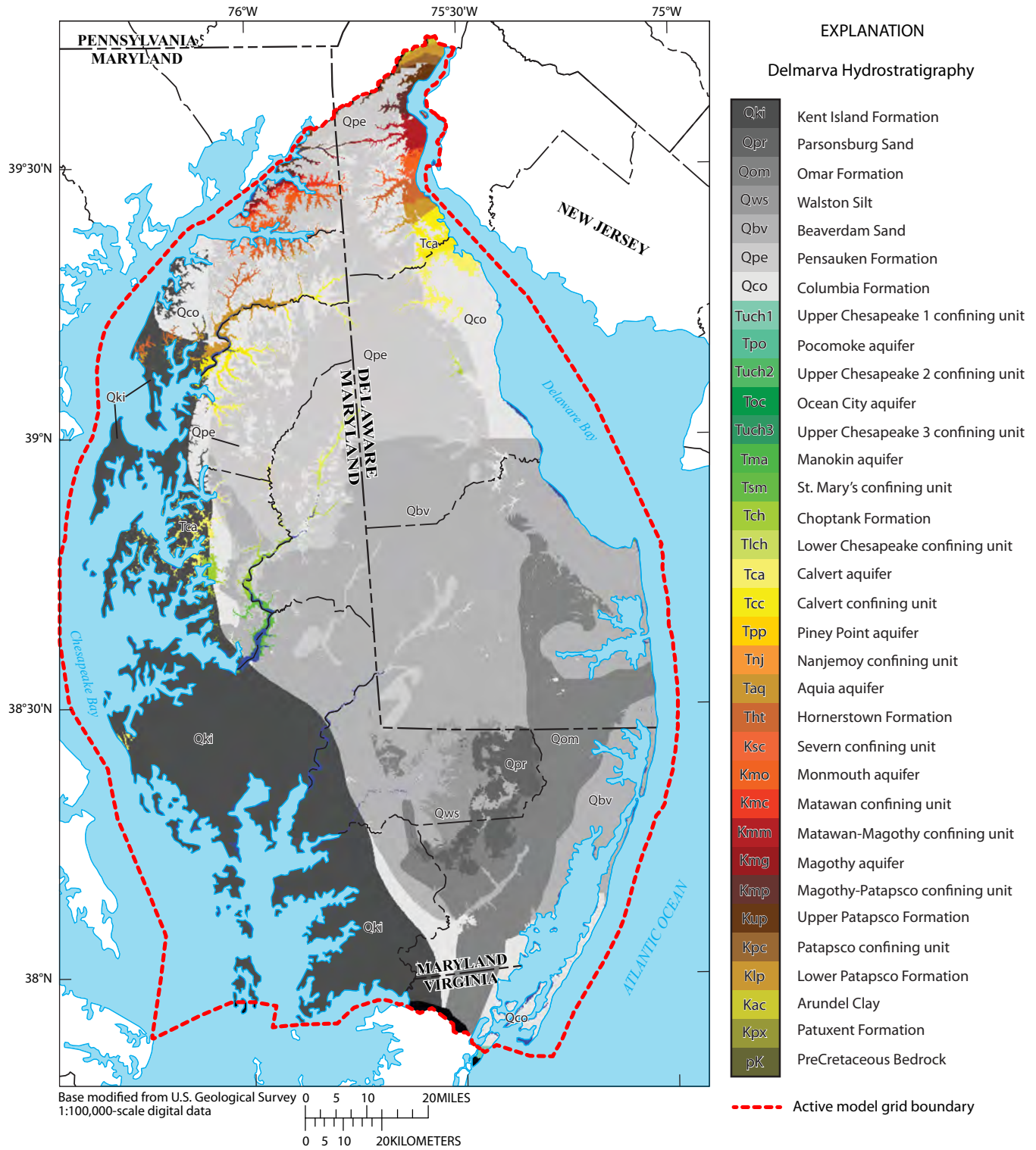


Figure 23. Distribution of geologic units within layer 1 of the model grid. The top of layer 1 is the land surface and the bottom is 10 feet below land surface. Formations also extend under the water bodies in the active model area (fig. 3).

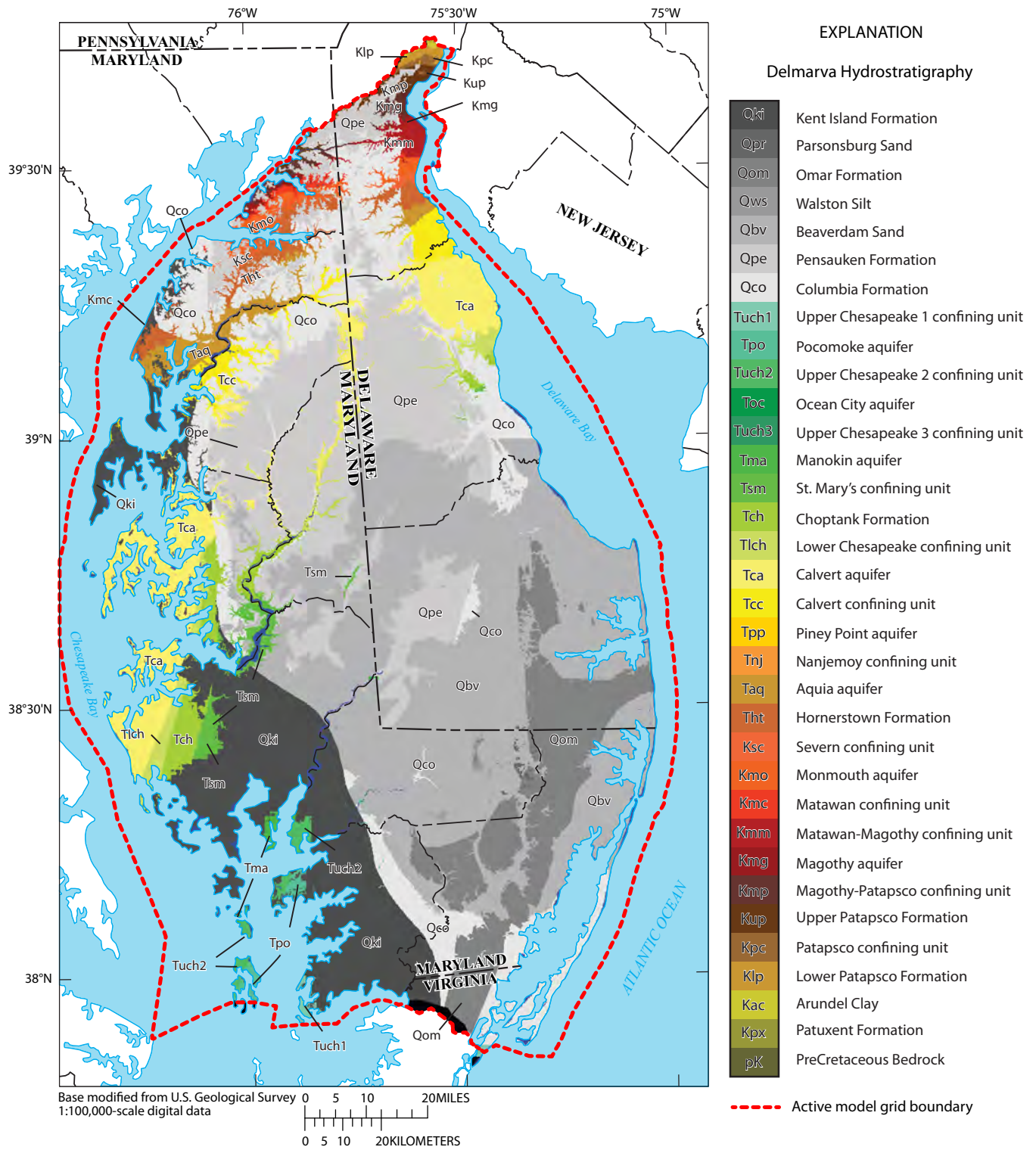


Figure 24. Distribution of geologic units within layer 2 of the model grid. The top and bottom of layer 2 are 10 and 30 ft below land surface. Formations also extend underneath the water bodies within the active model area (fig. 3).

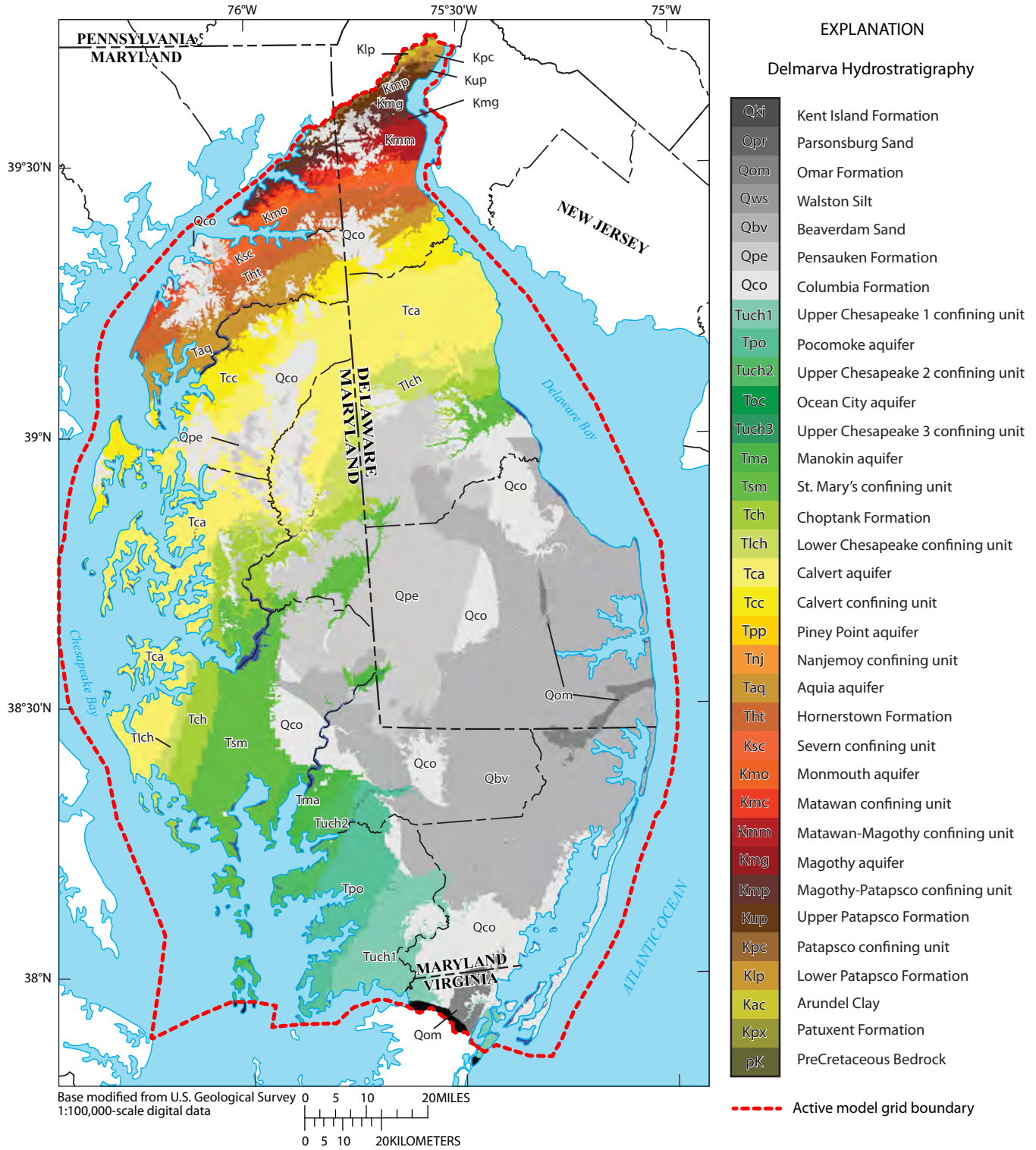


Figure 25. Distribution of geologic units within layer 3 of the model grid. The top and bottom of layer 3 are 30 and 60 feet below land surface. Formations also extend underneath the water bodies within the active model area (fig. 3).

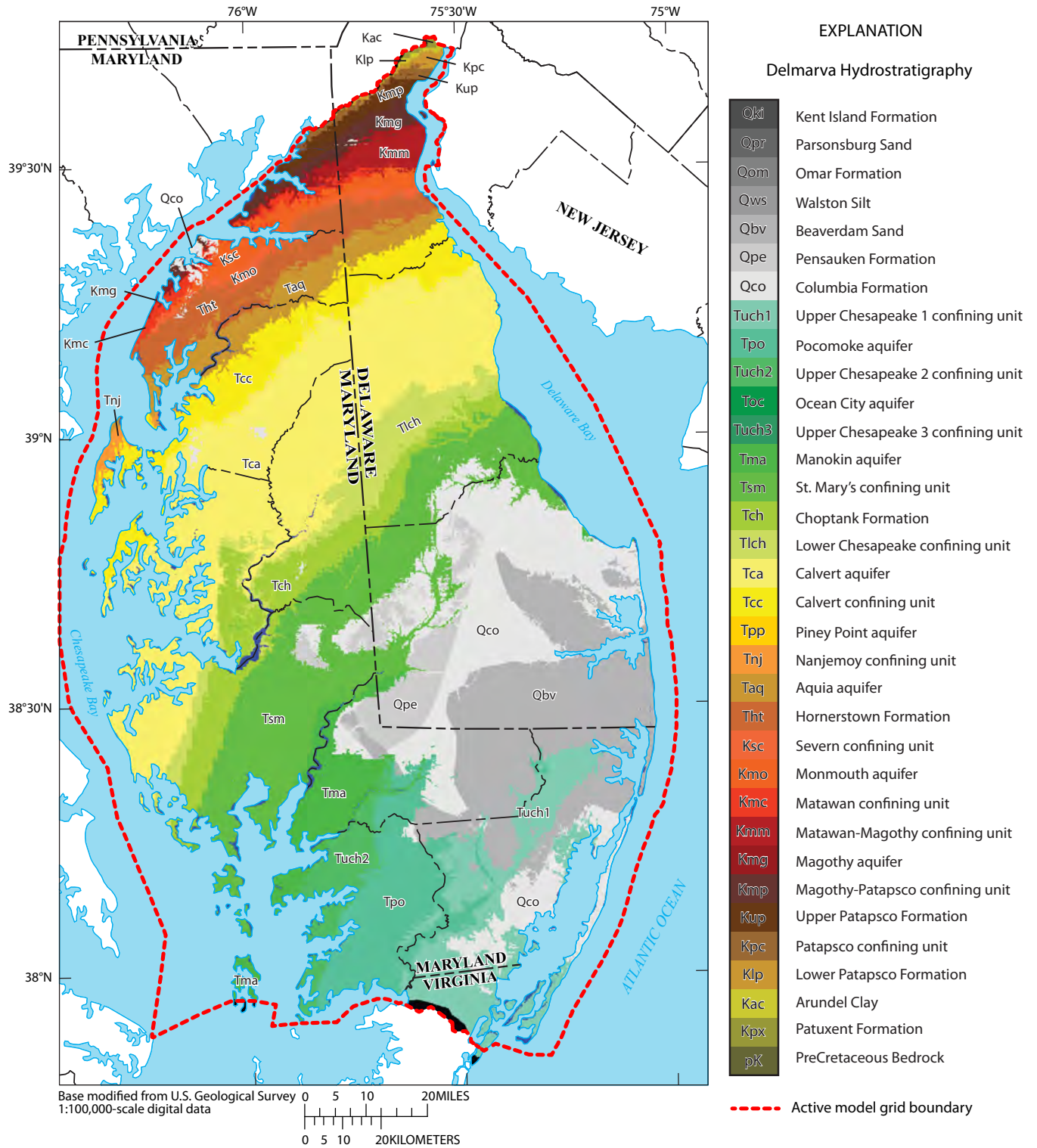


Figure 26. Distribution of geologic units within layer 4 of the model grid. The top and bottom of layer 4 are 60 and 100 feet below land surface. Formations also extend underneath the water bodies within the active model area (fig. 3).

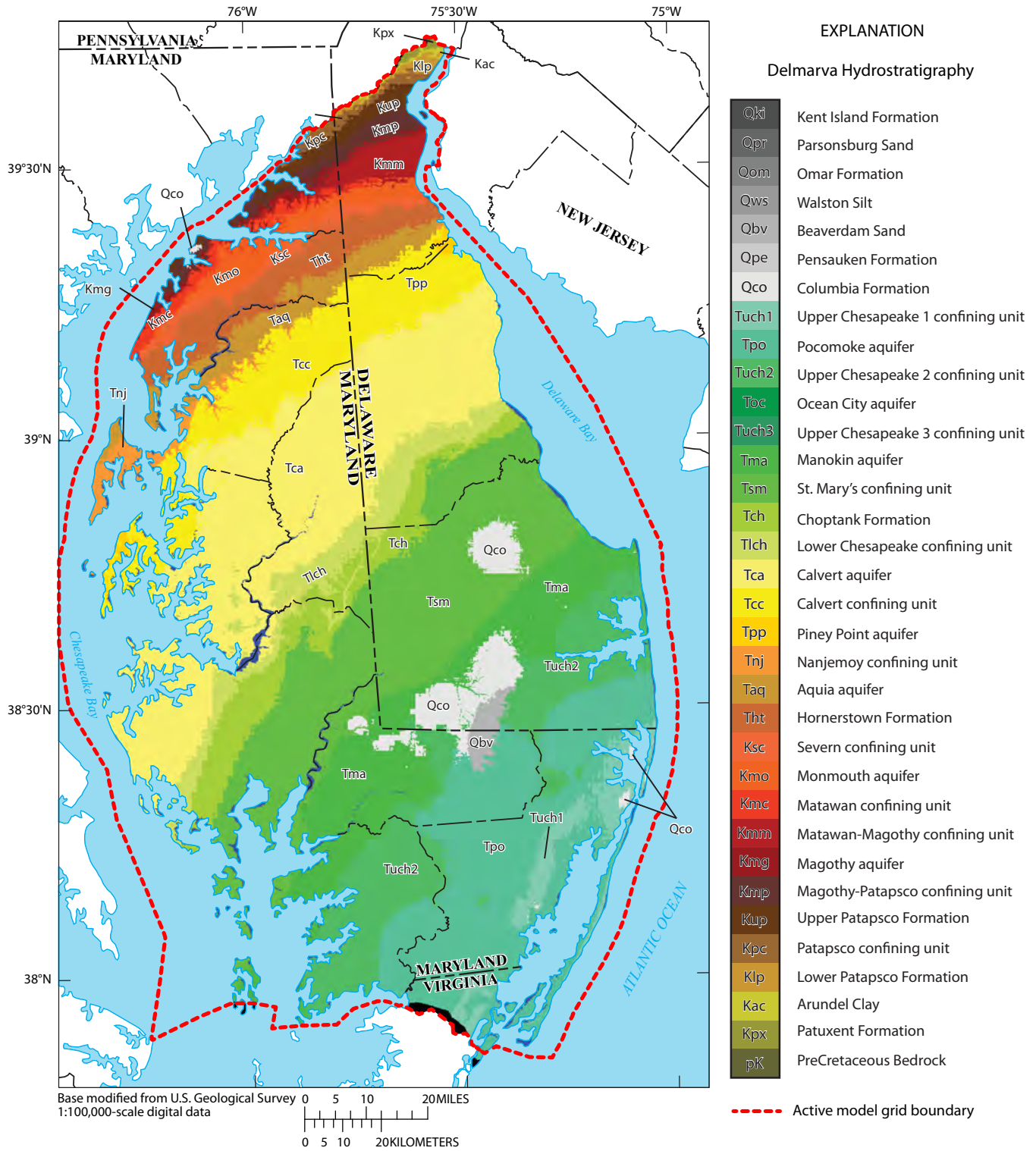


Figure 27. Distribution of geologic units within layer 5 of the model grid. The top and bottom of layer 5 are 100 and 150 feet below land surface. Formations also extend underneath the water bodies within the active model area (fig. 3).

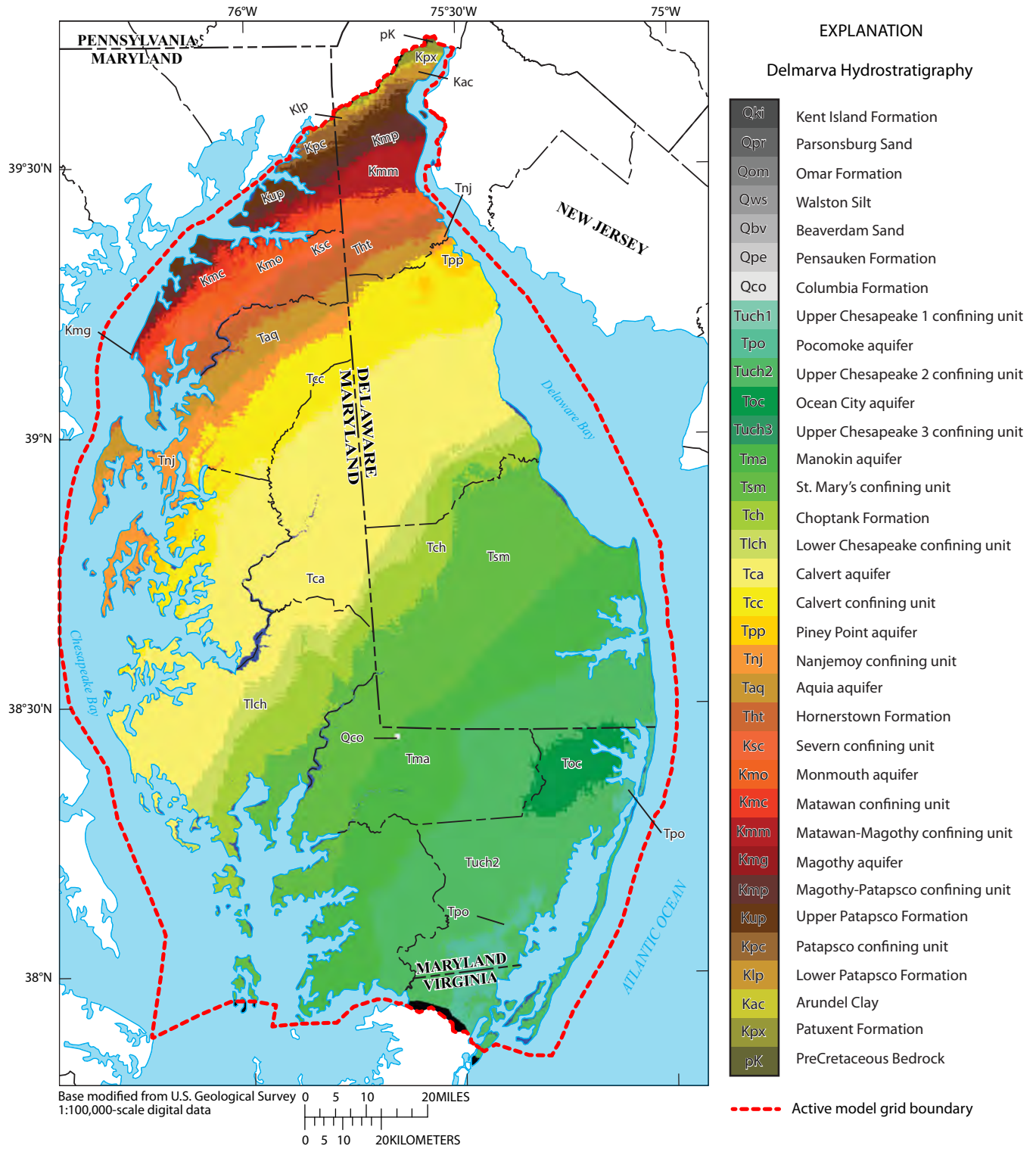


Figure 28. Distribution of geologic units within layer 6 of the model grid. The top and bottom of layer 6 are 150 and 210 feet below land surface. Formations also extend underneath the water bodies within the active model area (fig. 3).

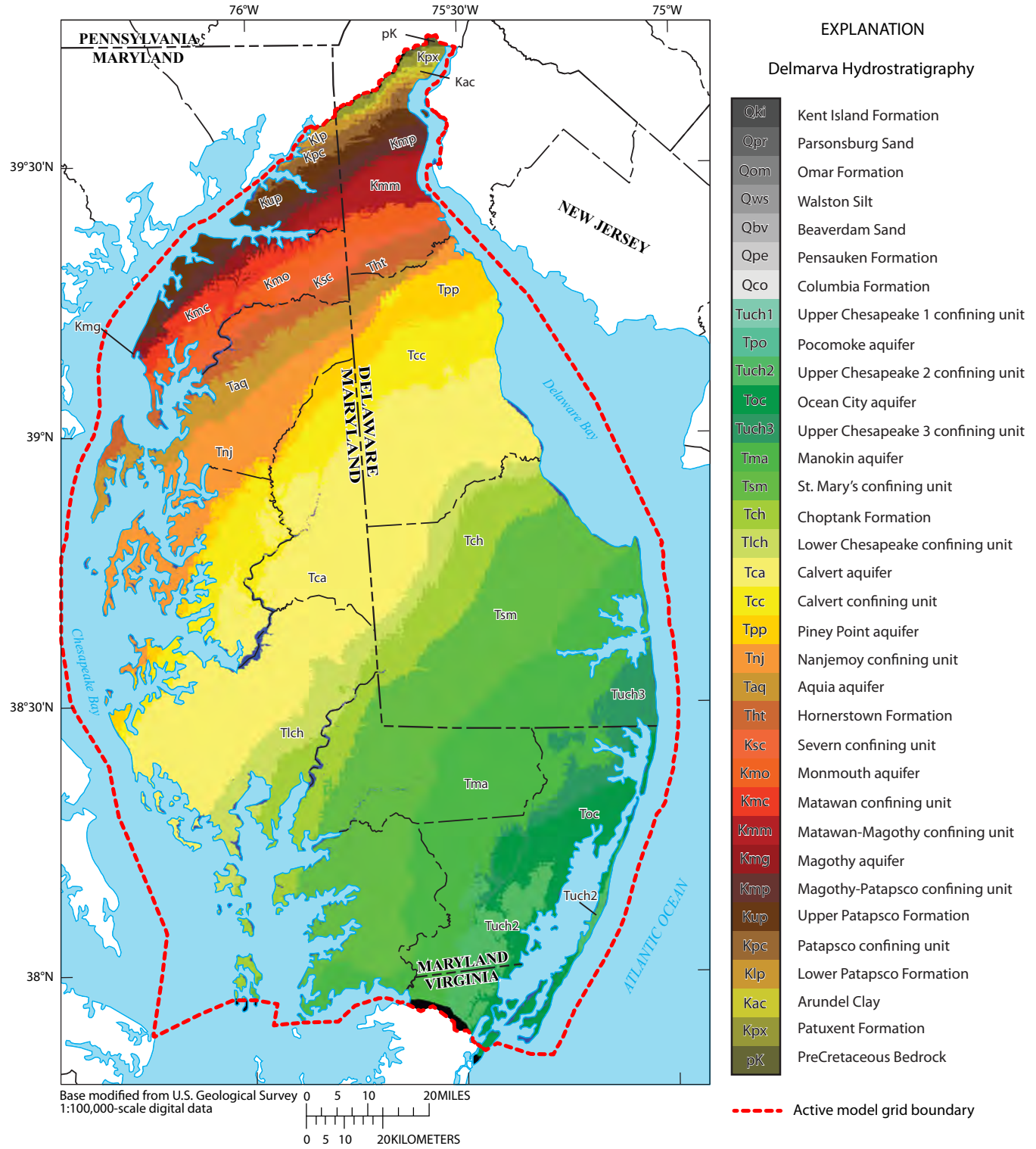


Figure 29. Distribution of geologic units within layer 7 of the model grid. The top and bottom of layer 7 are 210 and 300 feet below land surface. Formations also extend underneath the water bodies within the active model area (fig. 3).

Table 1. Observation wells and associated groundwater levels used to calibrate the groundwater model in this study.

[ID, identifier; no., number; Md, Maryland; Del., Delaware]

Well no.	Local well ID number	State	County	Latitude	Longitude	Grid row no.	Grid column no.	Well depth, in feet	Land surface elevation ^a	Grid layer no.	Depth to water	Water-level elevation ^a	Final simulated water level ^a	Error
1	CO Fd 4	Md.	Caroline	38°42'23"	75°47'13"	774	378	10.0	30.0	1	2.0	28.0	31.0	-3.0
2	CO Dc 145	Md.	Caroline	38°52'06"	75°52'06"	656	330	23.0	55.0	2	7.0	48.0	41.5	6.5
3	CO Dd 67	Md.	Caroline	38°52'13"	75°47'08"	654	377	11.0	42.0	1	4.0	38.0	39.2	-1.2
4	CO Dc 146	Md.	Caroline	38°53'02"	75°54'01"	645	311	20.0	45.0	2	6.0	39.0	41.5	-2.5
5	CO Bc 1	Md.	Caroline	39°03'33"	75°50'45"	517	341	20.5	54.0	2	2.0	52.0	53.8	-1.8
6	CE Ee 2	Md.	Cecil	39°23'38"	75°52'15"	273	324	21.5	70.0	2	8.0	62.0	60.4	1.6
7	DO Fd 1	Md.	Dorchester	38°19'03"	76°07'03"	1,059	192	17.0	3.0	2	1.0	2.0	1.7	0.3
8	DO Dh 27	Md.	Dorchester	38°29'16"	75°49'17"	933	360	63.0	9.1	4	10.0	-0.9	2.1	-3.1
9	DO Cg 46	Md.	Dorchester	38°32'18"	75°52'28"	897	329	17.0	18.0	2	3.0	15.0	12.0	3.0
10	KE Dc 89	Md.	Kent	39°06'26"	76°08'33"	484	172	29.0	4.5	2	3.5	1.0	1.9	-0.9
11	KE Cc 28	Md.	Kent	39°10'28"	76°08'53"	435	168	51.5	30.0	3	13.0	17.0	16.0	1.0
12	KE Cb 100	Md.	Kent	39°11'24"	76°10'10"	424	156	67.0	66.0	4	39.0	27.0	25.4	1.6
13	KE Cd 53	Md.	Kent	39°12'45"	76°03'48"	407	216	60.0	15.0	3	8.0	7.0	5.1	1.9
14	KE Cb 32	Md.	Kent	39°12'52"	76°13'57"	406	120	45.0	25.0	3	22.0	3.0	23.6	-20.6
15	KE Cd 44	Md.	Kent	39°14'32"	76°01'55"	385	234	84.0	50.0	4	30.0	20.0	12.6	7.4
16	KE Bd 39	Md.	Kent	39°16'45"	76°03'50"	358	215	38.5	75.0	3	15.0	60.0	58.5	1.5
17	KE Bc 185	Md.	Kent	39°16'50"	76°05'04"	357	204	55.0	82.0	3	12.0	70.0	69.5	0.5
18	KE Bd 188	Md.	Kent	39°16'54"	76°00'09"	356	250	39.0	50.0	3	18.0	32.0	37.1	-5.1
19	KE Be 162	Md.	Kent	39°17'42"	75°55'48"	346	291	67.0	61.0	4	10.0	51.0	54.4	-3.4
20	KE Bg 35	Md.	Kent	39°19'57"	75°49'06"	318	354	47.5	62.0	3	18.0	44.0	56.7	-12.7
21	KE Ag 15	Md.	Kent	39°20'06"	75°46'46"	316	376	13.0	70.0	2	2.0	68.0	68.1	-0.1
22	QA Ed 39	Md.	Queen Anne's	38°55'55"	76°07'54"	611	179	26.0	60.0	2	8.0	52.0	47.2	4.8
23	QA Ec 1	Md.	Queen Anne's	38°57'56"	76°10'53"	587	151	21.0	20.0	2	3.0	17.0	19.3	-2.3
24	QA Cg 69	Md.	Queen Anne's	39°08'39"	75°51'50"	455	330	69.0	65.0	4	5.0	60.0	64.5	-4.5
25	QA Cg 1	Md.	Queen Anne's	39°08'41"	75°51'52"	455	329	60.0	69.0	3	4.0	65.0	63.4	1.6

Table 1. Observation wells and associated groundwater levels used to calibrate the groundwater model in this study.—Continued

[ID, identifier; no., number; Md, Maryland; Del., Delaware]

Well no.	Local well ID number	State	County	Latitude	Longitude	Grid row no.	Grid column no.	Well depth, in feet	Land surface elevation ^a	Grid layer no.	Depth to water	Water-level elevation ^a	Final simulated water level ^a	Error
26	SO Cf 2	Md.	Somerset	38°06'16"	75°38'07"	1,211	471	15.0	20.0	2	2.0	18.0	18.3	-0.3
27	TA Be 44	Md.	Talbot	38°51'12"	76°03'39"	669	220	37.0	18.0	3	6.0	12.0	25.2	-13.2
28	TA Bf 74	Md.	Talbot	38°52'42"	75°59'31"	650	259	48.4	42.0	3	13.0	29.0	45.4	-16.4
29	TA Bf 54	Md.	Talbot	38°54'13"	75°58'53"	631	265	25.0	55.0	2	2.0	53.0	45.8	7.2
30	TA Be 85	Md.	Talbot	38°54'40"	76°02'44"	626	229	23.0	45.0	2	9.0	36.0	44.7	-8.7
31	WI Ce 13	Md.	Wicomico	38°21'50"	75°35'21"	1,021	494	65.0	7.0	4	4.0	3.0	5.4	-2.4
32	WI Ce 315	Md.	Wicomico	38°22'34"	75°39'26"	1,013	455	85.0	38.0	4	6.0	32.0	29.5	2.5
33	WI Cg 20	Md.	Wicomico	38°23'29"	75°26'37"	1,000	578	25.0	68.0	2	5.0	63.0	57.9	5.1
34	WI Cf 147	Md.	Wicomico	38°24'29"	75°34'45"	989	500	80.0	42.0	4	17.0	25.0	28.7	-3.7
35	WI Bh 4	Md.	Wicomico	38°25'43"	75°21'22"	972	627	12.0	40.0	1	5.0	35.0	34.4	0.6
36	WO Dd 9	Md.	Worcester	38°11'16"	75°22'41"	1,148	618	20.0	15.0	2	11.0	4.0	5.1	-1.1
37	Jd 42-3	Del.	Kent	39°06'07"	75°33'15"	483	506	11.0	44.0	1	6.0	38.0	40.9	-2.9
38	Hb 14-1	Del.	New Castle	39°19'11"	75°34'52"	325	488	18.6	70.0	2	6.0	64.0	66.7	-2.7
39	Md 24-1	Del.	New Castle	38°53'32"	75°31'54"	636	521	45.0	55.0	3	5.0	50.0	51.4	-1.4
40	Md 22-1	Del.	New Castle	38°53'10"	75°33'13"	641	509	17.0	58.0	2	5.0	53.0	56.5	-3.5
41	Mc 51-1	Del.	Sussex	38°50'41"	75°39'56"	672	445	18.0	55.0	2	10.0	45.0	44.1	0.9
42	Ng 11-1	Del.	Sussex	38°49'55"	75°19'28"	678	640	19.0	24.0	2	12.0	12.0	14.7	-2.7
43	Pf 24-2	Del.	Sussex	38°37'30"	75°21'35"	829	623	49.0	50.0	3	10.0	40.0	34.6	5.4
44	Of 23-5	Del.	Sussex	38°43'41"	75°22'38"	754	611	18.0	50.0	2	8.0	42.0	45.0	-3.0
45	Nf 51-3	Del.	Sussex	38°45'04"	75°24'26"	738	594	18.0	45.0	2	3.0	42.0	43.8	-1.8
46	Qe 44-1	Del.	Sussex	38°31'38"	75°26'20"	901	581	25.0	50.0	2	8.0	42.0	42.9	-0.9
47	Ne 54-3	Del.	Sussex	38°45'51"	75°26'48"	728	571	81.5	50.0	4	7.0	43.0	38.7	4.3
48	Nc 45-1	Del.	Sussex	38°46'39"	75°35'31"	720	488	15.5	43.0	2	9.0	34.0	33.6	0.4

^aElevations are in feet relative to NGVD 29.

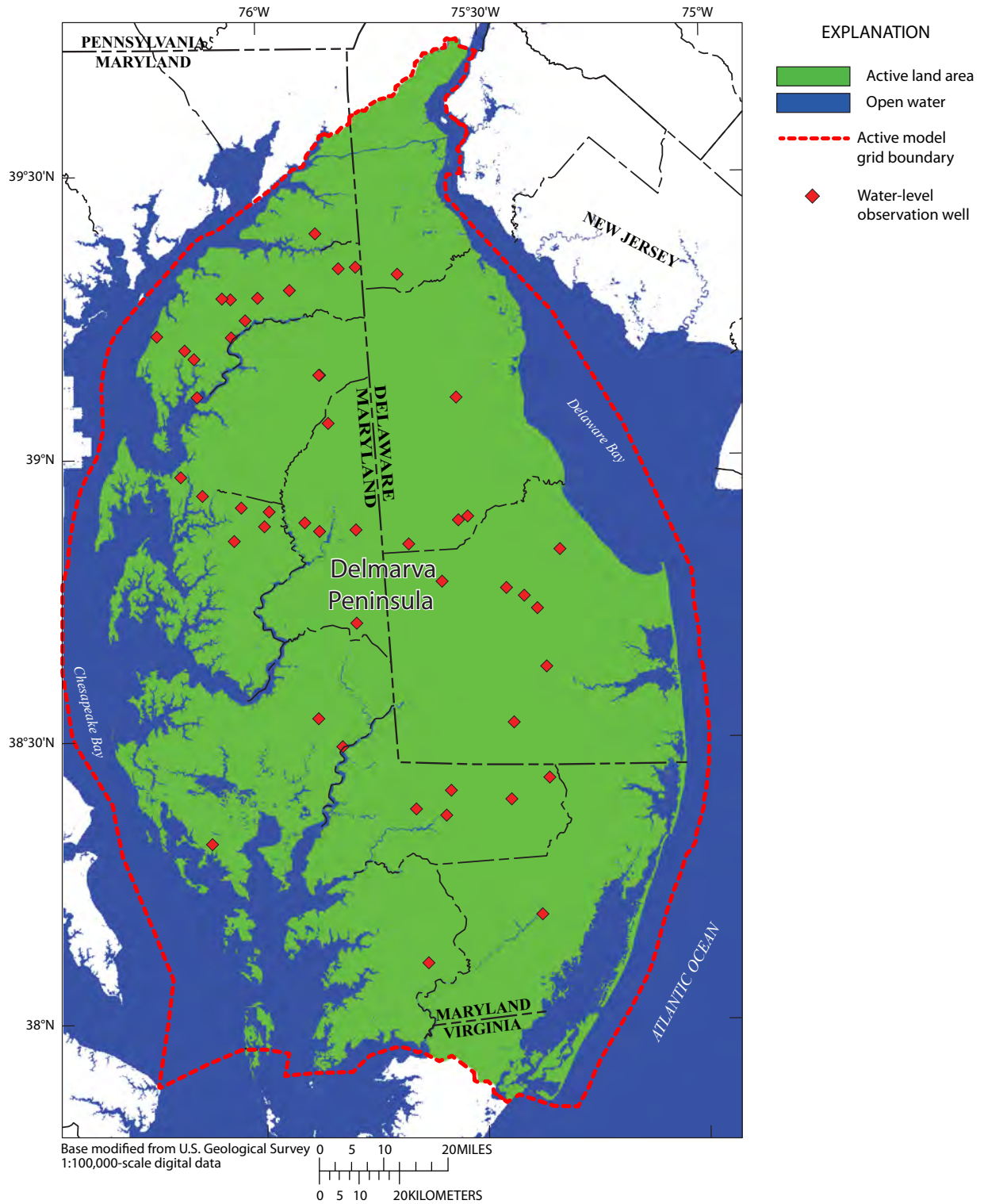


Figure 30. Locations of the 48 wells used for water-level observations.

Table 2. Watersheds used to compare observed and simulated total runoff from the land surface.[ft³/s, cubic foot per second]

Watershed no.	Watershed name	USGS station number	Drainage outlet	Area, in square miles	Mean flow 1971–2000, in ft ³ /s	Observed total runoff, in inches	Simulated total runoff, in inches	Error, in percent
1	Morgan Creek	01493500	Chesapeake Bay	12.7	12.4	13.3	17.1	25.3
2	Unicorn Branch	01493000	Chesapeake Bay	19.7	27.5	19.0	16.8	12.1
3	St. Jones River	01483700	Delaware Bay	31.9	40.1	17.1	17.1	0.1
4	Choptank River	01491000	Chesapeake Bay	113.0	143.7	17.3	16.5	4.6
5	Marshyhope Creek	01488500	Chesapeake Bay	46.8	59.0	17.1	16.6	3.1
6	Nanticoke River	01487000	Chesapeake Bay	75.4	92.7	16.7	16.8	0.6
7	Pocomoke River	01485000	Chesapeake Bay	60.5	77.6	17.4	16.9	3.0
8	Nassawango River	01485500	Chesapeake Bay	44.9	57.2	17.3	17.0	1.8

discharge, and in the mid-Atlantic Coastal Plain, that fraction is typically at least 70 to 90 percent (Sanford and others, 2012). In this study, recharge could be estimated with enough certainty that the fluxes were already considered to be adequately constrained, and therefore, base flows were not included in the calibration procedure. In addition, the procedure used to estimate the recharge was based on the base-flow calculations obtained from the Coastal Plain of Maryland (Sanford and others, 2012). To ensure that the base flows were represented adequately by the assigned recharge rates, however, total runoff was estimated from eight watersheds across the peninsula (table 2). These watersheds were a subset of 12 watersheds on the peninsula that have real-time water data collected at stream gages (fig. 31). The remaining four watersheds did not have an adequate period of flow data with which to make a comparison to simulated flow. The simulated total runoff was calculated from the model output by adding the base flow calculated from the drain discharges within the watershed to the estimated surface runoff for the watershed (fig. 16). The simulated and measured total runoff were within 5 percent of each other for six of the watersheds; values differed by 12 and 25 percent in two watersheds the northeastern peninsula (table 2).

Groundwater ages based on environmental tracer concentrations are frequently used to calibrate either fluxes (such as recharge rates), effective porosity, or both (Sanford, 2011). In this study, recharge was specified and not calibrated, but groundwater age proved to be useful for validating the recharge rates and calibrating effective porosity. Several dozen ages had previously been calculated for groundwater in shallow wells across the peninsula (Dunkle and others, 1993). A subset of 24 of these wells (table 3) was used to calibrate effective porosity. Groundwater age ranged from 2 to 44 years in wells whose screens were between 11 and 65 ft below land surface. Although several dozen ages were measured on the peninsula by Dunkle and others (1993), many of these were concentrated in a few local clusters; therefore,

a subset of 24 age measurements was chosen to obtain the best spatial coverage possible. The areal distribution of these measurements across the peninsula (fig. 32) reflects three of the east-west cross sections used in the original study. Two of the measurements are located at the same site but at different depths (table 3).

Representing the numerous geologic units in the model grid required 35 different hydraulic conductivity values to be assigned during the calibration procedure (table 4). The model was originally run using the USGS parameter-estimation code UCODE (Poeter and others, 2005) in order to complete a rough sensitivity analysis. From this analysis, it was determined that only some of the hydraulic conductivity parameters affected simulated water levels strongly enough to allow for their parameters to be estimated. As a result, the remaining hydraulic conductivity values were specified based on best estimates from field data (table 4), and the values for the seven most prevalent and influential unit were calibrated by a combination of UCODE inverse estimation and trial and error. The final values of the calibrated parameters are listed in table 4. The calibrated values were for the Kent Island Formation, the Omar Formation, the Beaverdam Sand, the Pensauken Formation, the Columbia Formation, the Aquia aquifer, and the Hornerstown Formation. All confining units were assigned a specified hydraulic conductivity value of 0.001. Although actual values for these units may be smaller locally in the field, the value was sufficiently low for the purpose of estimating age distributions to the streams. Use of a smaller value created severe solver convergence problems, and the tiny fraction of very old water created using smaller values does not impact forecasting trends in nitrate fluxes to the streams because all groundwater more than several decades old is relatively nitrate free. The composite-scaled sensitivity (CSS) for each hydraulic conductivity parameter is listed in table 5. Parameters with large CSS values either had corresponding geologic units that were areally extensive or contained numerous observation wells completed within them.

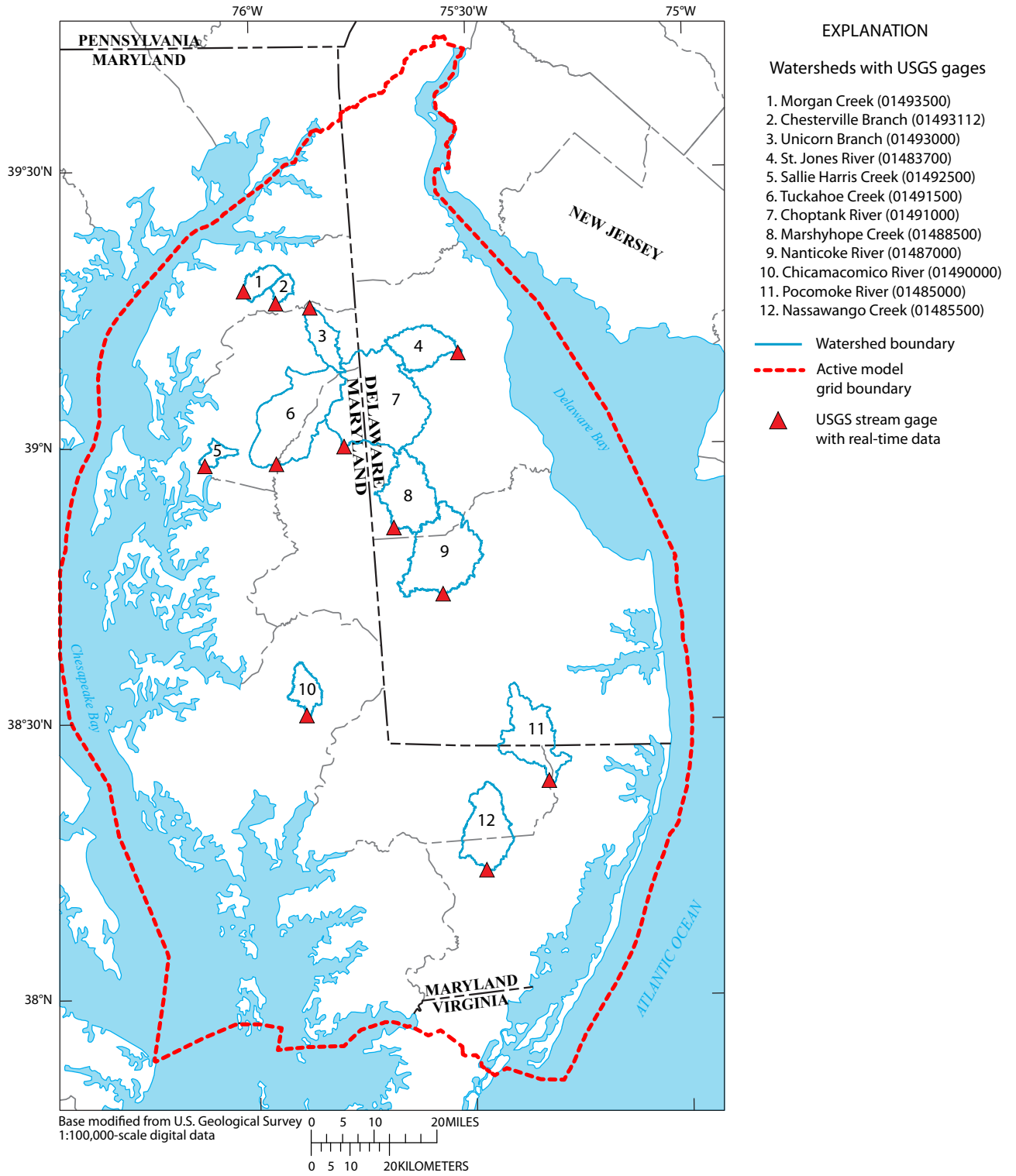


Figure 31. Locations of U.S. Geological Survey stream gages and watersheds on the Delmarva Peninsula with real-time water data.

Table 3. Observation wells and associated groundwater ages used for comparison with simulated groundwater ages in this study.

[Md., Maryland; Del., Delaware; ID, identifier]

Well no.	Local well ID number	State	County	Latitude	Longitude	Grid row no.	Grid column no.	Well depth, in feet	Land surface elevation ^a	Grid layer no.	Tracer-based age ^b , in years	Simulated age, in years	Error
1	KE Cc 28	Md.	Kent	39°10'28"	76°08'53"	435	168	50	30	3	30.5	23.9	6.6
2	KE Bd 39	Md.	Kent	39°16'45"	76°03'50"	358	215	37	75	2	32.6	18.8	13.8
3	Hd 15–7	Del.	New Castle	39°19'38"	75°40'14"	320	438	19	68	2	18.2	17.2	1.0
4	Hd 14–1	Del.	New Castle	39°18'04"	75°30'51"	338	526	27	15	2	21.0	40.3	-19.3
5	KE Bg 35	Md.	Kent	39°19'57"	75°49'06"	318	354	50	62	3	8.0	18.5	-10.5
6	KE Bg 65	Md.	Kent	39°16'08"	75°59'43"	365	254	20	49	2	4.0	7.0	-3.0
7	KE Be 62	Md.	Kent	39°17'42"	75°55'48"	346	291	24	61	2	5.0	8.3	-3.3
8	KE Be 162	Md.	Kent	39°17'42"	75°55'48"	346	291	65	61	3	36.0	28.8	7.2
9	KE Be 158	Md.	Kent	39°18'14"	75°57'55"	340	271	32	67	2	7.0	10.8	-3.8
10	GB 41–22	Del.	New Castle	39°21'20"	75°44'19"	300	399	23	80	2	6.0	6.8	-0.8
11	QA Fd 2	Md.	Queen Anne's	38°54'56"	76°09'03"	624	169	37	15	2	43.0	13.2	29.8
12	QA Ed 39	Md.	Queen Anne's	38°55'55"	76°07'54"	611	179	24	60	2	11.0	7.0	4.0
13	TA Be 85	Md.	Talbot	38°54'40"	76°02'44"	626	229	21	45	2	9.0	7.2	1.8
14	CO Dc 146	Md.	Caroline	38°53'02"	75°54'01"	645	311	19	45	2	5.0	5.8	-0.8
15	Nd 41–4	Del.	Sussex	38°46'30"	75°34'51"	722	495	19	45	2	2.0	5.6	-3.6
16	Og 43–2	Del.	Sussex	38°41'18"	75°17'31"	782	660	19	44	2	5.0	12.3	-7.3
17	Nb 24–3	Del.	Sussex	38°48'37"	75°41'52"	697	427	12	38	1	15.0	4.5	10.5
18	DO Ce 89	Md.	Dorchester	38°31'23"	76°03'13"	909	227	16	12	2	44.0	18.2	25.8
19	DO Cg 45	Md.	Dorchester	38°32'18"	75°52'28"	897	329	48	18	3	33.0	788.2	-755.2
20	WI Be 52	Md.	Wicomico	38°26'44"	75°36'12"	962	485	47	47	3	11.0	22.1	-11.1
21	WI Bg 18	Md.	Wicomico	38°25'08"	75°27'08"	980	572	13	65	1	15.0	4.6	10.4
22	WO Bf 86	Md.	Worcester	38°23'32"	75°14'18"	997	695	48	33	3	14.0	41.5	-27.5
23	WI Bh 4	Md.	Wicomico	38°25'43"	75°21'22"	972	627	11	40	1	10.0	3.3	6.7
24	WI Ch 56	Md.	Wicomico	38°24'52"	75°20'29"	982	636	16	41	1	8.0	8.0	0.0

^aElevations are in feet above NGVD 29.^bData from Dunkle and others (1993).

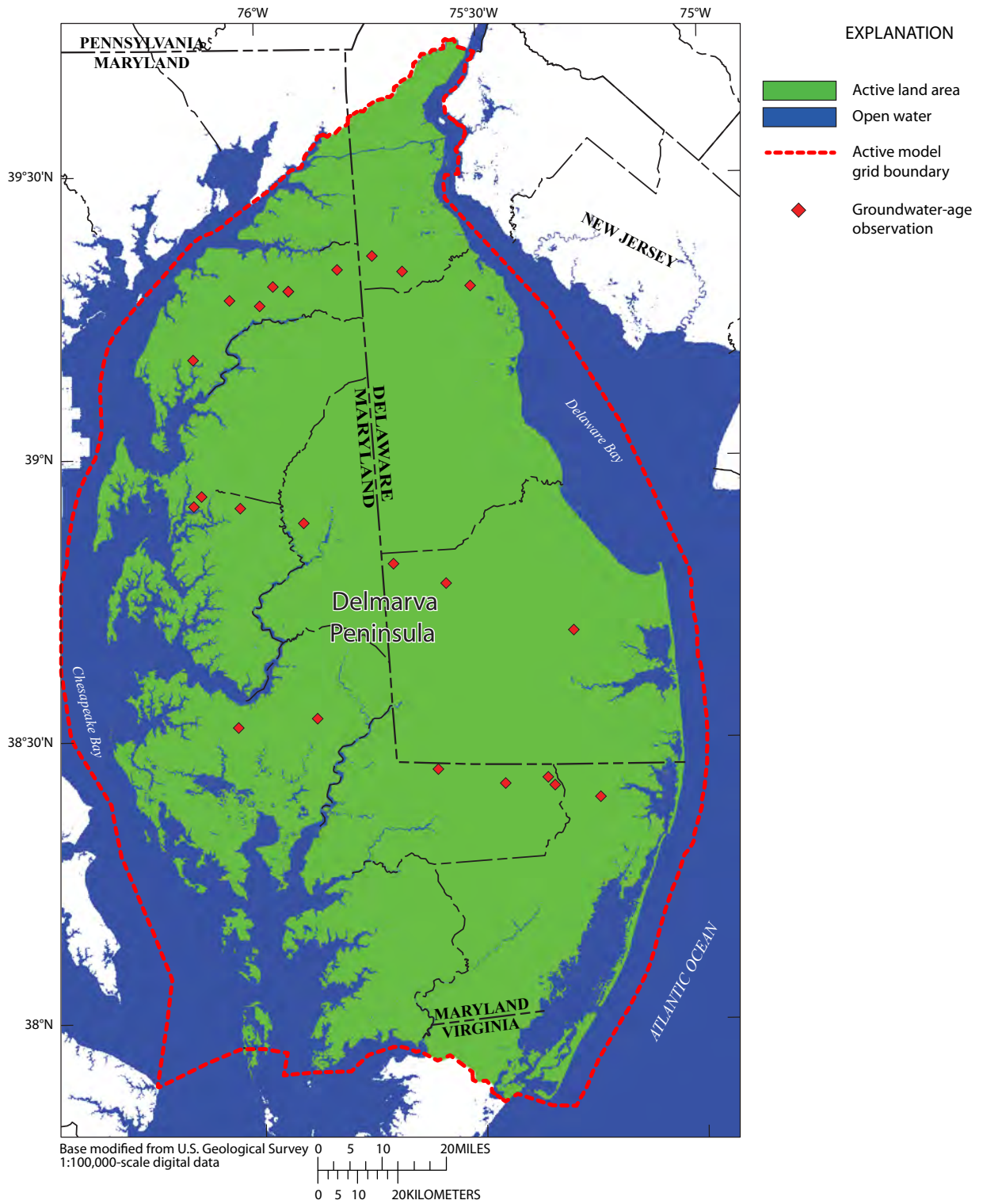


Figure 32. Locations of the 23 well sites where samples were collected for groundwater-age observations.

Table 4. Hydraulic conductivity values reported and specified or calibrated in the groundwater model in this study.[ft²/d, foot squared per day; nd, no data acquired or reported]

Unit number	Stratigraphic or hydrogeologic unit name	Map symbol used in this report	Mean reported value of transmissivity, in ft ² /d ^a	Number of values reported	Mean thickness, in feet	Average hydraulic conductivity, in feet per day	Value of hydraulic conductivity used in model, in feet per day ^b
1	Kent Island Formation	Qki	nd	nd	nd	nd	<i>1</i>
2	Parsonsborg sand	Qpr	nd	nd	20	nd	50
3	Omar Formation	Qom	nd	nd	50	nd	<i>1</i>
4	Walston silt	Qws	nd	nd	20	nd	1
5	Beaverdam sand	Qbv	nd	nd	75	nd	75
6	Pensauken Formation	Qpe	8,500	26	50	170	100
7	Columbia Formation	Qco	nd	nd	50	nd	10
8	Upper Chesapeake Confining Unit UC1	Tuch1	nd	nd	90	nd	0.001
9	Pocomoke aquifer	Tpo	7,100	1	50	36	25
10	Upper Chesapeake Confining Unit UC2	Tuch2	0	1	70	0.002	0.001
11	Ocean City aquifer	Toc	5,300	1	40	133	25
12	Upper Chesapeake Confining Unit UC3	Tuch3	nd	nd	30	nd	0.001
13	Manokin aquifer	Tma	570	7	110	20	25
14	St. Mary's confining unit	Tsm	nd	nd	150	nd	0.001
15	Choptank aquifer	Tch	nd	nd	100	nd	1
16	Lower Chesapeake confining unit	Tlch	nd	nd	60	nd	0.001
17	Calvert aquifer system	Tca	1,656	11	240	7	1
18	Calvert confining unit	Tec	1	18	90	0.008	0.001
19	Piney Point aquifer	Tpp	3,700	17	100	37	50
20	Nanjemoy confining unit	Tnj	40	4	30	1.3	0.001
21	Aquia aquifer	Taq	2,340	32	100	23	50
22	Hornerstown Formation	Tht	nd	nd	100	nd	8
23	Severn confining unit	Ksc	nd	nd	40	nd	0.001
24	Monmouth aquifer	Kmo	570	1	80	7	10
25	Matawan confining unit	Kmc	0	6	60	0.001	0.001
26	Matawan aquifer	Kma	nd	nd	nd	nd	20
27	Matawan-Magothy confining unit	Kmm	0	1	120	0.000	0.001
28	Magothy aquifer	Kmg	3,800	33	52	73	20
29	Magothy-Patapsco confining unit	Kmp	0	3	70	0.003	0.001
30	Upper Patapsco aquifer	Kup	2,000	25	400	5	20
31	Patapsco confining unit	Kpc	0	nd	150	0.000	0.001
32	Lower Patapsco aquifer	Klp	1,754	41	550	3	20
33	Arundel Clay confining unit	Kac	nd	nd	300	nd	0.001
34	Patuxent aquifer	Kpx	1,142	39	1,200	1	10
35	Pre-Cretaceous crystalline	pK	nd	nd	nd	nd	1

^aValues reported in Andreasen and others (2007).^bNumbers in bold-italic were calibrated; those not in bold-italic were specified.

Table 5. Composite scaled sensitivities for hydraulic conductivity parameters in the groundwater model.

[CSS, Composite Scaled Sensitivity]

Unit number	Stratigraphic or hydrogeologic unit name	Map symbol on figures in this report	Parameter name	Hydraulic conductivity, in feet per day	CSS	Percent CSS of maximum value of CSS
1	Kent Island Formation	Qki	kntislnd	1	0.061	3.5
2	Parsonsburg sand	Qpr	prsnsbrg	50	0.011	0.6
3	Omar Formation	Qom	omarform	1	0.031	1.8
4	Walston silt	Qws	walstons	1	0.026	1.5
5	Beaverdam sand	Qbv	beavrdm	75	1.317	75.0
6	Pensauken Formation	Qpe	pensaukn	100	1.487	85.0
7	Columbia Formation	Qco	columbia	10	1.020	58.0
8	Upper Chesapeake Confining Unit UC1	Tuch1	aquitard ^a	0.001	0.013	7.5
9	Pocomoke aquifer	Tpo	pocomoke	25	0.152	8.7
10	Upper Chesapeake Confining Unit UC2	Tuch2	aquitard ^a	0.001	0.013	7.5
11	Ocean City aquifer	Toc	oceancty	25	0.064	3.6
12	Upper Chesapeake Confining Unit UC3	Tuch3	aquitard ^a	0.001	0.013	7.5
13	Manokin aquifer	Tma	manokina	25	0.763	43.4
14	St. Mary's confining unit	Tsm	aquitard ^a	0.001	0.013	7.5
15	Choptank aquifer	Tch	choptank	1	0.071	4.0
16	Lower Chesapeake confining unit	Tlch	aquitard ^a	0.001	0.013	7.5
17	Calvert aquifer system	Tca	calverta	1	0.390	22.2
18	Calvert confining unit	Tcc	aquitard ^a	0.001	0.013	7.5
19	Piney Point aquifer	Tpp	pineypta	50	0.014	0.8
20	Nanjemoy confining unit	Tnj	aquitard ^a	0.001	0.013	7.5
21	Aquia aquifer	Taq	aquiaaqf	50	1.069	60.9
22	Hornerstown Formation	Tht	hnrstwn	8	1.745	100.0
23	Severn confining unit	Ksc	aquitard ^a	0.001	0.013	7.5
24	Monmouth aquifer	Kmo	monmouth	10	0.772	44.0
25	Matawan confining unit	Kmc	aquitard ^a	0.001	0.013	7.5
25	Matawan Aquifer	Kma	matawana	20	0.001	0.1
26	Matawan-Magothy confining unit	Kmm	aquitard ^a	0.001	0.013	7.5
27	Magothy aquifer	Kmg	magothya	20	0.111	0.1
28	Magothy-Patapsco confining unit	Kmp	aquitard ^a	0.001	0.013	7.5
29	Upper Patapsco aquifer	Kup	uptapsco	20	0.009	0.5
30	Patapsco confining unit	Kpc	aquitard ^a	0.001	0.013	7.5
31	Lower Patapsco aquifer	Klp	lptapsco	20	0.001	0.1
33	Arundel Clay confining unit	Kac	aquitard ^a	0.001	0.013	7.5
34	Patuxent aquifer	Kpx	patuxent	10	0.001	0.1
35	Pre-Cretaceous crystalline	pK	aquitard ^a	1	0.013	7.5

^aThe aquitard parameter is a combination of all of the confining units, and thus the CSS represents this composite of units.

The final calibrated model produced a set of simulated water levels that were then compared to the observed water levels (fig. 33). The fit to the data is shown in figure 33A, with the largest single error being 24 ft (fig. 33B). Errors can be attributed to local variations in hydraulic conductivity that cannot be represented by assigning a constant value for each formation for the entire peninsula. Thus, although the error between observed and simulated water-level values could potentially be high at the local cell level, the overall system (and especially fluxes) is represented in a manner appropriate for estimating the age distributions in streams, which is the intended use of this model. The distribution of the error in the simulated water-level observations does not show any obvious spatial trend in observed error (fig. 34).

Groundwater ages were simulated for each of the corresponding observation wells using backward tracking of particles in the USGS code MODPATH (Pollock, 1994). The resulting plot of observed and simulated advective age (fig. 35) reveals a distribution that is not highly correlated, but this pattern is typical of simulated groundwater-age observations (Sanford, 2011). Flow direction and age vary greatly at this scale, which is typically too small for age to be simulated in adequate detail by the flow model; therefore, a general fit to the mean and range of groundwater ages is usually sought as an indicator of reasonable fit. In this case, the mean observed age was 11 years and the mean simulated age was 11.5 years. Simulated age ranged from 3 to 42 years (except for one outlier), which was very close to the range of 2 to 45 years for the observed values. The outlier can be explained by the fact that the tritium-helium-based tracer at that particular observation was near its limit of about 40 to 50 years. Thus, because it is possible that given water sampled from wells can represent a mixture of ages (Cook and Herzceg, 2000), the groundwater at this observation location may easily have a substantial percentage of water much older than 40 to 50 years, such as that suggested by the simulated age of 755 years.

The final simulated ages were calculated after adjusting porosity to achieve the best fit for the mean age. This adjustment yielded a calibrated effective porosity of 35 percent for the entire system. This value is very reasonable for the sediments on the Coastal Plain because measured total porosity, which will be greater than the effective porosity, is typically between 40 and 50 percent for the Quaternary (least compacted) sediments (Sanford and Pope, 2009). The spatial distribution of simulated ages does not show any obvious spatial trend in error (fig. 36).

Simulation Results

The primary result of the flow model in this study is a distribution of hydraulic head (groundwater levels) that represents the steady-state flow condition. The water levels in layer 1 of the model (fig. 37) most closely represent the elevation of the water table, which for most of the peninsula, strongly reflects the topography. Water levels in the deepest

part of the model grid, at 245 ft below land surface in layer 7, are a slightly subdued replica of the water table (fig. 38) because the groundwater system simulated here is very thin (300 ft) compared to its areal extent (tens of miles) and controlled mostly by local variation in topography. The water table is close to land surface (within 3 ft) over much of the peninsula (fig. 39), especially in low-lying areas near the bays. Marshy areas in the center of the peninsula in Delaware and southeastern Maryland also have very shallow water tables. The areas that have deeper water tables (more than 10 ft) are typically located along the upper topographic rims of incised stream valleys, especially in the northeastern peninsula, which has the most deeply incised valleys.

Information can also be obtained by examining the overall water budget of the model. The post-processing code ZONEBUDGET (Harbaugh, 1990) was used to analyze the spatial water budget for the model. A layer-by-layer analysis (table 6) revealed that much of the flow is concentrated in the upper part of the model grid (shallowest part of the flow system), with two-thirds of the flow occurring in the top 10 percent of the model grid and 90 percent of the flow occurring in the top half of the model grid. Although the mean recharge to the peninsula is 3,320 Mgal/d, only 56 Mgal/d exits by submarine groundwater discharge (less than 2 percent of the total discharge); the remainder discharges in the stream valleys. By dividing the total water volume of each layer (using the calibrated porosity of 0.35) by the total flux in each layer, mean residence times were obtained for each layer. The higher flows in the upper layers are reflected in these residence times, which range from 2.5 years for layer 1 to over 900 years for layer 7. ZONEBUDGET was also used to apportion the fluxes by geologic unit (table 7). The highest fluxes are in those aquifers with the broadest areal extent, and the lowest fluxes are in the deeper units and those with a limited areal extent. Water volumes and residence times were also calculated for the geologic units. In general, the units with the shortest residence times are the shallowest Quaternary units, and those with the longest residence times are the confining units, especially the deeper ones.

Other useful information can be obtained by directly analyzing the fluxes between cells from the final head distribution. One example is the distribution of net recharge (or discharge) across the peninsula (fig. 40). As described earlier in the report, the land-surface boundary condition was treated as a combination of specified recharge and a seepage face. The net recharge can be calculated by subtracting the drain discharge at each cell from its specified value of recharge. Plotting this net recharge areally yields the locations and magnitudes of net groundwater discharge. These discharge locations, shown in red in figure 40, are in stream valleys where base flow to the streams occurs. In the broad marshy areas, nearly all of the specified recharge is calculated by the model to discharge again within, or close to, the same cell at land surface (representing riparian ET), resulting in a net recharge of nearly zero.

Another important example of flux-related information obtained from the simulation results is the residence time of

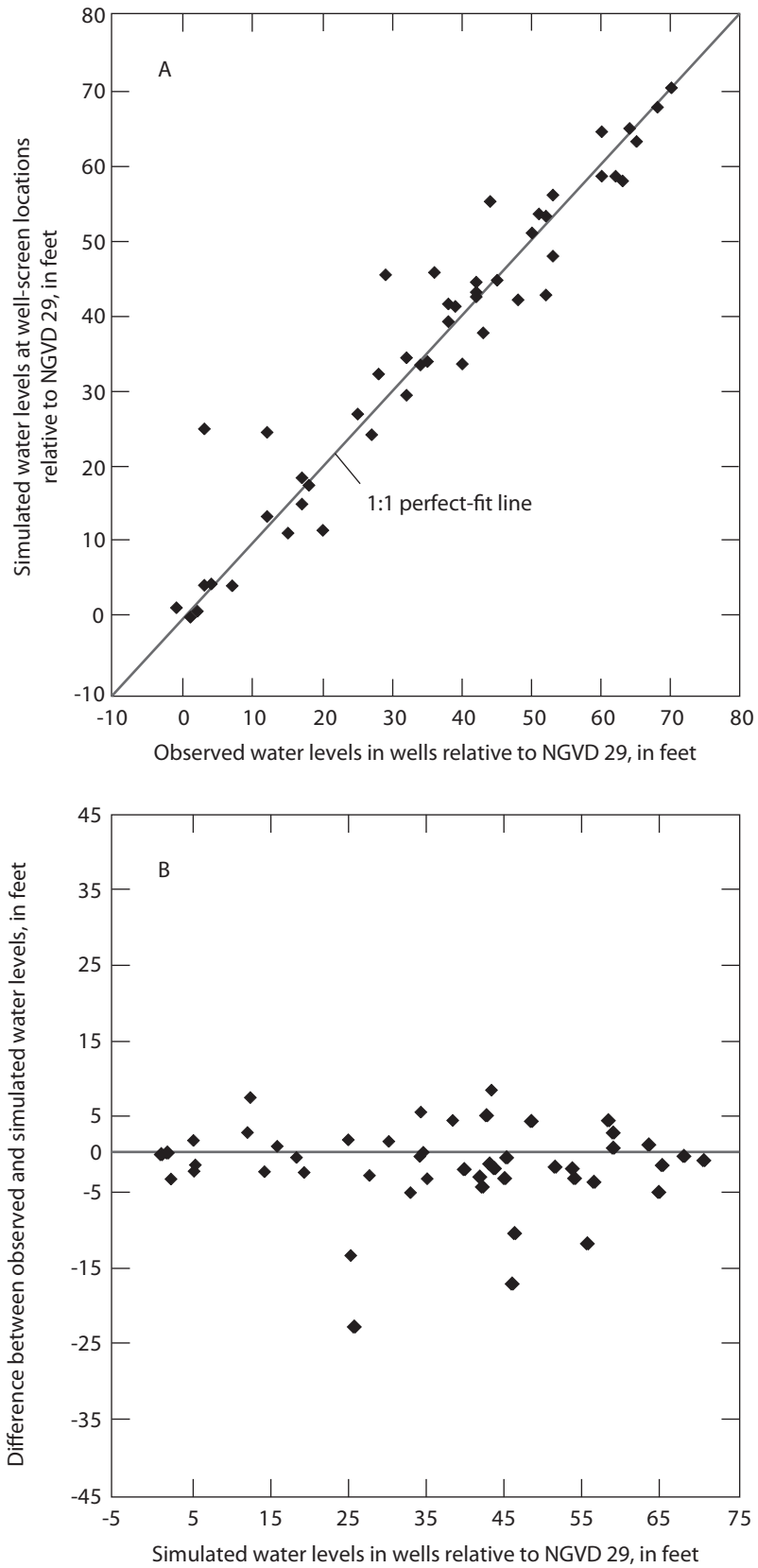


Figure 33. A, Observed versus simulated water levels, and B, simulated water levels versus the difference between the observed and simulated water levels.

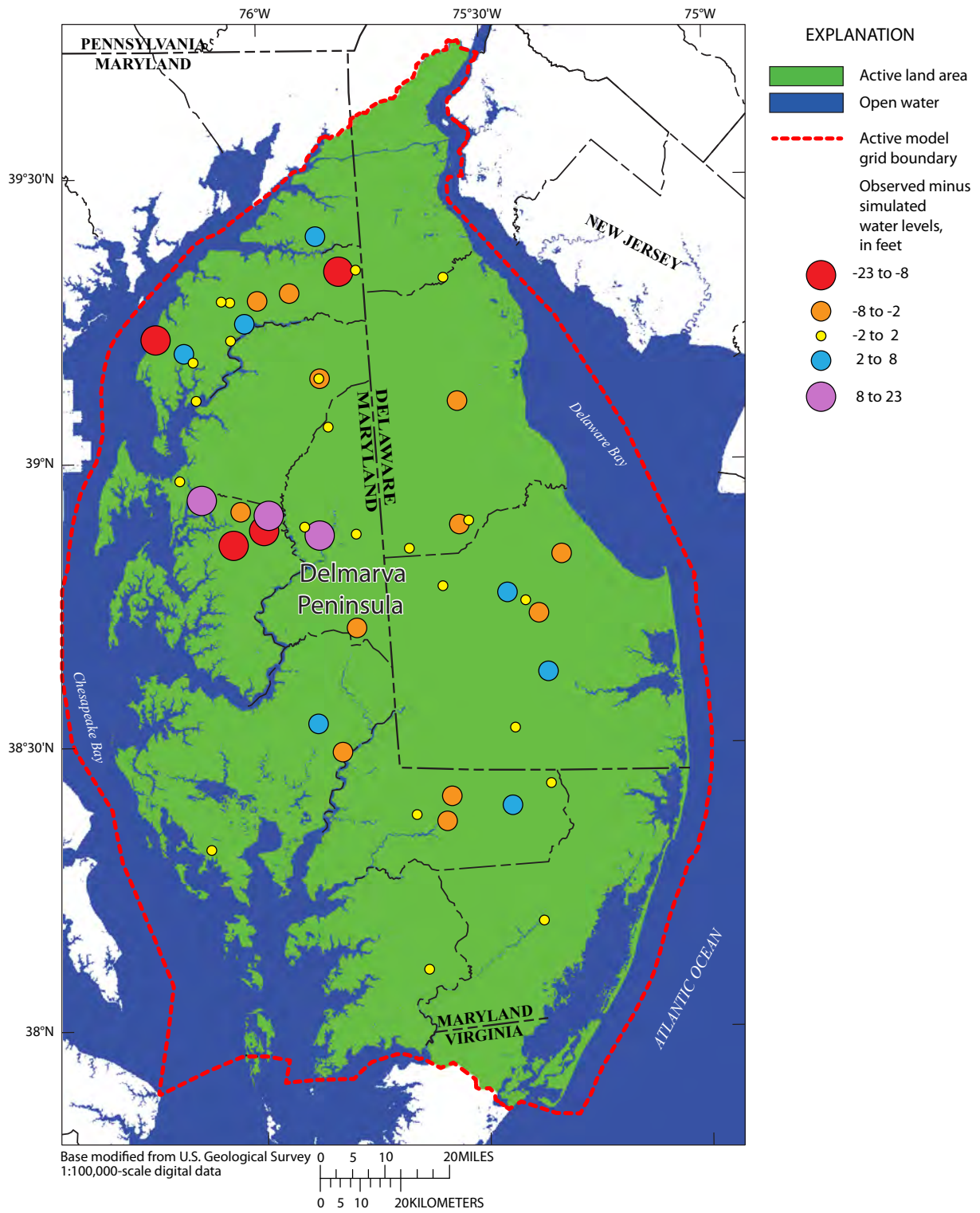


Figure 34. Spatial distribution of errors in the simulated water-level observations.

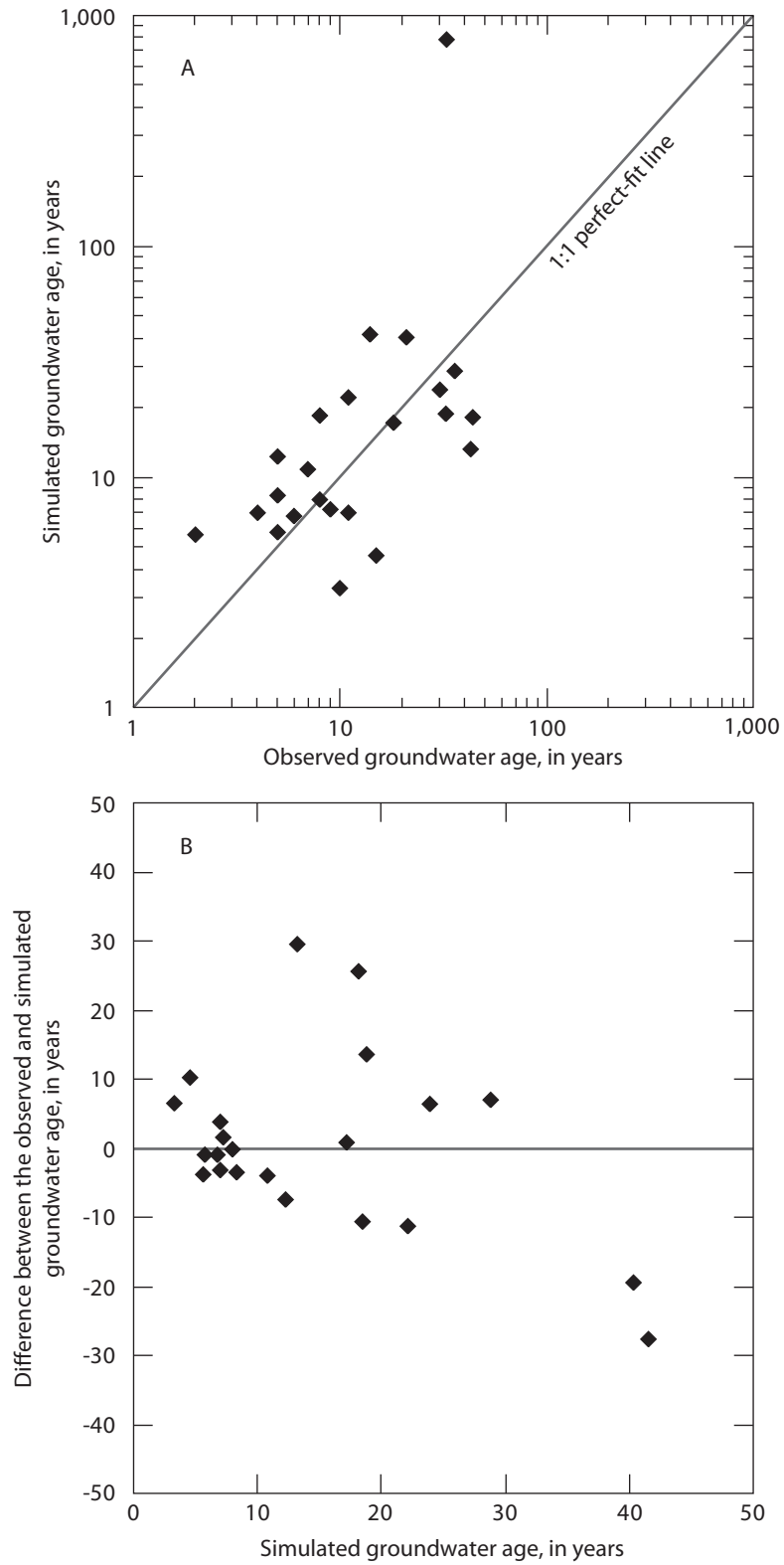


Figure 35. A, Observed versus simulated groundwater ages, and B, simulated ages versus the difference between the observed and simulated ages.

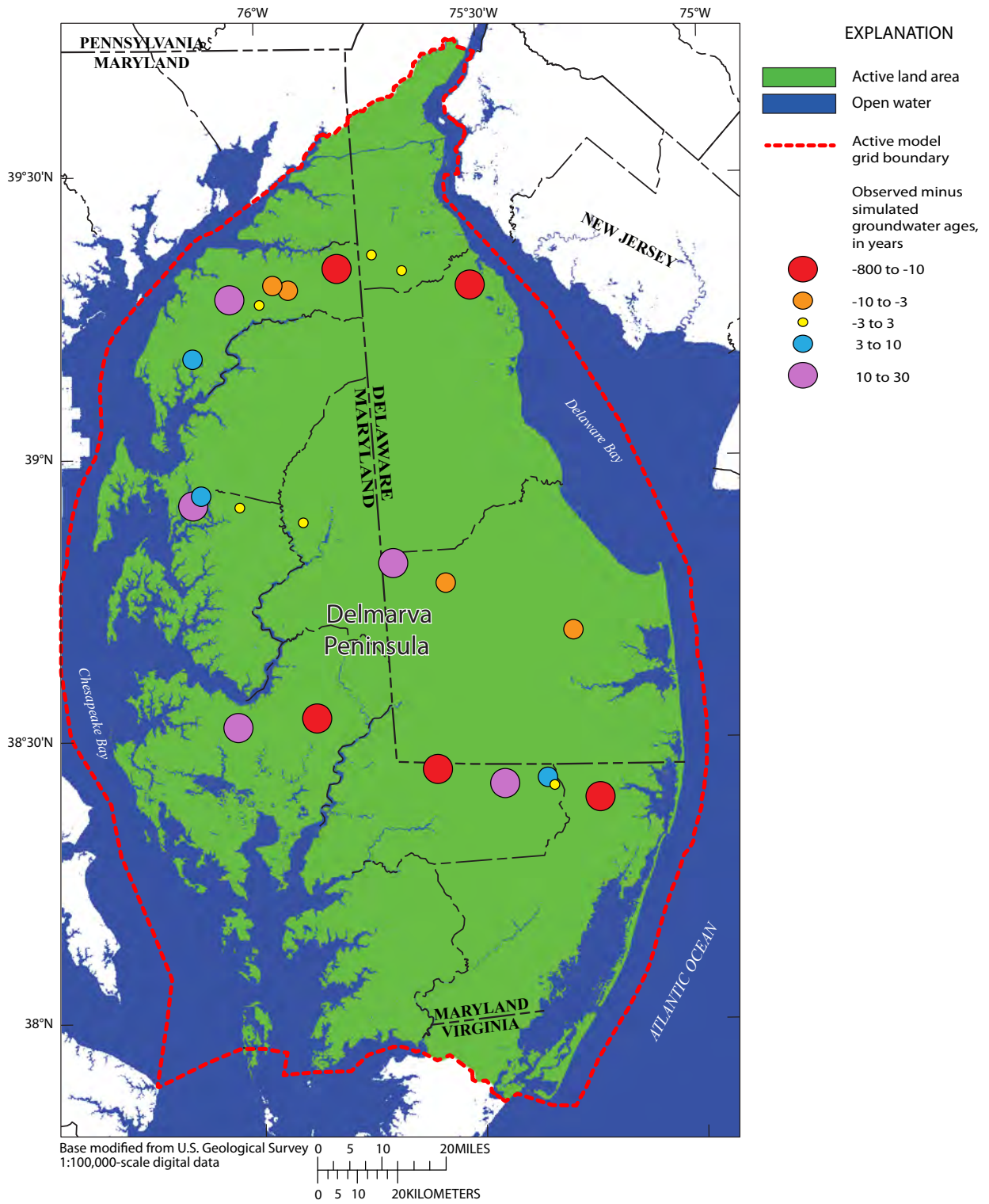


Figure 36. Spatial distribution of errors in the simulated age observations.

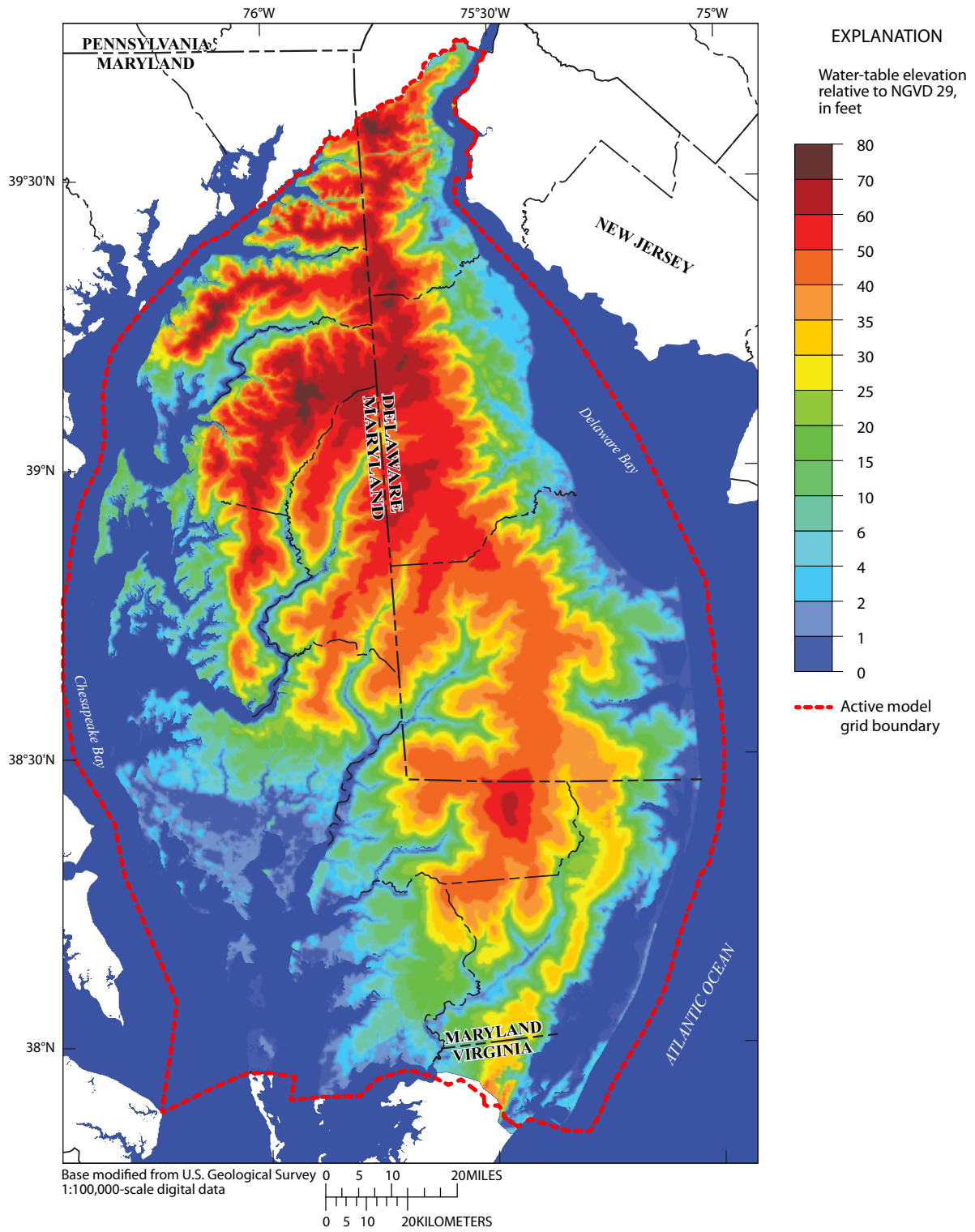


Figure 37. The simulated water table on the Delmarva Peninsula represented by water levels in layer 1 of the model.

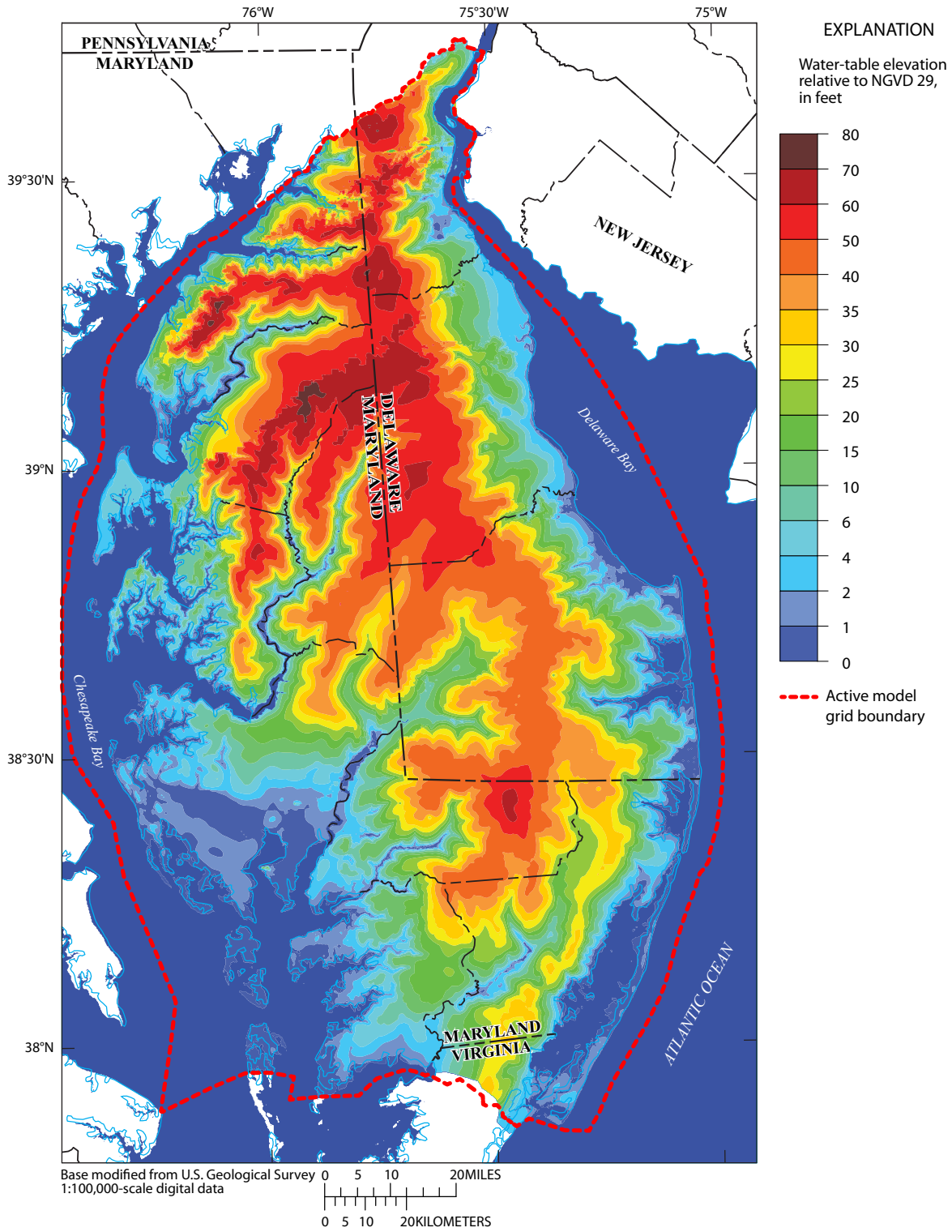


Figure 38. The simulated water levels in layer 7 of the model.

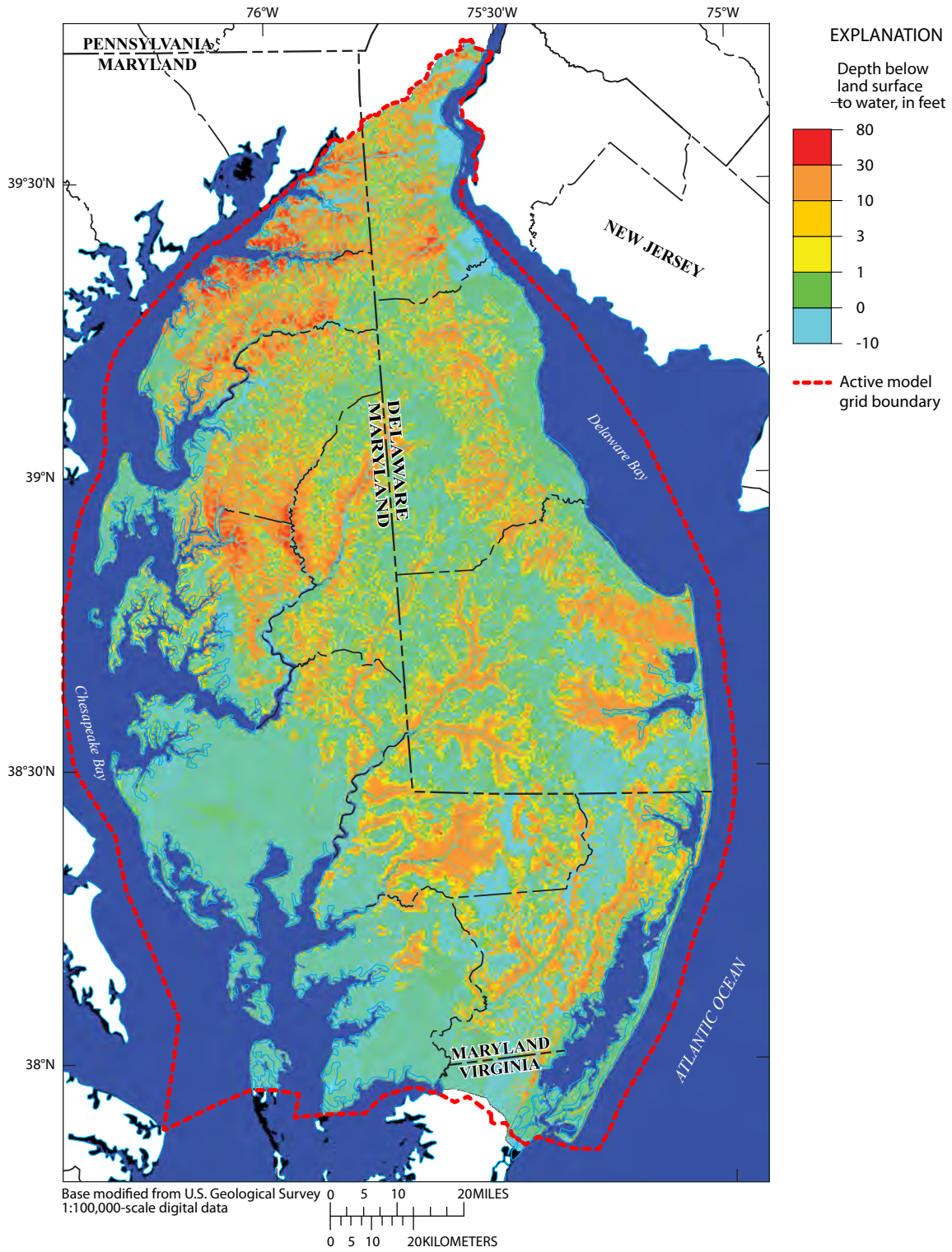


Figure 39. The simulated depth of the water table beneath the land surface. Negative values represent artesian conditions.

Table 6. Water budget terms in the groundwater model by model layer.

[Mgal/d, millions of gallons per day; SGD, submarine groundwater discharge; Bgal, billions of gallons]

Layer number	Inflows, in Mgal/d		Outflows, in Mgal/d			Total flux, in Mgal/d	Percentage of total flux	Volume of water, in Bgal	Mean residence time of water, in years
	Recharge	From other layers	To other layers	To drain cells	Net to seafloor (SGD)				
1	3,320	2,117	2,117	3,264	56	5,437	40.4	5,034	2.5
2	0	3,520	3,520	0	0	3,520	26.1	9,982	7.8
3	0	2,158	2,158	0	0	2,158	16.0	15,104	19
4	0	1,176	1,176	0	0	1,176	8.7	20,129	47
5	0	674	674	0	0	674	5.0	25,297	103
6	0	385	385	0	0	385	2.9	30,208	215
7	0	133	133	0	0	133	1.0	45,313	932
Total	3,320			3,264	56	13,507		151,000	125

the groundwater within the flow system. This residence time is the primary object of concern with respect to the transport of nitrate from the infiltration point at land surface to Chesapeake Bay, and obtaining these results is the main objective of this study. The residence time can be viewed from two different perspectives. The first is from the perspective of groundwater age at any location in the flow system. This is calculated from the model results by using MODPATH to track a flow path-line backward from every cell of interest in the model to its recharge location at the water table, calculate its time of travel (age), and then plot each age according to its starting cell location. When this is done for layer 4 across the entire model area, a map of groundwater age 80 ft below land surface is produced (fig. 41). The ages range from less than 30 years to more than 1,000 years. There are two main controls on the age at these depths—the location within the local flow system and the hydraulic conductivity of the geologic unit that is represented locally at the cell. The youngest waters are located near recharge areas that are also close to local streams. The oldest waters are in confining units, where flow rates are small. As a result, these old waters only contribute minimally to streamflow compared to waters in shallower, more permeable sediments.

The second perspective from which to view residence time is return time, which is the time required for groundwater to flow from the water table where it is recharged to the land surface as discharge to a surface-water body. These return times were calculated using MODPATH by tracking a particle forward from the water table at each cell to its discharge location and then calculating the associated time of travel (return time). This time of travel is mapped for each starting location to yield a map of groundwater return times (fig. 42). Such a map reveals that the peninsula is dominated by local flow systems controlled by the drainage network, and that return times vary consistently from less than 3 years in the stream valley to more than 100 years near the stream divides. These return times can be used to determine the age distribution of

groundwater contributed to individual streams, which in turn can be used to predict the potential lag time between changes in the loading of nitrate at land surface and the resulting changes in nitrate concentrations in the streams.

The limitations of the model should be considered when interpreting or applying the results to other studies or to management decisions. These limitations are not likely to change the overall results, but may create errors more locally. These limitations include (1) anthropogenic stresses were not simulated, (2) calibration was made directly only to water-level and age observations (although base-flow observations were used to calibrate the specified recharge rates), (3) many local areas were not represented by water-level or age observations, (4) the bottom of the model is treated as a no-flow boundary, (5) long-term climate conditions were not considered (only a 30-year climate record was used to calibrate recharge), (6) only the impervious surface distribution from 2001 was used, and (7) variable-density effects on flow near the coastline were not simulated.

Summary and Conclusions

In this study, the U.S. Geological Survey (USGS) constructed a groundwater flow model for the Delmarva Peninsula including Delaware, Maryland and the northernmost section of Virginia. The model was constructed to simulate shallow groundwater flow system in the peninsula so that predictions can ultimately be made about the magnitude and variability of the lag time for nitrate between its application at land surface and its discharge into streams and Chesapeake Bay. The model was constructed and simulated using the newly released Newton version of the USGS code MODFLOW. A recharge value was specified at land surface based on a water-balance method used recently for the Coastal Plain that also incorporates a climate-regression equation for estimating evapotranspiration.

Table 7. Water budget terms in the groundwater model by geologic unit.

[Mgal/d, millions of gallons per day; SGD, submarine groundwater discharge; Bgal, billions of gallons]

Zone number in model	Stratigraphic or hydrogeologic unit name	Inflows, in Mgal/d		Outflows, in Mgal/d			Total flux, in Mgal/d	Volume of water, in Bgal	Mean residence time of water, in years
		Recharge	From other layers	To other layers	To drain cells	Net to seafloor (SGD)			
31	Kent Island Formation	603	157	173	573	13.6	761	2,208	7.9
32	Parsonsborg sand	73.4	18.5	70.4	21.5	0	92	83	2.5
33	Omar Formation	356	247	317	286	0.10	603	1,138	5.2
34	Walston silt	47.2	15.4	47.4	15.3	0	63	58	2.5
35	Beaverdam sand	1,029	908	940	995	1.55	1,947	8,237	12
36	Pensauken Formation	674	600	629	645	0.41	1,275	3,915	8.4
37	Columbia Formation	386	762	753	390	5.14	1,149	6,303	15
2	Upper Chesapeake Confining Unit UC1	3.62	11.4	11.31	2.73	0.96	15	7,582	1,370
3	Pocomoke aquifer	0.14	312	312	0.51	0	314	5,393	47
4	Upper Chesapeake Confining Unit UC2	0.048	262	262	0.00	0	265	8,522	88
5	Ocean City aquifer	0	35.2	35.2	0	0	35	3,595	280
6	Upper Chesapeake Confining Unit UC3	0	0.005	0.005	0	0	0	1,057	538,000
7	Manokin aquifer	0.21	232	233	0.12	0	236	11,094	129
8	St. Mary's confining unit	4.21	8.24	8.03	3.64	0.77	12	17,680	3,880
9	Choptank aquifer	7.25	71.2	50.0	26.1	2.33	79	7,538	262
10	Lower Chesapeake confining unit	3.39	14.0	13.3	2.36	1.75	17	5,167	812
11	Calvert aquifer system	26.3	141	105	57.9	4.52	168	24,143	393
12	Calvert confining unit	19.7	21.1	20.3	16.6	3.89	41	8,590	577
13	Piney Point aquifer	0	13.5	13.5	0	0	14	2,094	425
14	Nanjemoy confining unit	0	3.63	3.48	0	0.16	4	6,017	4,540
15	Aquia aquifer	16.8	172	99.0	79.8	9.53	190	4,326	62
16	Hornerstown Formation	1.86	198	140	58.3	1.15	200	3,644	50
17	Severn confining unit	4.95	9.32	11.5	2.21	0.56	14	1,252	240
18	Monmouth aquifer	11.6	81.8	55.7	36.1	1.58	93	2,076	61
19	Matawan confining unit	5.56	4.69	5.80	3.97	0.47	10	1,417	378
20	Matawan aquifer	0	0.002	0.002	0	0	0	3	4,640
21	Matawan-Magothy confining unit	7.34	1.77	1.36	7.64	0.11	9	1,414	425
22	Magothy aquifer	3.14	27.53	20.56	9.57	0.54	31	1,029	92
23	Magothy-Patapsco confining unit	2.06	12.0	6.55	4.48	3.06	14	1,882	366
24	Upper Patapsco aquifer	5.81	34.3	20.4	16.3	3.42	40	2,033	139
25	Patapsco confining unit	3.66	1.71	3.32	1.65	0.40	5	752	384
26	Lower Patapsco aquifer	4.37	6.67	4.33	6.21	0.51	11	452	112
27	Arundel Clay confining unit	0.95	0.29	0.88	0.37	0	1	161	355
28	Patuxent aquifer	0.16	2.80	2.32	0.64	0	3	231	214
30	Pre-Cretaceous crystalline	0	0.30	0.30	0	0	0	39	355
Total		3,320			3,264	56		151,000	125

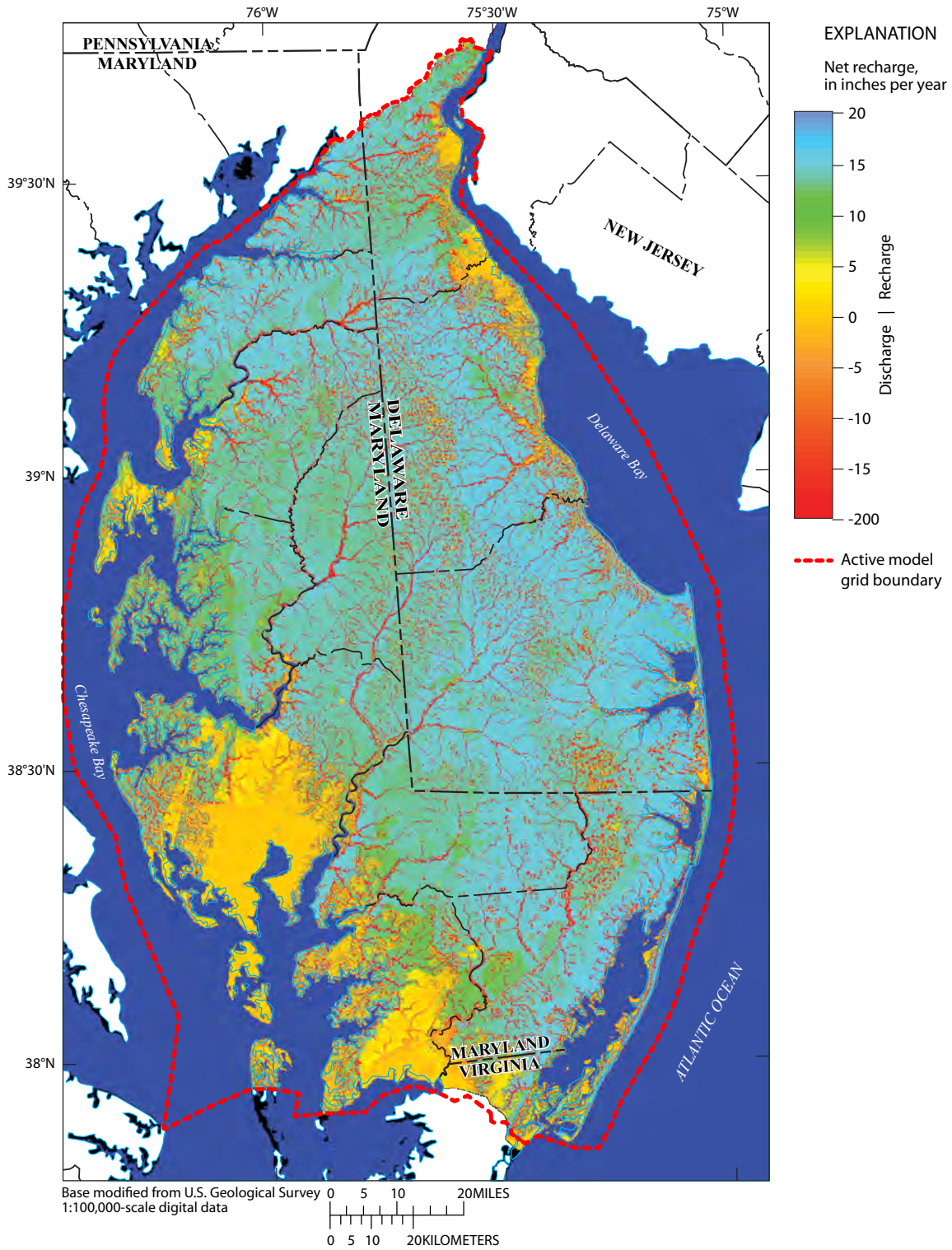


Figure 40. Simulated net recharge across the Delmarva Peninsula calculated by subtracting the seepage (drain) discharge from the recharge (fig. 18).

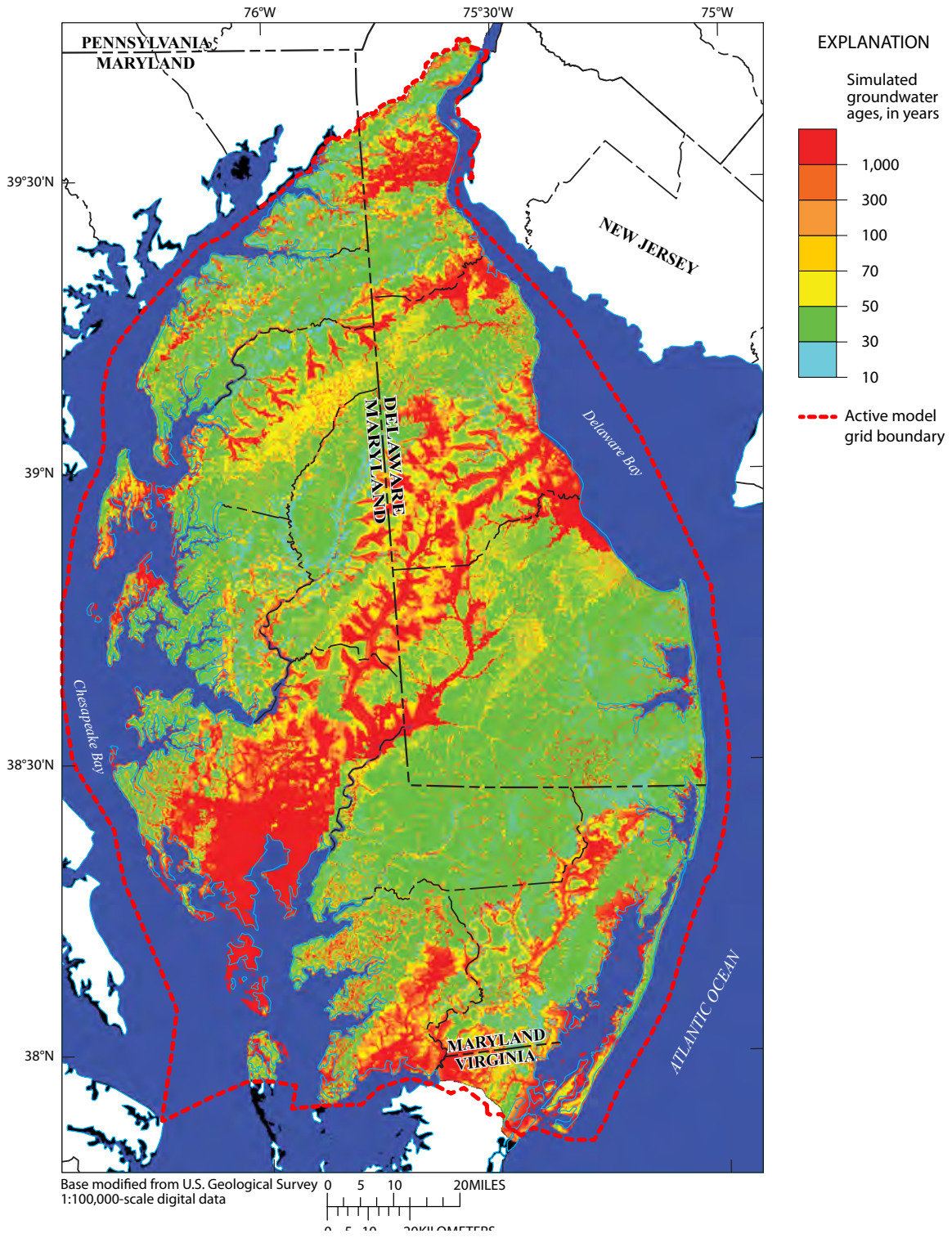


Figure 41. Simulated groundwater age 80 feet below land surface in layer 4 of the model grid.

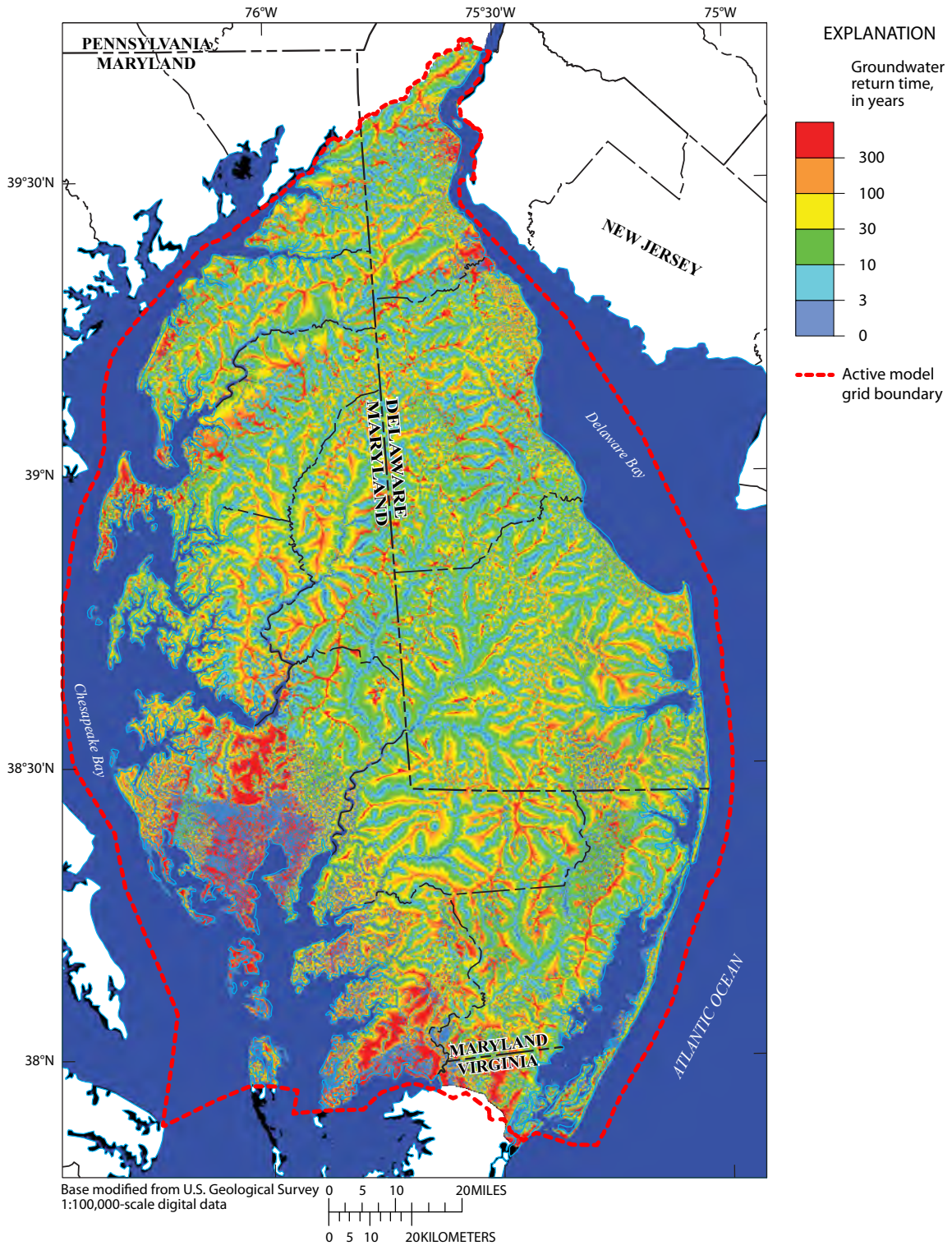


Figure 42. Simulated return time of groundwater travelling from the water table to its discharge location.

Seepage to streams as base flow was simulated with the drain package in MODFLOW by assigning drains to every active cell in the top layer with an elevation above NGVD 29. A hydrogeologic framework for the Coastal Plain sediments constructed by Andreasen and coworkers at the Maryland Geological Survey was incorporated into the model grid. Hydraulic conductivity values were assigned mostly based on reported field values, but seven values for the most prevalent and influential units were calibrated to a best fit using 48 groundwater levels in shallow wells across the peninsula. Groundwater ages were calculated using MODPATH and compared to tracer-based ages from 24 wells, and the difference between the mean simulated and mean observed age was minimized to yield a calibrated effective porosity for the entire system of 35 percent.

Results of the simulation reveal a water table that closely reflects the land surface topography, with depths to water greater than 10 feet being located only in upland locations that are adjacent to incised stream valleys. The shallow nature of this flow system relative to its spatial extent results in groundwater flow that is controlled mostly by the local topography. Most of the water that is recharged remains within its local flow system until it is discharged to a local stream. Groundwater ages and return times were calculated using MODPATH for every cell in the model. Mapped groundwater ages illustrate the local nature of the flow systems and the very slow movement of water through the confining units. A map of the groundwater return time illustrates that most groundwater reaches a stream between 3 and 100 years after it is recharged to the water table, with a strong positive correlation existing between the return time and the distance between the point of recharge and the nearest stream.

References Cited

- Andreasen, D.C., Achmad, G., Staley, A.W., and Hodo, R.M., 2007, Hydrogeologic framework of the Maryland Coastal Plain: Maryland Geological Survey and Maryland Department of Natural Resources Progress Report, 72 p.
- Ator, S.W., Denver, J.M., Krantz, D.E., Newell, W.L., and Martucci, S.K., 2005, A surficial hydrogeologic framework for the Mid-Atlantic Coastal Plain: U.S. Geological Survey Professional Paper 1680, 44 p., 4 pls.
- Bachman, L.J., and Wilson, J.M., 1984, The Columbia aquifer of the Eastern Shore of Maryland: Maryland Geological Survey Report of Investigations No. 40, 144 p.
- Böhlke, J.K., and Denver, J.M., 1995, Combined use of groundwater dating, chemical, and isotopic analyses to resolve the history and fate of nitrate contamination in two agricultural watersheds, Atlantic Coastal Plain, Maryland: Water Resources Research, v. 31, no. 9, p. 2319–2339.
- Cook, P.G., and Herzceg, A.L., 2000, Environmental tracers in subsurface hydrology: Boston, Kluwer Academic Publishers, 529 p.
- Daly, C., Halbleib, M., Smith, J.I., Gibson, W.P., Doggett, M.K., Taylor, G.H., Curtis, J., and Pasteris, P.P., 2008, Physiographically-sensitive mapping of temperature and precipitation across the conterminous United States: International Journal of Climatology, v. 28, p. 2031–2064.
- Dunkle, S.A., Plummer, L.N., Busenberg, E., Phillips, P.J., Denver, J.M., Hamilton, P.A., Michel, R.L., Coplen, T.B., 1993, Chlorofluorocarbons (CCl₃F and CCl₂F₂) as dating tools and hydrologic tracers in shallow groundwater of the Delmarva Peninsula, Atlantic Coastal Plain, United States: Water Resources Research, v. 29, no. 12, p. 3837–3860.
- Fleck, W.B., and Vroblesky, D.A., 1996, Simulation of ground-water flow of the Coastal Plain aquifers in parts of Maryland, Delaware, and the District of Columbia: U.S. Geological Survey Professional Paper 1404–J, 41 p.
- Harbaugh, A.W., 1990, A computer program for calculating subregional water budgets using results from the U.S. Geological Survey Modular three-dimensional finite-difference ground-water flow model: U.S. Geological Survey Open-File Report 90–392, 24 p.
- Harbaugh, A.W., 2005, MODFLOW–2005, The U.S. Geological Survey modular ground-water model—The ground-water flow process: U.S. Geological Survey Techniques and Methods, book 6, chap. 16, variously paged.
- Heywood, C.E., and Pope, J.P., 2009, Simulation of ground-water flow in the Coastal Plain aquifer system of Virginia: U.S. Geological Survey Scientific Investigations Report 2009–5039, 115 p.
- Hill, M.C., Tiedeman, C.R., 2007, Effective groundwater model calibration: Hoboken, N.J., John Wiley & Sons, 455 p.
- Homer, C., Huang, C., Yang, L., Wylie, B., and Coan, M., 2004, Development of a 2001 national land-cover database for the United States: Photogrammetric Engineering and Remote Sensing, v. 70, no. 7, p. 829–840.
- Kenny, J. F., Barber, N. L., Hutson, S. S., Linsey, K. S., Lovelace, J. K., and Maupin, M. A., 2009, Estimated use of water in the United States in 2005: U. S. Geological Survey Circular 1344, 52 p.
- Langevin, C.D., Shoemaker, W.B., and Guo, W., 2003, MODFLOW–2000, the U. S. Geological Survey Modular Ground-Water Model—Documentation of the SEAWAT–2000 version with variable-density flow process (VDF) and the integrated MT3DMS transport process (IMT): U.S. Geological Survey Open-File Report 03–426, 43 p.

- Leahy, P.P., and Martin, M., 1993, Geohydrology and simulation of ground-water flow in the northern Atlantic Coastal Plain aquifer system: U.S. Geological Survey Professional Paper 1404-K, 81 p., 22 pls.
- Niswonger, R.G., Panday, S., and Ibaraki, M., 2011, MODFLOW-NWT, A Newton formulation for MODFLOW-2005: U.S. Geological Survey Techniques and Methods book 6, chap. A37, 44 p.
- Owens, J.P., and Denny, C.S., 1979, Upper Cenozoic deposits of the central Delmarva Peninsula, Maryland and Delaware: U.S. Geological Survey Professional Paper 1067-A, variously paged.
- Phillips, S.W., and Lindsey, B.D., 2003, The influence of groundwater on nitrogen delivery to the Chesapeake Bay: U.S. Geological Survey Fact Sheet FS-091-03, 4 p.
- Poeter, E.P., Hill, M.C., Banta, E.R., Mehl, S., and Christensen, S., 2005, UCODE_2005 and six other computer codes for universal sensitivity analysis, calibration, and uncertainty evaluation: U.S. Geological Survey Techniques and Methods, book 6, chap. A-11, 283 p.
- Pollock, D.W., 1994, User's guide for MODPATH/MODPATH-PLOT, version 3: A particle tracking post-processing package for MODFLOW, the U.S. Geological Survey finite-difference ground-water flow model: U.S. Geological Survey Open-File Report 94-464, variously paged.
- Reilly, T.E., Plummer L.N., Phillips, L. J, and Busenberg, E., 1994, The use of simulation and multiple environmental tracers to quantify groundwater flow in a shallow aquifer: Water Resources Research, v. 30, p. 421-433.
- Reilly, T.E., and Pollock, D.W., 1996 Sources of water to wells for transient cyclic systems: Ground Water, v. 34, no. 6, p. 979-988.
- Sanford, W.E., 2002, Recharge and groundwater models—An overview: Hydrogeology Journal, v. 10, no. 1, p. 110-120.
- Sanford, W.E., 2011, Calibration of models using groundwater age: Hydrogeology Journal, v. 19, no. 1, p. 13-16.
- Sanford, W.E., Nelms, D.L., Pope, J.P., and Selnick, D.L., 2012, Quantifying components of the hydrologic cycle in Virginia using chemical hydrograph separation and multiple regression analysis: U.S. Geological Survey Scientific Investigations Report 2011-5198, 152 p.
- Sanford, W.E., and Pope, J.P., 2007, A simulation of groundwater discharge and nitrate delivery to the Chesapeake Bay from the lowermost Delmarva Peninsula, *in* Sanford W., Langevin, C., Polemio, M., and Povinec, P. (eds.), A New Focus on Groundwater-Seawater Interaction: IAHS Publication 312, p. 326-333.
- Sanford, W.E., Pope, J.P., and Nelms, D.L., 2009, Simulation of groundwater-level and salinity changes in the Eastern Shore, Virginia: U.S. Geological Survey Scientific Investigations Report 2009-5066, 125 p.

ISBN 978-1-4113-3508-0



9 781411 335080



Printed on recycled paper